DM Physics w/o & w/ Dark Higgs Boson

Pyungwon Ko (KIAS)

LIO International Conference and
France-Korea STAR Workshop on
"Fundamental Forces from Colliders to GW"

Contents

- Motivations
- VDM w/ Higgs Portal : $\Gamma_{\rm inv}(H \to VV)$ for $m_V \to 0$
- Inelastic DM and XENON1T Excess
- $U(1)_{L_\mu - L_\tau}$-charged DM : Z' only vs. $Z' + \phi$
- Higgs-Portal Assisted Higgs Inflation
- Summary

Motivations

- Existence of DM established from astro/cosmo observations
- DM-DM, DM-SM force carried by some mediators
- Dark photon : the most common. Usually the origin of its mass is ignored, or assume Stueckelberg mechanism
- Dark Higgs : a kind of the must for massive dark photon within perturbation → Main theme of this talk
- And mediators with both dark and SM charges

- DM physics with massive dark photon can not be complete without Dark Higgs or some mass generation mechanism (well known from the SM W boson) !
- Dark photon : better be connected with conserved quantum #'s dark sector, exact or approximate
- DM with local dark gauge symmetry : can guarantee stability of EW scale DM in the standard QFT framework
- Dark gauge symmetry breaking needs dark Higgs

DM is stable because...

- Symmetries

  - (ad hoc) Z_2 symmetry, etc
  - R-parity
  - Topology (from a broken sym.)

- Very small mass and weak coupling

  e.g: QCD-axion ($m_a \sim \Lambda_{QCD}^2/f_a$; $f_a \sim 10^{9-12}$ GeV)

$$\Gamma_a \sim \mathcal{O}(10^{-5})\frac{m_a^3}{f_a^2} \ll H_0 \sim 10^{-42}\mathrm{GeV}$$

But for WIMP ...

S.Baek, P.Ko, W.I.Park, arXIv:1303.4280 [hep-ph], JHEP (2013)

- Global symmetry is not enough since

$$-\mathcal{L}_{\rm int} = \begin{cases} \lambda \frac{\phi}{M_{\rm P}} F_{\mu\nu} F \mu\nu & \text{for boson} \\ \lambda \frac{1}{M_{\rm P}} \bar{\psi} \gamma^\mu D_\mu \ell_{Li} H^\dagger & \text{for fermion} \end{cases}$$

Observation requires [M.Ackermann et al. (LAT Collaboration), PRD 86, 022002 (2012)]

$$\tau_{\rm DM} \gtrsim 10^{26-30} {\rm sec} \Rightarrow \begin{cases} m_\phi \lesssim \mathcal{O}(10){\rm keV} \\ m_\psi \lesssim \mathcal{O}(1){\rm GeV} \end{cases}$$

$\Rightarrow$ WIMP is unlikely to be stable

- SM is guided by gauge principle

It looks natural and may need to consider a gauge symmetry in dark sector, too.

Why Dark Gauge Symmetry ?

S.Baek, P.Ko, W.I.Park, arXIv:1303.4280 [hep-ph], JHEP (2013)

- Is DM absolutely stable or very long lived ?
- If DM is absolutely stable, one can assume it carries a new conserved dark charge, associated with unbroken dark gauge sym
- DM can be long lived (lower bound on DM lifetime is much weaker than that on proton lifetime) if dark sym is spontaneously broken

Higgs can be harmful to weak scale DM stability

Z_2 sym Scalar DM

$$\mathcal{L} = \frac{1}{2}\partial_\mu S \partial^\mu S - \frac{1}{2} m_S^2 S^2 - \frac{\lambda_S}{4!} S^4 - \frac{\lambda_{SH}}{2} S^2 H^\dagger H.$$

- Very popular alternative to SUSY LSP
- Simplest in terms of the # of new dof's
- But, where does this Z2 symmetry come from ?
- Is it Global or Local ?

Fate of CDM with Z2 sym

- Global Z2 cannot save DM from decay with long enough lifetime

Consider Z_2 breaking operators such as

$$\frac{1}{M_{\rm Planck}} S O_{\rm SM}$$

keeping dim-4 SM operators only

The lifetime of the Z_2 symmetric scalar CDM S is roughly given by

$$\Gamma(S) \sim \frac{m_S^3}{M_{\rm Planck}^2} \sim (\frac{m_S}{100{\rm GeV}})^3 10^{-37} GeV$$

The lifetime is too short for ~100 GeV DM

Fate of CDM with Z_2 sym

- Spontaneously broken local $U(1)_X$ can do the job to some extent, but there is still a problem

Let us assume a local $U(1)_X$ is spontaneously broken by $\langle \phi_X \rangle \neq 0$ with

$$Q_X(\phi_X) = Q_X(X) = 1$$

Then, there are two types of dangerous operators:

$\phi_X^\dagger X H^\dagger H$, and $\phi_X^\dagger X O_{\rm SM}^{(dim-4)}$

Problematic !

Perfectly fine !

- These arguments will apply to all the CDM models based on ad hoc Z_2 symmetry
- One way out is to implement Z_2 symmetry as local U(1) symmetry (arXiv:1407.6588 with Seungwon Baek and Wan-Il Park)
- See a paper by Ko and Tang on local Z_3 scalar DM, and another by Ko, Omura and Yu on inert 2HDM with local $U(1)_H$

arXiv:1407.6588 w/ WIPark and SBaek

$$Q_X(\phi) = 2, \quad Q_X(X) = 1$$

$$\mathcal{L} = \mathcal{L}_{\rm SM} + -\frac{1}{4}X_{\mu\nu}X^{\mu\nu} - \frac{1}{2}\epsilon X_{\mu\nu}B^{\mu\nu} + D_\mu\phi_X^\dagger D^\mu\phi_X - \frac{\lambda_X}{4}\left(\phi_X^\dagger\phi_X - v_\phi^2\right)^2 + D_\mu X^\dagger D^\mu X - m_X^2 X^\dagger X$$
$$- \frac{\lambda_X}{4}\left(X^\dagger X\right)^2 - \left(\mu X^2\phi^\dagger + H.c.\right) - \frac{\lambda_{XH}}{4}X^\dagger X H^\dagger H - \frac{\lambda_{\phi_X H}}{4}\phi_X^\dagger\phi_X H^\dagger H - \frac{\lambda_{XH}}{4}X^\dagger X\phi_X^\dagger\phi_X$$

The lagrangian is invariant under $X \to -X$ even after $U(1)_X$ symmetry breaking.

Unbroken Local Z2 symmetry

$X_R \to X_I \gamma_h^*$ followed by $\gamma_h^* \to \gamma \to e^+e^-$ **etc.**

The heavier state decays into the lighter state

The local Z2 model is not that simple as the usual Z2 scalar DM model (also for the fermion CDM)

VDM w/ Higgs Portal

$\Gamma_{\rm inv}(H \to VV)$ for $m_V \to 0$

arXiv: 2112.11983, PRD 105 (2022) 015007,with S. Baek, W.I. Park
And references therein by P. Ko et al

Higgs portal DM models

$$\mathcal{L}_{\rm scalar} = \frac{1}{2}\partial_\mu S \partial^\mu S - \frac{1}{2} m_S^2 S^2 - \frac{\lambda_{HS}}{2} H^\dagger H S^2 - \frac{\lambda_S}{4} S^4$$

$$\mathcal{L}_{\rm fermion} = \overline{\psi}\left[i\gamma\cdot\partial - m_\psi\right]\psi - \frac{\lambda_{H\psi}}{\Lambda} H^\dagger H\, \overline{\psi}\psi$$

$$\mathcal{L}_{\rm vector} = -\frac{1}{4} V_{\mu\nu} V^{\mu\nu} + \frac{1}{2} m_V^2 V_\mu V^\mu + \frac{1}{4}\lambda_V (V_\mu V^\mu)^2 + \frac{1}{2}\lambda_{HV} H^\dagger H V_\mu V^\mu .$$

All invariant under ad hoc Z2 symmetry

arXiv:1112.3299, … 1402.6287, etc.

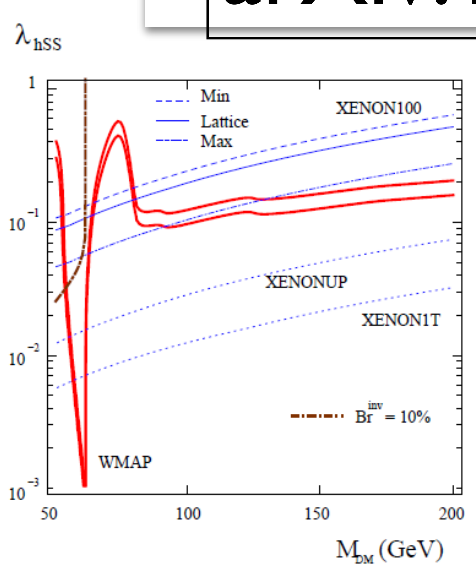

FIG. 1. Scalar Higgs-portal parameter space allowed by WMAP (between the solid red curves), XENON100 and $BR^{inv} = 10\%$ for $m_h = 125$ GeV. Shown also are the prospects for XENON upgrades.

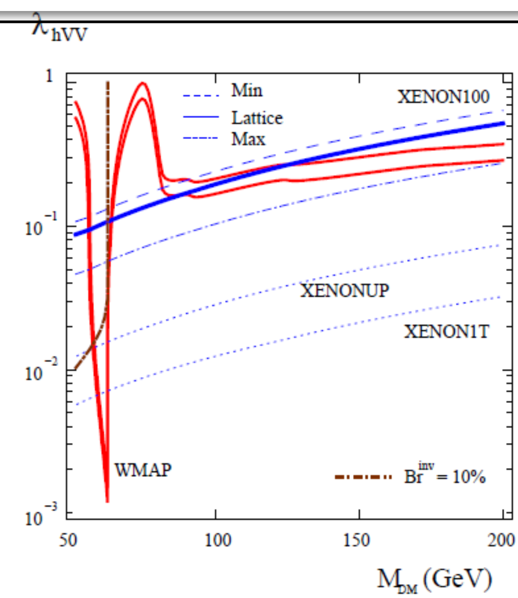

FIG. 2. Same as Fig. 1 for vector DM particles.

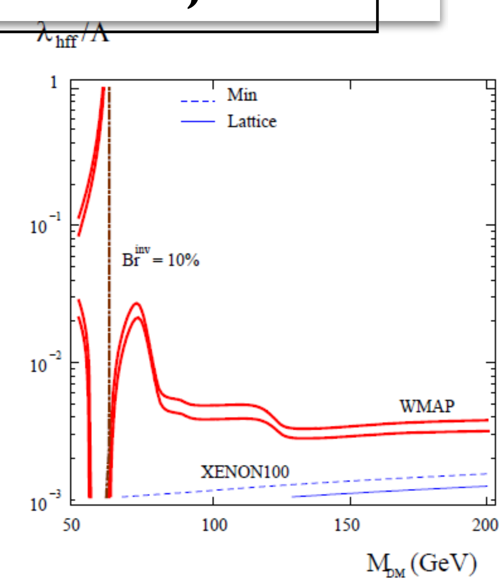

FIG. 3. Same as in Fig.1 for fermion DM; λ_{hff}/Λ is in GeV^{-1}.

Higgs portal DM as examples

$$\mathcal{L}_{\rm scalar} = \frac{1}{2}\partial_\mu S \partial^\mu S - \frac{1}{2} m_S^2 S^2 - \frac{\lambda_{HS}}{2} H^\dagger H S^2 - \frac{\lambda_S}{4} S^4$$

$$\mathcal{L}_{\rm fermion} = \overline{\psi}\left[i\gamma \cdot \partial - m_\psi \right] \psi - \frac{\lambda_{H\psi}}{\Lambda} H^\dagger H \, \overline{\psi}\psi$$

$$\mathcal{L}_{\rm vector} = -\frac{1}{4} V_{\mu\nu} V^{\mu\nu} + \frac{1}{2} m_V^2 V_\mu V^\mu + \frac{1}{4}\lambda_V (V_\mu V^\mu)^2 + \frac{1}{2}\lambda_{HV} H^\dagger H V_\mu V^\mu .$$

All invariant under ad hoc Z2 symmetry

arXiv:1112.3299, … 1402.6287, etc.

And Revived recent papers

We need to include dark Higgs or singlet scalar to get renormalizable/unitary models for Higgs portal singlet fermion or vector DM

[NB: UV Completions : Not unique]

$m_h = 125$ GeV. Shown also are the prospects for XENON upgrades.

FIG. 2. Same as Fig. 1 for vector DM particles.

FIG. 3. Same as in Fig.1 for fermion DM; λ_{hff}/Λ is in GeV

Models for HP SFDM & VDM

UV Completion of HP Singlet Fermion DM (SFDM)

$$\begin{aligned}\mathcal{L} &= \mathcal{L}_{\rm SM} - \mu_{HS} S H^\dagger H - \frac{\lambda_{HS}}{2} S^2 H^\dagger H \\ &+ \frac{1}{2}(\partial_\mu S \partial^\mu S - m_S^2 S^2) - \mu_S^3 S - \frac{\mu_S'}{3} S^3 - \frac{\lambda_S}{4} S^4 \\ &+ \overline{\psi}(i \not{\partial} - m_{\psi_0})\psi - \lambda S \overline{\psi}\psi\end{aligned}$$

UV Completion of HP VDM

$$\begin{aligned}\mathcal{L}_{VDM} &= -\frac{1}{4} X_{\mu\nu} X^{\mu\nu} + (D_\mu \Phi)^\dagger (D^\mu \Phi) - \frac{\lambda_\Phi}{4}\left(\Phi^\dagger\Phi - \frac{v_\Phi^2}{2}\right)^2 \\ &\quad -\lambda_{H\Phi}\left(H^\dagger H - \frac{v_H^2}{2}\right)\left(\Phi^\dagger\Phi - \frac{v_\Phi^2}{2}\right) ,\end{aligned}$$

- **The simplest UV completions in terms of # of new d.o.f.**
- **At least, 2 more parameters, (m_ϕ , $\sin\alpha$) for DM physics**

UV Completion for HP FDM

Baek, Ko, Park, arXiv:1112.1847

$$\begin{aligned}\mathcal{L} &= \mathcal{L}_{\rm SM} - \mu_{HS} S H^\dagger H - \frac{\lambda_{HS}}{2} S^2 H^\dagger H \\ &+ \frac{1}{2}(\partial_\mu S \partial^\mu S - m_S^2 S^2) - \mu_S^3 S - \frac{\mu_S'}{3} S^3 - \frac{\lambda_S}{4} S^4 \\ &+ \overline{\psi}(i \not{\partial} - m_{\psi_0})\psi - \lambda S \overline{\psi}\psi\end{aligned}$$

mixing

invisible decay

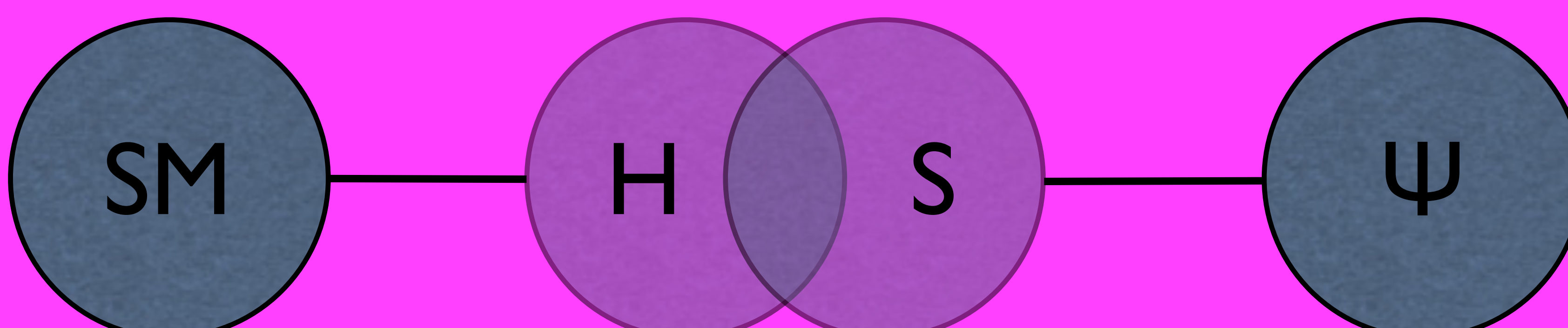

Production and decay rates are suppressed relative to SM.

Higgs-Singlet Mixing

- Mixing and Eigenstates of Higgs-like bosons

$$\mu_H^2 = \lambda_H v_H^2 + \mu_{HS} v_S + \frac{1}{2}\lambda_{HS} v_S^2,$$
$$m_S^2 = -\frac{\mu_S^3}{v_S} - \mu_S' v_S - \lambda_S v_S^2 - \frac{\mu_{HS} v_H^2}{2 v_S} - \frac{1}{2}\lambda_{HS} v_H^2,$$

at vacuum

$$M^2_{\rm Higgs} \equiv \begin{pmatrix} m^2_{hh} & m^2_{hs} \\ m^2_{hs} & m^2_{ss} \end{pmatrix} \equiv \begin{pmatrix} \cos\alpha & \sin\alpha \\ -\sin\alpha & \cos\alpha \end{pmatrix} \begin{pmatrix} m_1^2 & 0 \\ 0 & m_2^2 \end{pmatrix} \begin{pmatrix} \cos\alpha & -\sin\alpha \\ \sin\alpha & \cos\alpha \end{pmatrix}$$

$$H_1 = h\cos\alpha - s\sin\alpha,$$
$$H_2 = h\sin\alpha + s\cos\alpha.$$

Mixing of Higgs and singlet

Constraints

- Dark matter to nucleon cross section (constraint)

$$\sigma_p \approx \frac{1}{\pi}\mu^2\lambda_p^2 \simeq 2.7\times 10^{-2}\frac{m_p^2}{\pi}\left|\left(\frac{m_p}{v}\right)\lambda \sin\alpha\cos\alpha\left(\frac{1}{m_1^2}-\frac{1}{m_2^2}\right)\right|^2$$

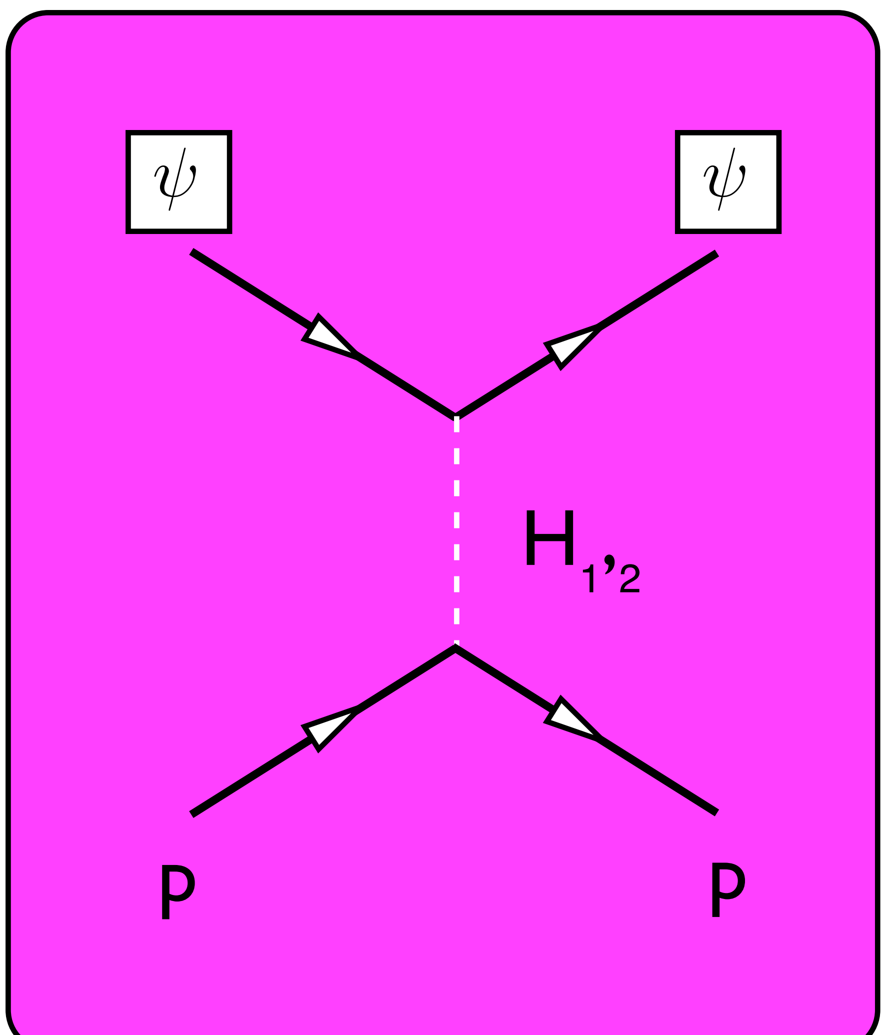

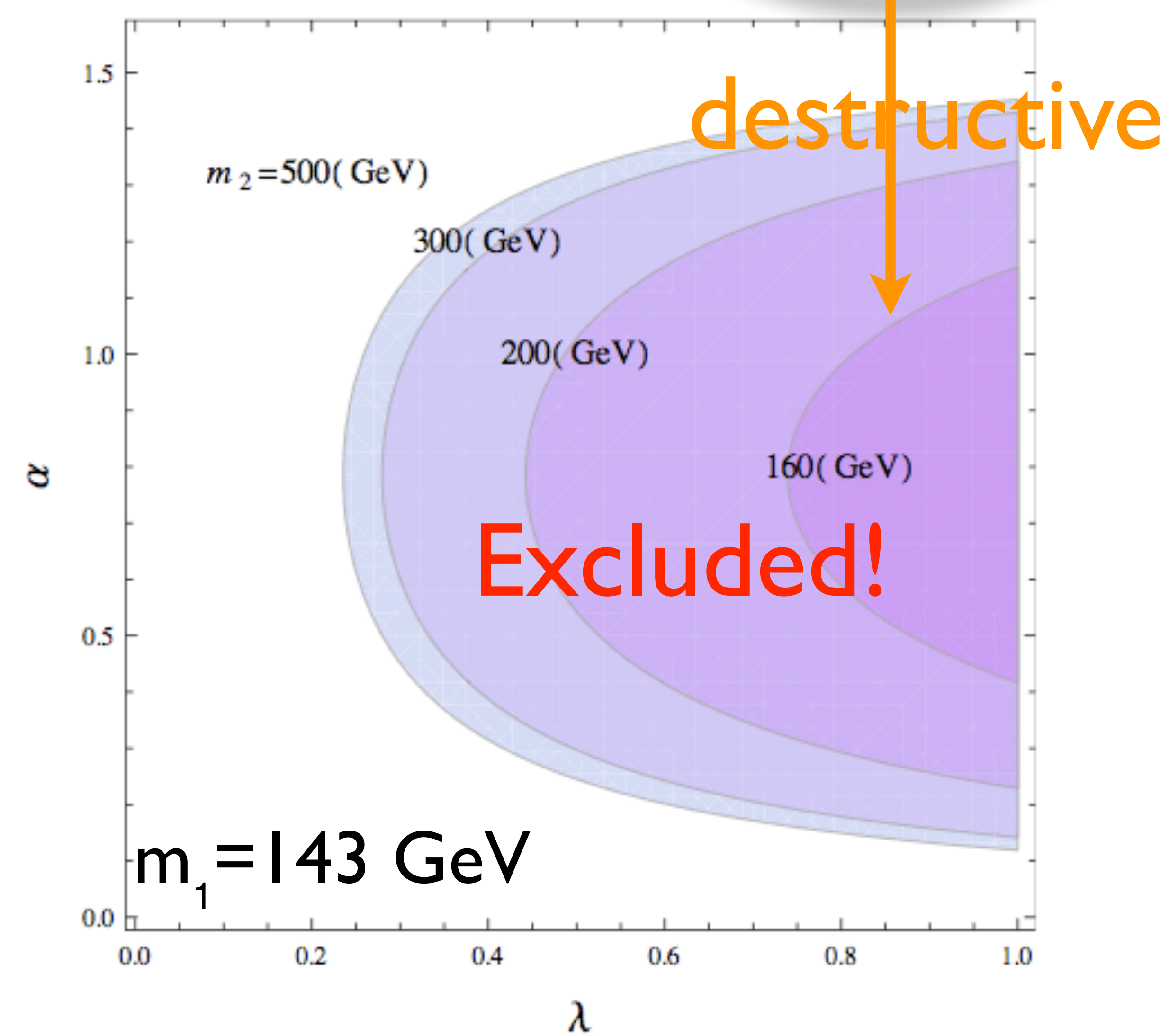

Low energy pheno.

- Universal suppression of collider SM signals

[See 1112.1847, Seungwon Baek, P. Ko & WIP]

- If "$m_h > 2\, m_\phi$", non-SM Higgs decay!

- Tree-level shift of $\lambda_{H,SM}$ (& loop correction)

$$\lambda_{\Phi H} \Rightarrow \lambda_H = \left[1 + \left(\frac{m_\phi^2}{m_h^2} - 1\right)\sin^2\alpha\right]\lambda_H^{SM}$$

If "$m_\phi > m_h$", vacuum instability can be cured.

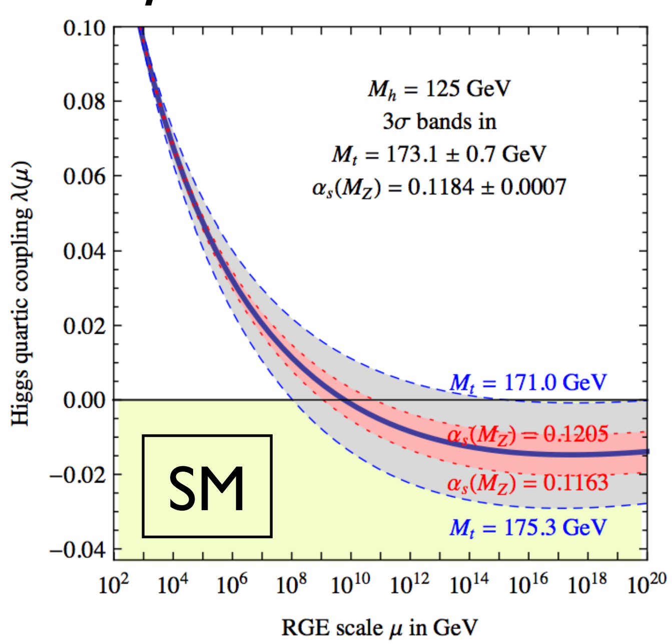

[G. Degrassi et al., 1205.6497]

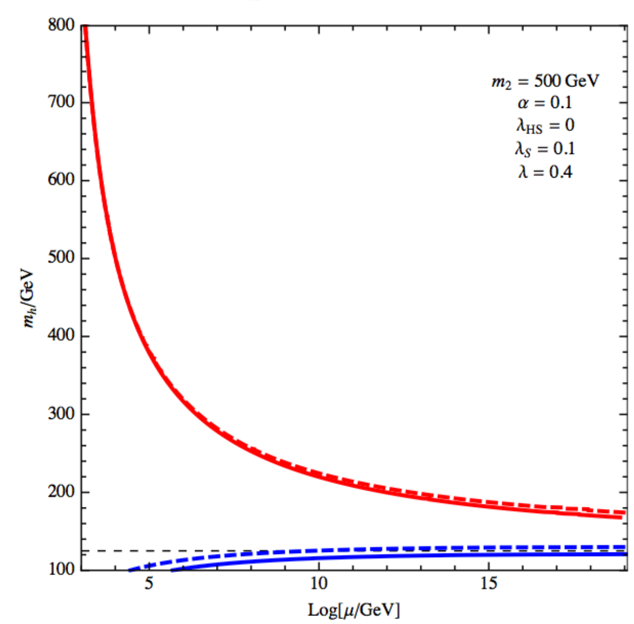

[S. Baek, P. Ko, WIP & E. Senaha, JHEP(2012)]

UV Completion of HP VDM

[S Baek, P Ko, WI Park, E Senaha, arXiv:1212.2131 (JHEP)]

$$\mathcal{L}_{VDM} = -\frac{1}{4}X_{\mu\nu}X^{\mu\nu} + (D_\mu\Phi)^\dagger(D^\mu\Phi) - \frac{\lambda_\Phi}{4}\left(\Phi^\dagger\Phi - \frac{v_\Phi^2}{2}\right)^2 - \lambda_{H\Phi}\left(H^\dagger H - \frac{v_H^2}{2}\right)\left(\Phi^\dagger\Phi - \frac{v_\Phi^2}{2}\right) ,$$

$X_\mu \equiv V_\mu$ here

$$\Phi(x) = (v_\phi + \phi(x))/\sqrt{2}$$

- There appear a new singlet scalar (dark Higgs) $\phi(x)$ from $\Phi(x)$, which mixes with the SM Higgs boson through Higgs portal interaction ($\lambda_{H\Phi}$ term)
- The effects must be similar to the singlet scalar in the fermion CDM model, and generically true in the DM with dark gauge symmetry
- Can accommodate GeV scale gamma ray excess from GC with $VV \to \phi\phi$
- **Can modify the Higgs inflation : No tight correlation with top mass**

New scalar (Dark Higgs) improves EW vacuum stability

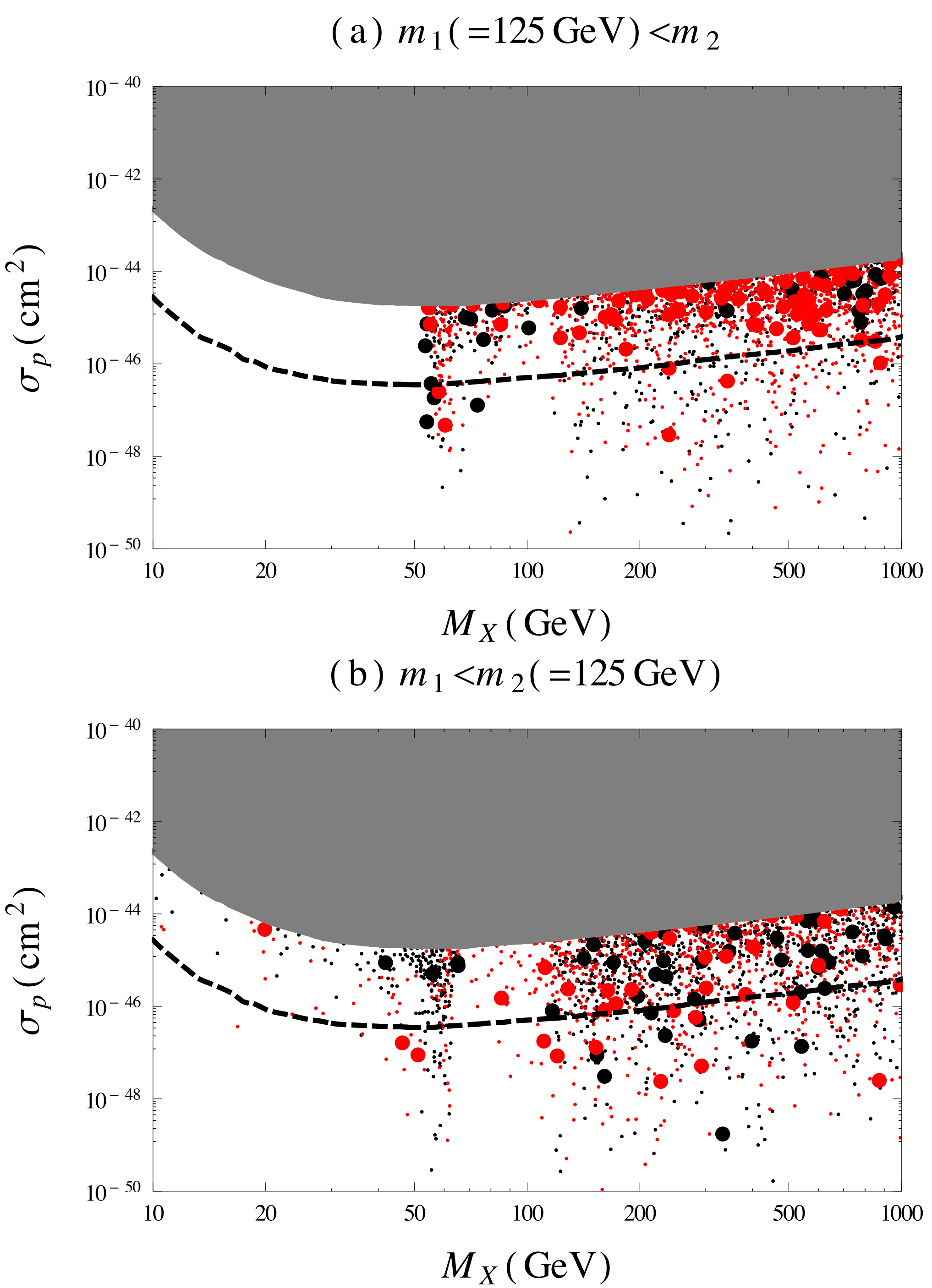

Figure 6. The scattered plot of σ_p as a function of M_X. The big (small) points (do not) satisfy the WMAP relic density constraint within 3 σ, while the red-(black-)colored points gives $r_1 > 0.7 (r_1 < 0.7)$. The grey region is excluded by the XENON100 experiment. The dashed line denotes the sensitivity of the next XENON experiment, XENON1T.

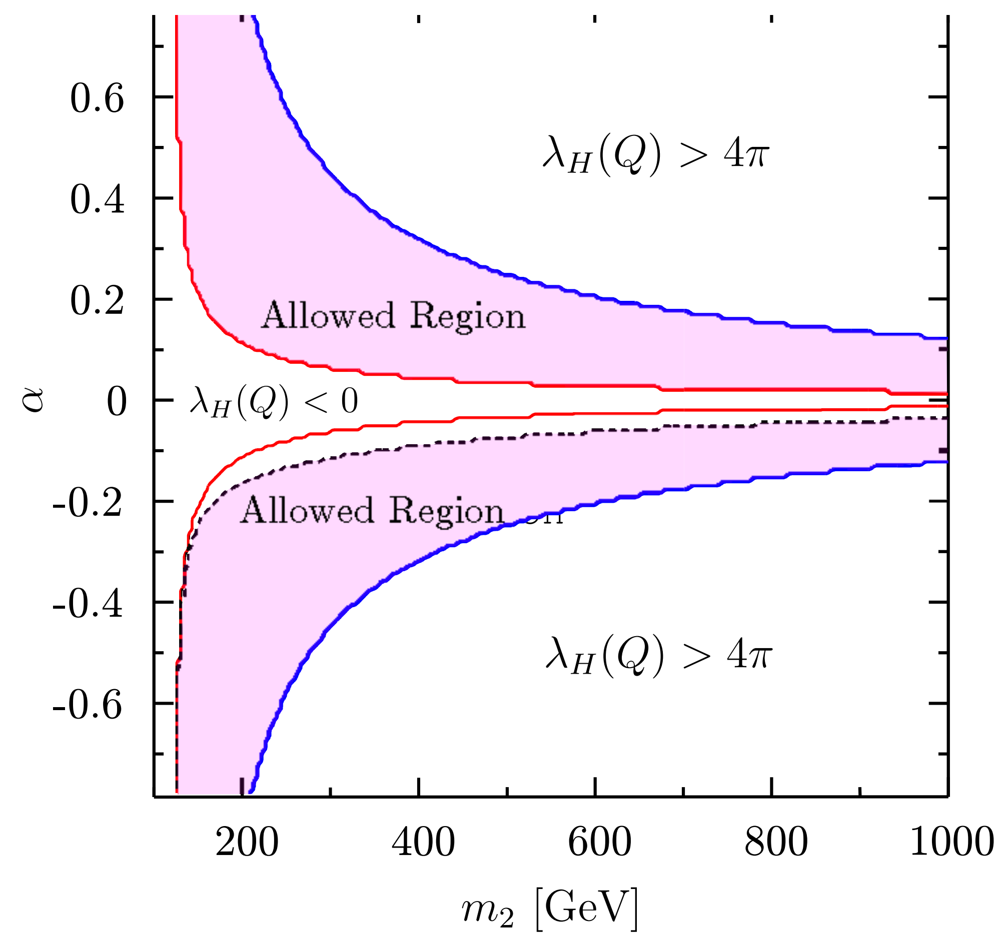

Figure 8. The vacuum stability and perturbativity constraints in the α-m_2 plane. We take $m_1 = 125$ GeV, $g_X = 0.05$, $M_X = m_2/2$ and $v_\Phi = M_X/(g_X Q_\Phi)$.

Interaction Lagrangians

Scalar DM

$$\mathcal{L}^{\rm int}_{\rm SDM} = -h\ \left(\frac{2m_W^2}{v_h} W^+_\mu W^{-\mu} + \frac{m_Z^2}{v_h} Z_\mu Z^\mu\right) - \lambda_{HS} v_h\ hS^2 .$$

Singlet FDM

$$\mathcal{L}^{\rm int}_{\rm FDM} = -\left(H_1 \cos\alpha + H_2 \sin\alpha\right) \left(\sum_f \frac{m_f}{v_h} \bar{f} f - \frac{2m_W^2}{v_h} W^+_\mu W^{-\mu} - \frac{m_Z^2}{v_h} Z_\mu Z^\mu\right) + g_\chi \left(H_1 \sin\alpha - H_2 \cos\alpha\right)\ \bar{\chi}\chi\ .$$

Vector DM

$$\mathcal{L}^{\rm int}_{\rm VDM} = -\left(H_1 \cos\alpha + H_2 \sin\alpha\right) \left(\sum_f \frac{m_f}{v_h} \bar{f} f - \frac{2m_W^2}{v_h} W^+_\mu W^{-\mu} - \frac{m_Z^2}{v_h} Z_\mu Z^\mu\right) - \frac{1}{2} g_V m_V \left(H_1 \sin\alpha - H_2 \cos\alpha\right)\ V_\mu V^\mu\ .$$

NB: One can not ignore 125 GeV Higgs Boson or singlet scalar by hand : Not Well defined EFT, Breaks gauge invariance, etc.

Collider Implications

$m_h = 125\text{GeV},\ \text{Br}(H \to \text{inv}) < 0.51$ at 90% CL

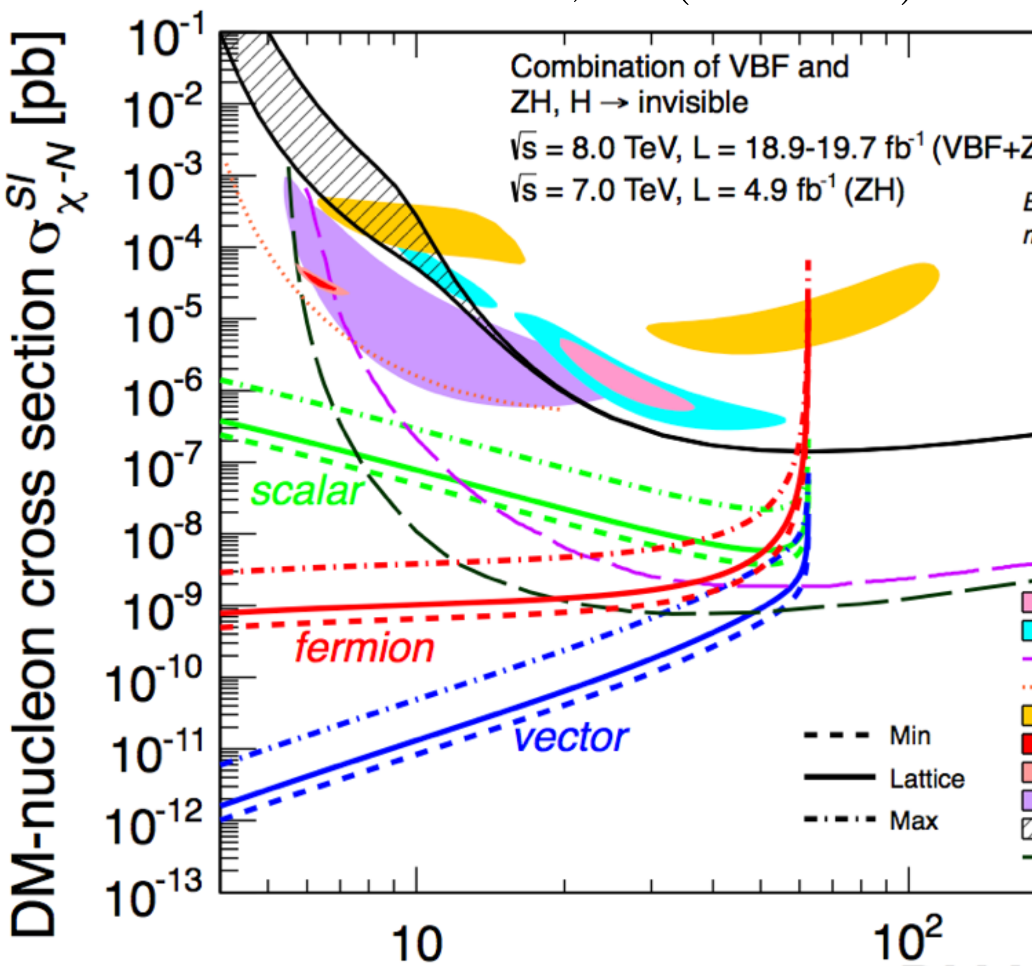

[arXiv:1404.1344]

Based on EFTs

$m_h = 125.5\text{GeV},\ \text{Br}(H \to \text{inv}) < 0.52$ at 90% CL

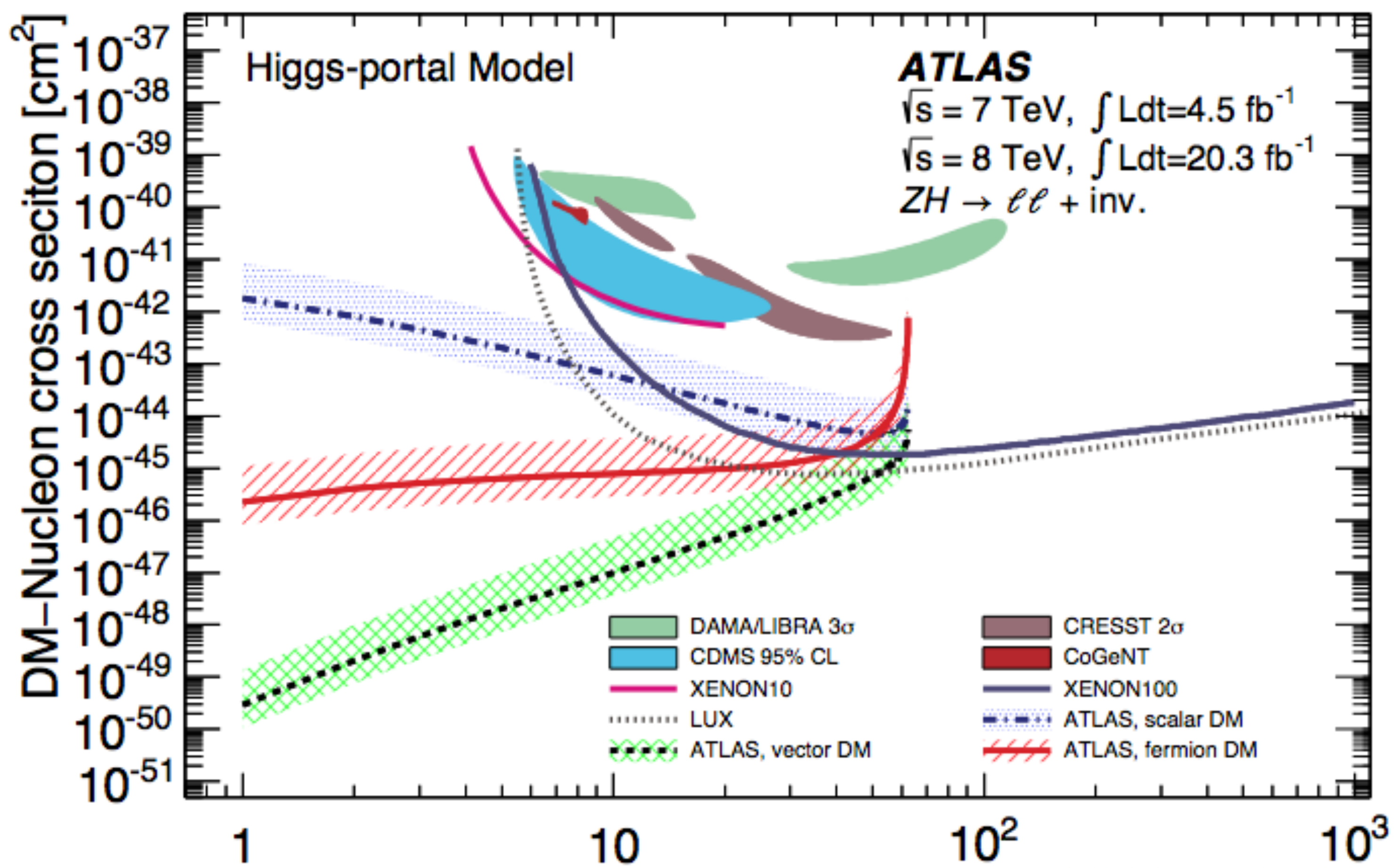

[arXiv:1402.3244]

- However, in renormalizable unitary models of Higgs portals, 2 more relevant parameters !

[arXiv: 1405.3530, S. Baek, P. Ko & WIPark, PRD]

$$\mathcal{L}_{\rm SFDM} = \overline{\psi}(i\partial - m_\psi - \lambda_\psi S) - \mu_{HS} S H^\dagger H - \frac{\lambda_{HS}}{2} S^2 H^\dagger H + \frac{1}{2}\partial_\mu S \partial^\mu S - \frac{1}{2} m_S^2 S^2 - \mu_S^3 S - \frac{\mu_S'}{3} S^3 - \frac{\lambda_S}{4} S^4.$$

$$\sigma_p^{\rm SI} = (\sigma_p^{\rm SI})_{\rm EFT}\, c_\alpha^4 m_h^4 \mathcal{F}(m_{\rm DM}, \{m_i\}, v) \simeq (\sigma_p^{\rm SI})_{\rm EFT}\, c_\alpha^4 \left(1 - \frac{m_h^2}{m_2^2}\right)^2$$

$$\mathcal{L}_{\rm VDM} = -\frac{1}{4} V_{\mu\nu} V^{\mu\nu} + D_\mu \Phi^\dagger D^\mu \Phi - \lambda_\Phi \left(\Phi^\dagger \Phi - \frac{v_\Phi^2}{2}\right)^2 - \lambda_{\Phi H} \left(\Phi^\dagger \Phi - \frac{v_\Phi^2}{2}\right)\left(H^\dagger H - \frac{v_H^2}{2}\right)$$

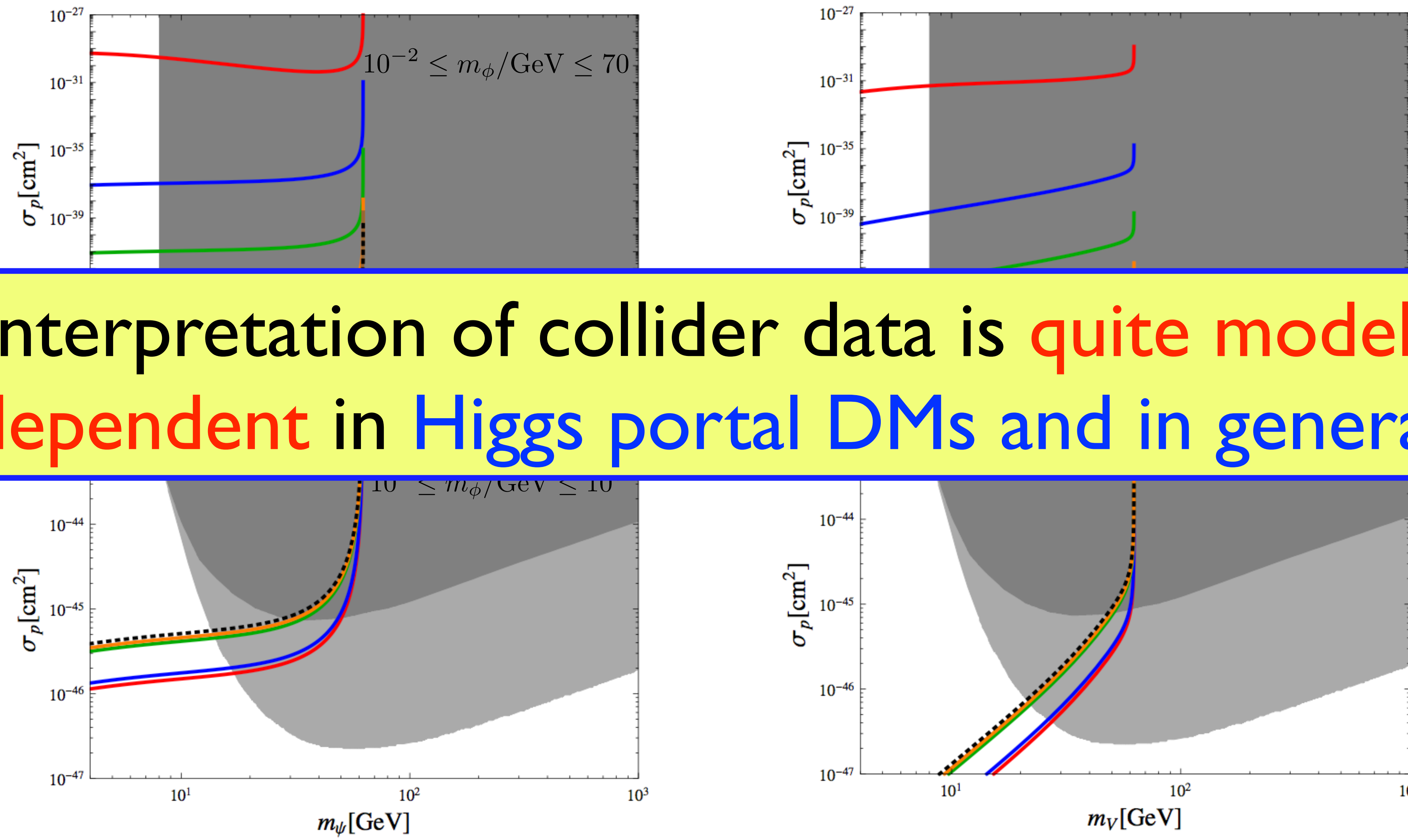

Dashed curve ATLAS,CMS

Interpretation of collider data is quite model-dependent in Higgs portal DMs and in general

- However, in renormalizable unitary models of Higgs portals, 2 more relevant parameters !

[arXiv: 1405.3530, S. Baek, P. Ko & WIPark, PRD]

$$\mathcal{L}_{\rm SFDM} = \overline{\psi}\left(i\partial\!\!\!/ - m_\psi - \lambda_\psi S\right) - \mu_{HS} S H^\dagger H - \frac{\lambda_{HS}}{2} S^2 H^\dagger H + \frac{1}{2}\partial_\mu S \partial^\mu S - \frac{1}{2} m_S^2 S^2 - \mu_S^3 S - \frac{\mu_S^{'}}{3} S^3 - \frac{\lambda_S}{4} S^4.$$

$$\mathcal{L}_{\rm VDM} = -\frac{1}{4} V_{\mu\nu} V^{\mu\nu} + D_\mu \Phi^\dagger D^\mu \Phi - \lambda_\Phi \left(\Phi^\dagger \Phi - \frac{v_\Phi^2}{2}\right)^2 - \lambda_{\Phi H}\left(\Phi^\dagger \Phi - \frac{v_\Phi^2}{2}\right)\left(H^\dagger H - \frac{v_H^2}{2}\right)$$

$$\begin{aligned}\sigma_p^{\rm SI} &= (\sigma_p^{\rm SI})_{\rm EFT}\; c_\alpha^4 m_h^4 \mathcal{F}(m_{\rm DM}, \{m_i\}, v) \\ &\simeq (\sigma_p^{\rm SI})_{\rm EFT}\; c_\alpha^4 \left(1 - \frac{m_h^2}{m_2^2}\right)^2\end{aligned}$$

Dashed curves:EFT, ATLAS,CMS results

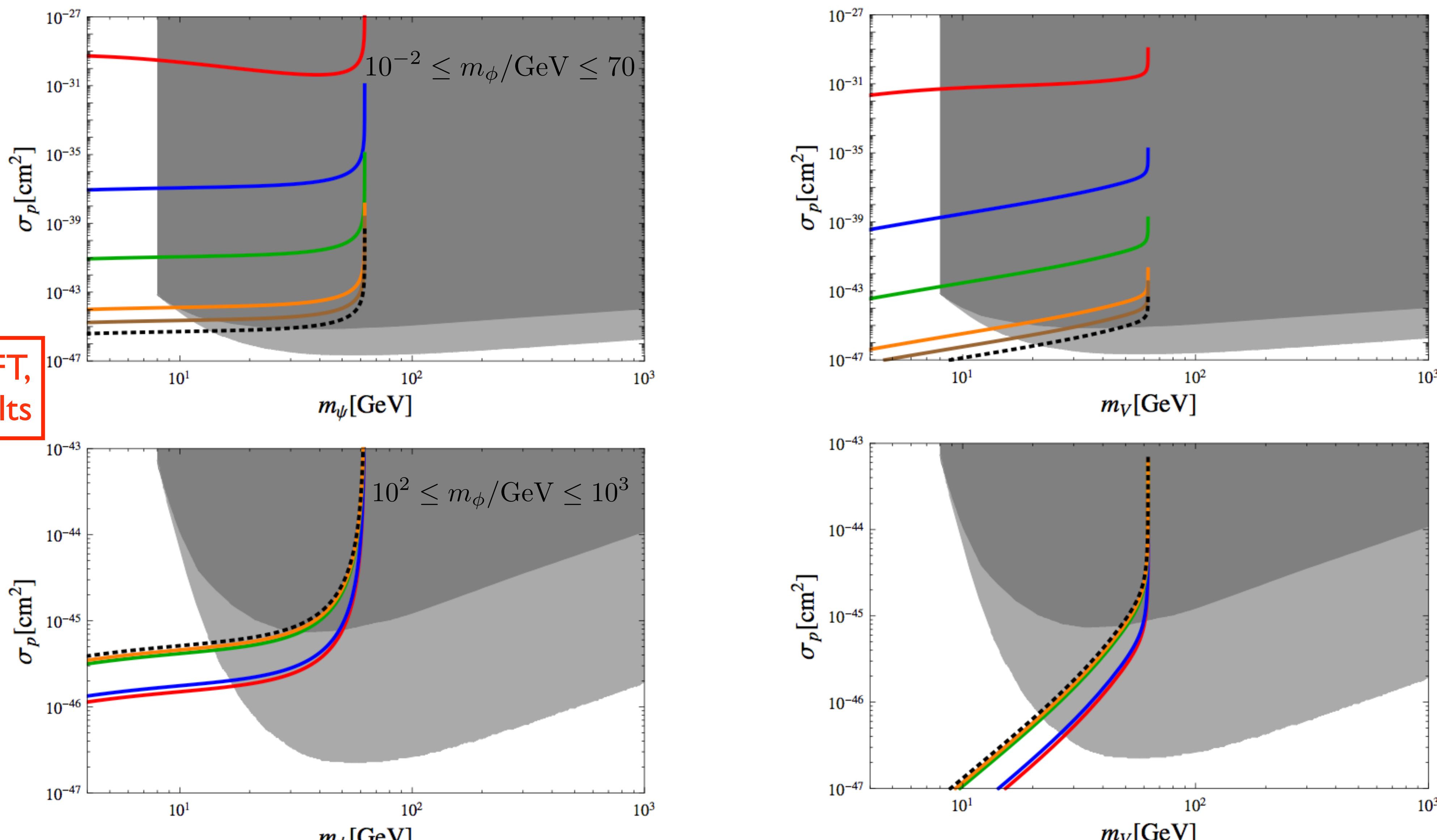

Invisible H decay into a pair of VDM

[arXiv: 1405.3530, S. Baek, P. Ko & WIPark, PRD]

$$(\Gamma_h^{\rm inv})_{\rm EFT} = \frac{\lambda_{VH}^2}{128\pi} \frac{v_H^2 m_h^3}{m_V^4} \times \left(1 - \frac{4m_V^2}{m_h^2} + 12\frac{m_V^4}{m_h^4}\right)\left(1 - \frac{4m_V^2}{m_h^2}\right)^{1/2} \quad (23)$$

Diverge when $m_V \to 0$!!

$$m_V \propto g_x Q_\Phi v_\Phi$$

$$\frac{g_X^2}{m_V^2} = \frac{g_X^2}{g_X^2 Q_\Phi^2 v_\Phi^2} \to \frac{1}{v_\Phi^2} = \text{finite}$$

VS.

$$\Gamma_i^{\rm inv} = \frac{g_X^2}{32\pi} \frac{m_i^3}{m_V^2} \left(1 - \frac{4m_V^2}{m_i^2} + 12\frac{m_V^4}{m_i^4}\right)\left(1 - \frac{4m_V^2}{m_i^2}\right)^{1/2} \sin^2\alpha \quad (22)$$

Invisible H decay width : finite for small mV in unitary/renormalizable model

Two Limits for $m_V \to 0$

Also see the addendum:
by S Baek, P Ko, WI Park

- $m_V = g_X Q_\Phi v_\Phi$ in the UV completion with dark Higgs boson

- Case I : $g_X \to 0$ with finite $v_\Phi \neq 0$

$$\frac{g_X^2 Q_\Phi^2}{m_V^2} = \frac{g_X^2 Q_\Phi^2}{g_X^2 Q_\Phi^2 v_\Phi^2} = \frac{1}{v_\Phi^2} = \text{finite.}$$

$$\left(\Gamma_h^{\rm inv}\right)_{\rm UV} = \frac{1}{32\pi} \frac{m_h^3}{v_\Phi^2} \sin^2\alpha = \Gamma(h \to a_\Phi a_\Phi)$$

with a_Φ being the NG boson for spontaneously broken global $U(1)_X$

- Case II : $v_\Phi \to 0$ with finite $g_X \neq 0$

$$\alpha \xrightarrow{v_\Phi \to 0^+} \frac{2\lambda_{H\Phi} v_\Phi}{\lambda_H v_H}$$

$$\frac{g_X^2 Q_\Phi^2}{m_V^2} \sin^2\alpha \xrightarrow{v_\Phi \to 0^+} \frac{4\lambda_{H\Phi}^2}{\lambda_H^2 v_H^2} = \frac{2\lambda_{H\Phi}^2}{\lambda_H m_h^2} = \text{finite,}$$

$$\left(\Gamma_h^{\rm inv}\right)_{\rm UV} \xrightarrow{v_\Phi \to 0^+} \frac{1}{16\pi} \frac{\lambda_{H\Phi}^2 m_h}{\lambda_H}$$

Therefore $\Gamma(h \to VV)$ is finite when $m_V \to 0$ in the UV completions

S. Baek, P. Ko, M. Park, WIPark, C.Yu, arXiv:1506.06556, PLB (2016)

- EFT : Effective operator $\mathcal{L}_{int} = \frac{m_q}{\Lambda_{dd}^3}\bar{q}q\bar{\chi}\chi$
- S.M.: Simple scalar mediator S of
  $\mathcal{L}_{int} = \left(\frac{m_q}{v_H}\sin\alpha\right) S\bar{q}q - \lambda_s \cos\alpha S\bar{\chi}\chi$
- H.M.: A case where a Higgs is a mediator
  $\mathcal{L}_{int} = -\left(\frac{m_q}{v_H}\cos\alpha\right) H\bar{q}q - \lambda_s \sin\alpha H\bar{\chi}\chi$
- H.P.: Higgs portal model as in eq. (2).

$$\frac{d\sigma_i}{dm_{\chi\chi}} \propto \left|\frac{\sin 2\alpha\ g_\chi}{m_{\chi\chi}^2 - m_{H_1}^2 + i m_{H_1}\Gamma_{H_1}} - \frac{\sin 2\alpha\ g_\chi}{m_{\chi\chi}^2 - m_{H_2}^2 + i m_{H_2}\Gamma_{H_2}}\right|^2$$

$$\text{H.P.} \xrightarrow[m_{H_2}^2 \gg \hat{s}]{} \text{H.M.},$$

$$\text{S.M.} \xrightarrow[m_S^2 \gg \hat{s}]{} \text{EFT},$$

$$\text{H.M.} \neq \text{EFT}.$$

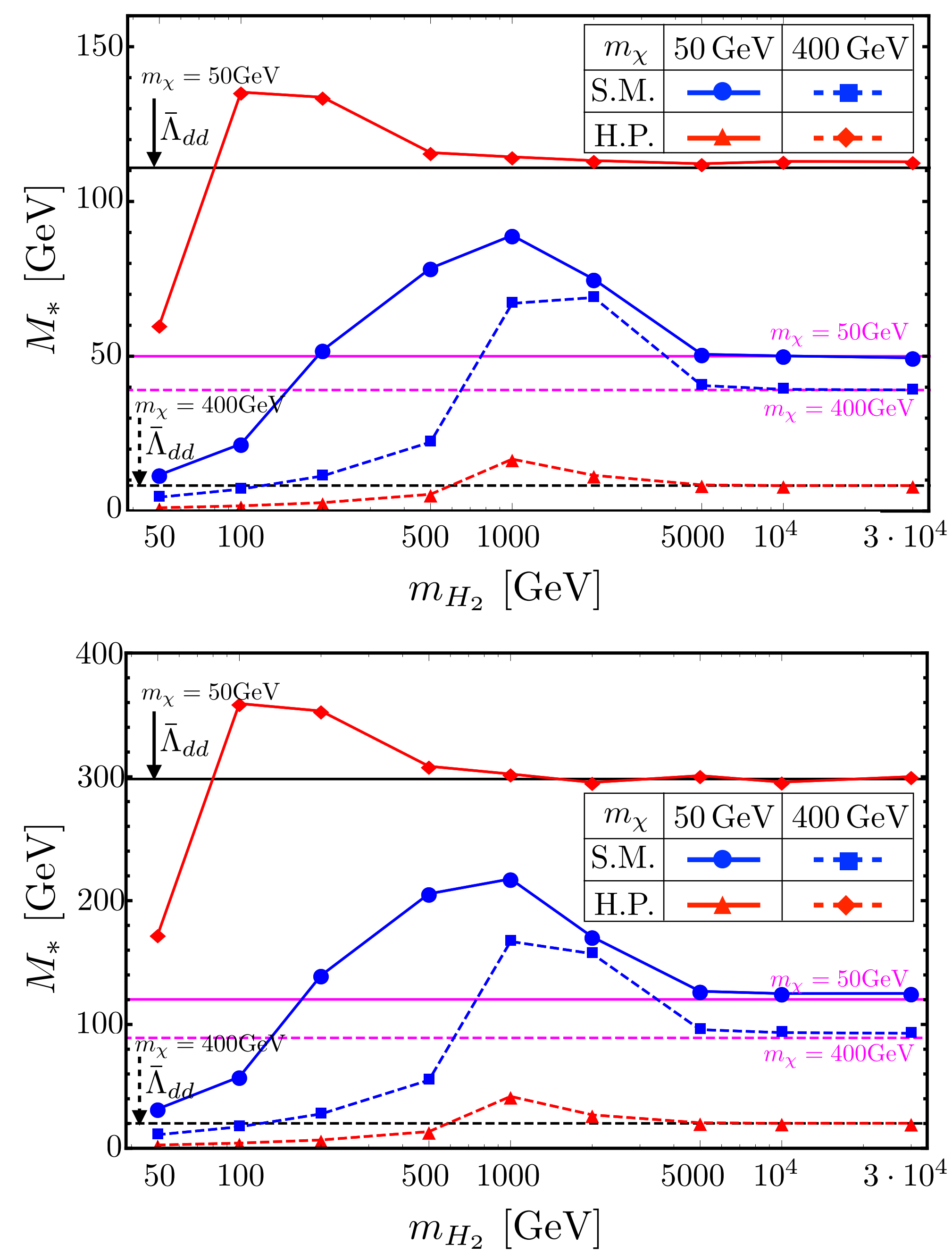

FIG. 3: The experimental bounds on M_* at 90% C.L. as a function of m_{H_2} (m_S in S.M. case) in the monojet+$\not{E}_T$ search (upper) and $t\bar{t} + \not{E}_T$ search (lower). Each line corresponds to the EFT approach (magenta), S.M. (blue), H.M. (black), and H.P. (red), respectively. The bound of S.M., H.M., and H.P., are expressed in terms of the effective mass M_* through the Eq.(16)-(20). The solid and dashed lines correspond to $m_\chi = 50$ GeV and 400 GeV in each model, respectively.

Fermi-LAT GC γ-ray

see arXiv:1612.05687 for a recent overview by C.Karwin, S. Murgia, T. Tait, T.A. Porter, P. Tanedo

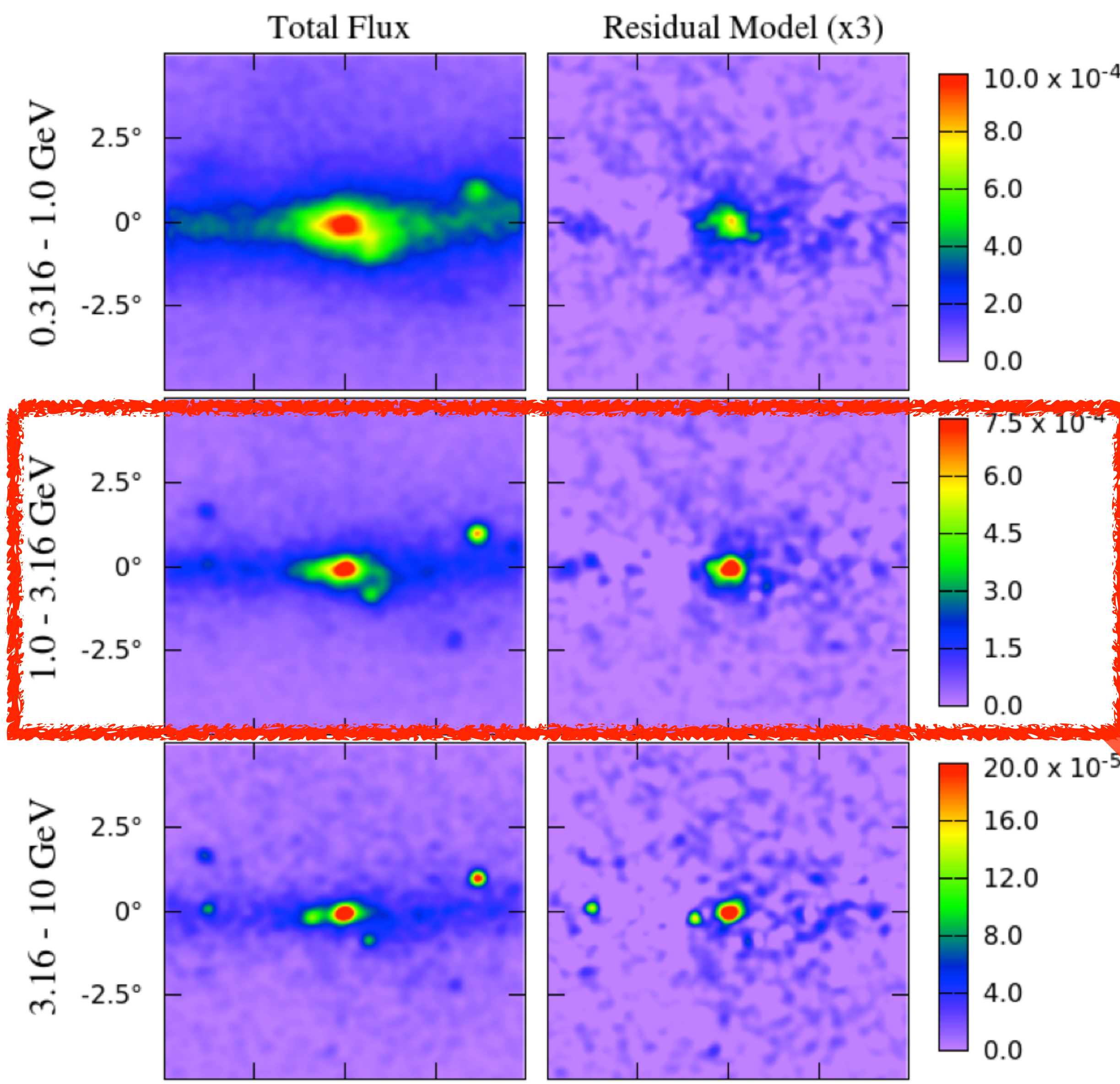

[1402.6703, T. Daylan et.al.]

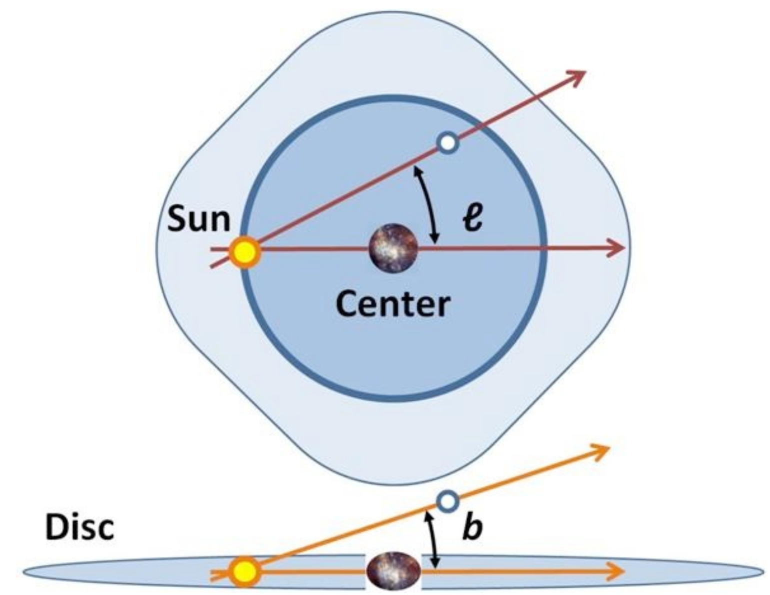

$$\mathrm{GC} : b \sim l \lesssim 0.1^\circ$$

extended

GeV scale excess!

• A DM interpretation

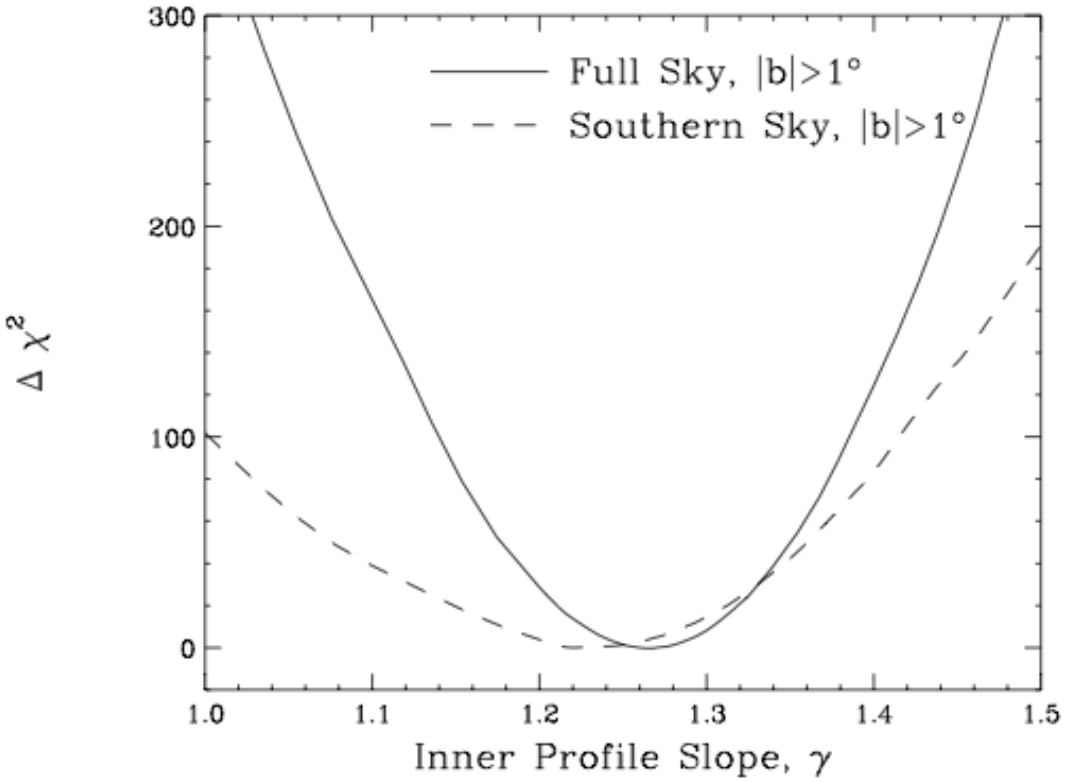

$\mathrm{DM} + \mathrm{DM} \to b\bar{b}$ with $\sigma v = 1.7 \times 10^{-26}\mathrm{cm}^3/\mathrm{s}$

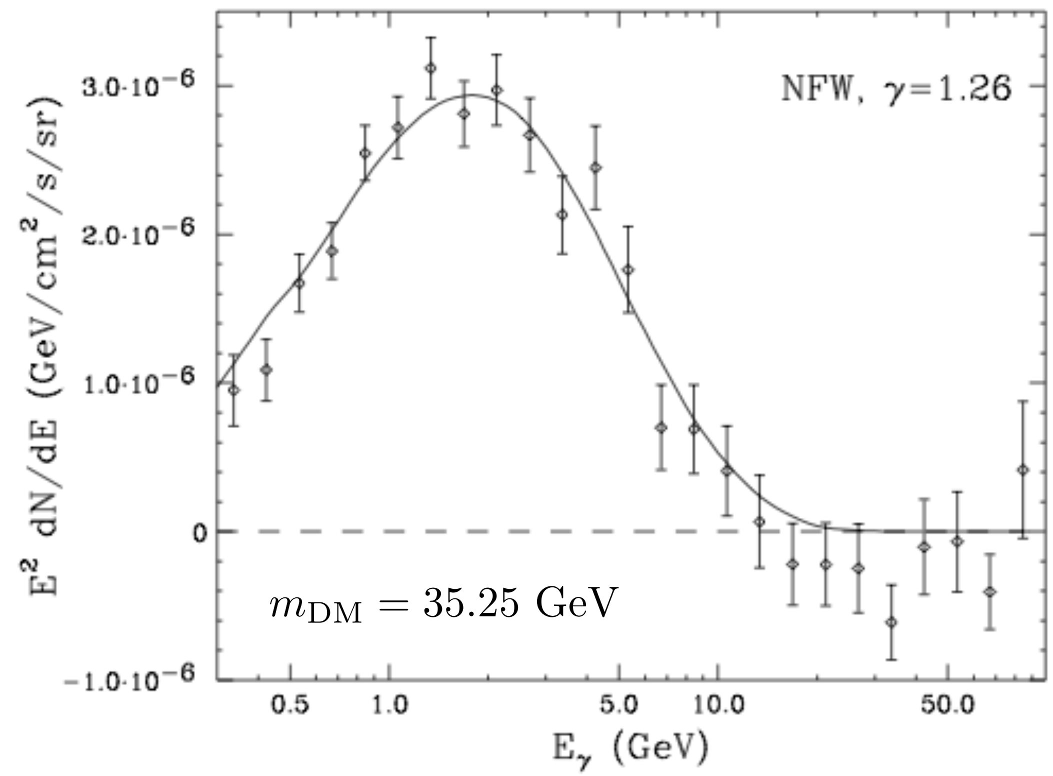

* See "1402.6703, T. Daylan et.al." for other possible channels

• Millisecond Pulars (astrophysical alternative)

It may or may not be the main source, depending on

- luminosity func.
- bulge population
- distribution of bulge population

* See "1404.2318, Q. Yuan & B. Zhang" and "1407.5625, I. Cholis, D. Hooper & T. Linden"

GC gamma ray in HP VDM

P. Ko, WI Park, Y. Tang. arXiv:1404.5257, JCAP

H2 : 125 GeV Higgs
H1 : absent in EFT

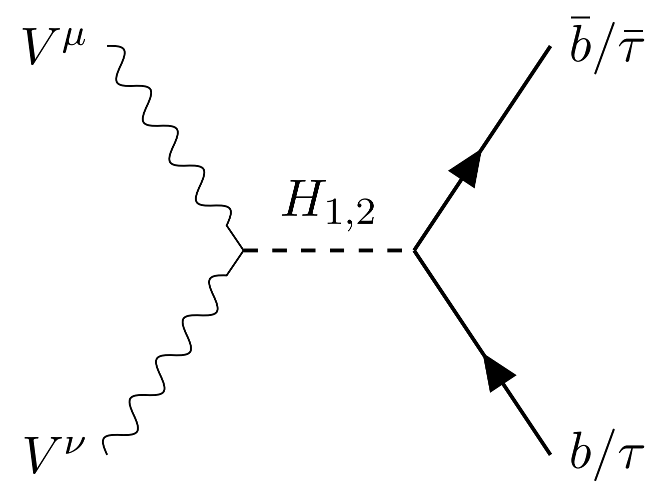

Figure 2. Dominant s channel $b + \bar{b}$ (and $\tau + \bar{\tau}$) production

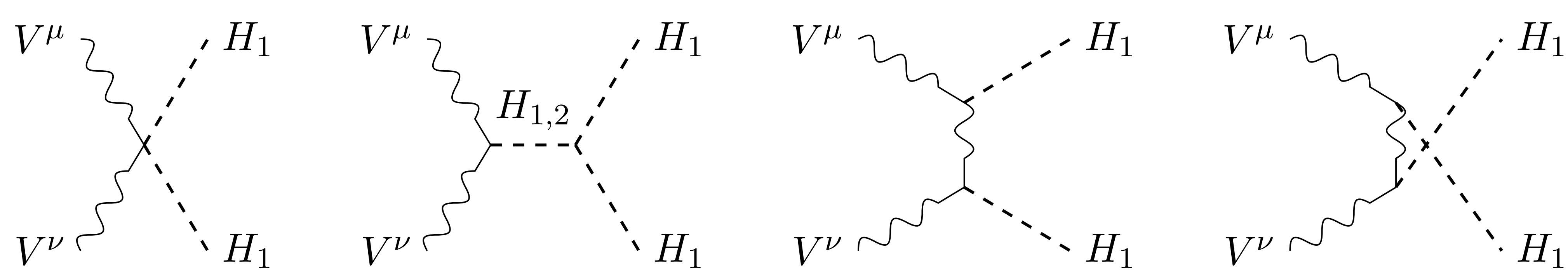

Figure 3. Dominant s/t-channel production of H_1s that decay dominantly to $b + \bar{b}$

Importance of HP VDM with Dark Higgs Boson

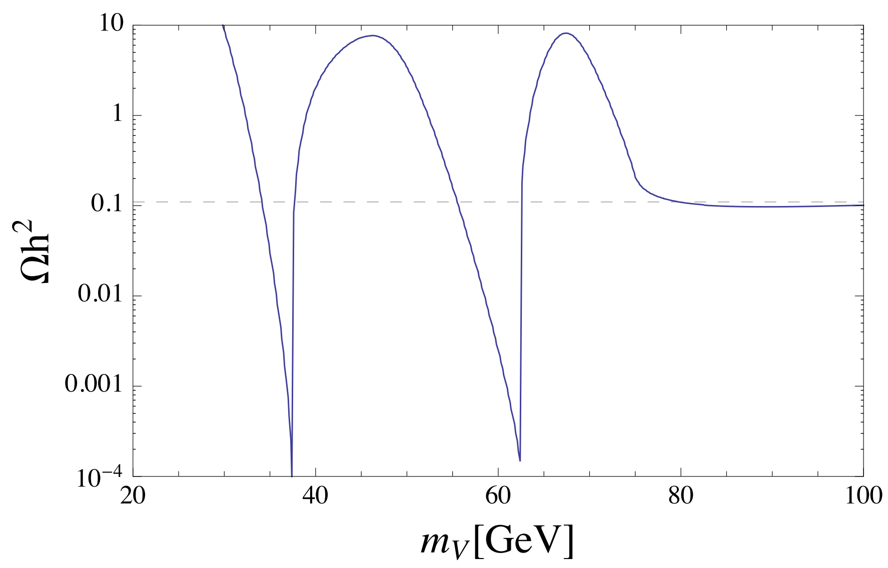

Figure 4. Relic density of dark matter as function of m_ψ for $m_h = 125$, $m_\phi = 75\,\text{GeV}$, $g_X = 0.2$, and $\alpha = 0.1$.

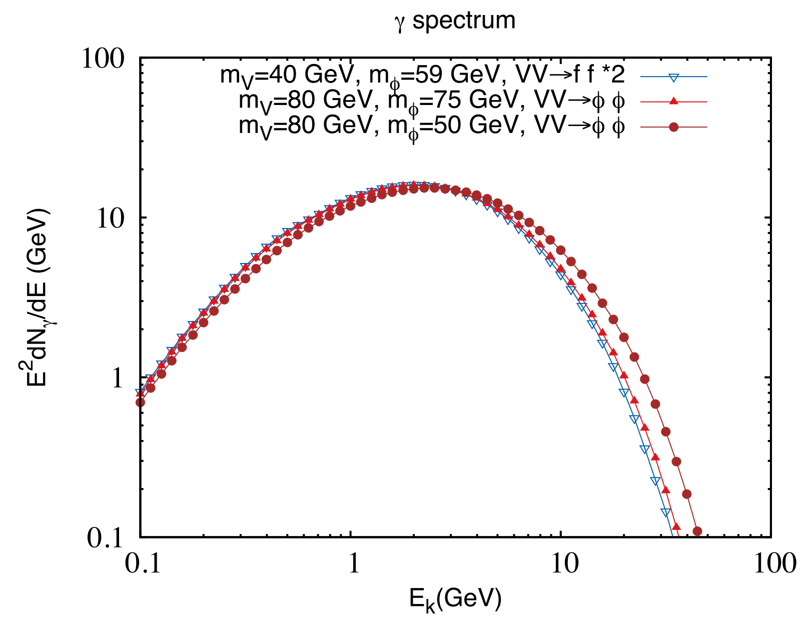

Figure 5. Illustration of γ spectra from different channels. The first two cases give almost the same spectra while in the third case γ is boosted so the spectrum is shifted to higher energy.

This mass range of VDM would have been impossible in the VDM model (EFT)

And No 2nd neutral scalar (Dark Higgs) in EFT

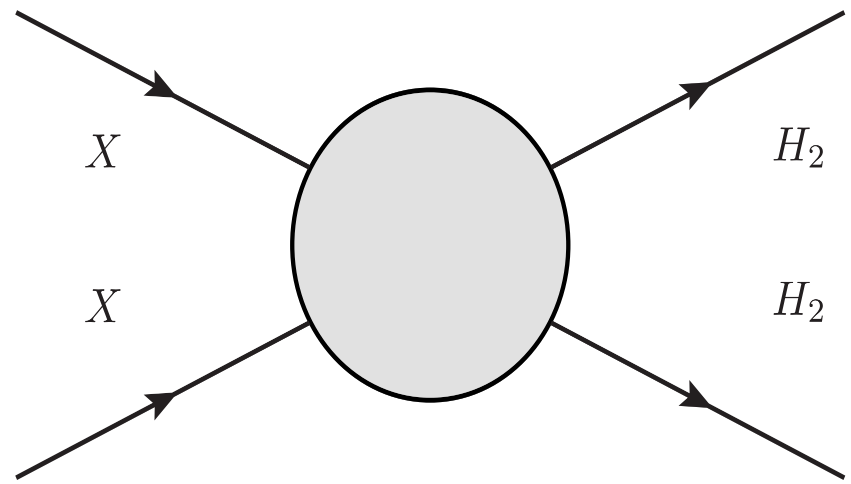

P.Ko, Yong Tang.
arXiv:1504.03908

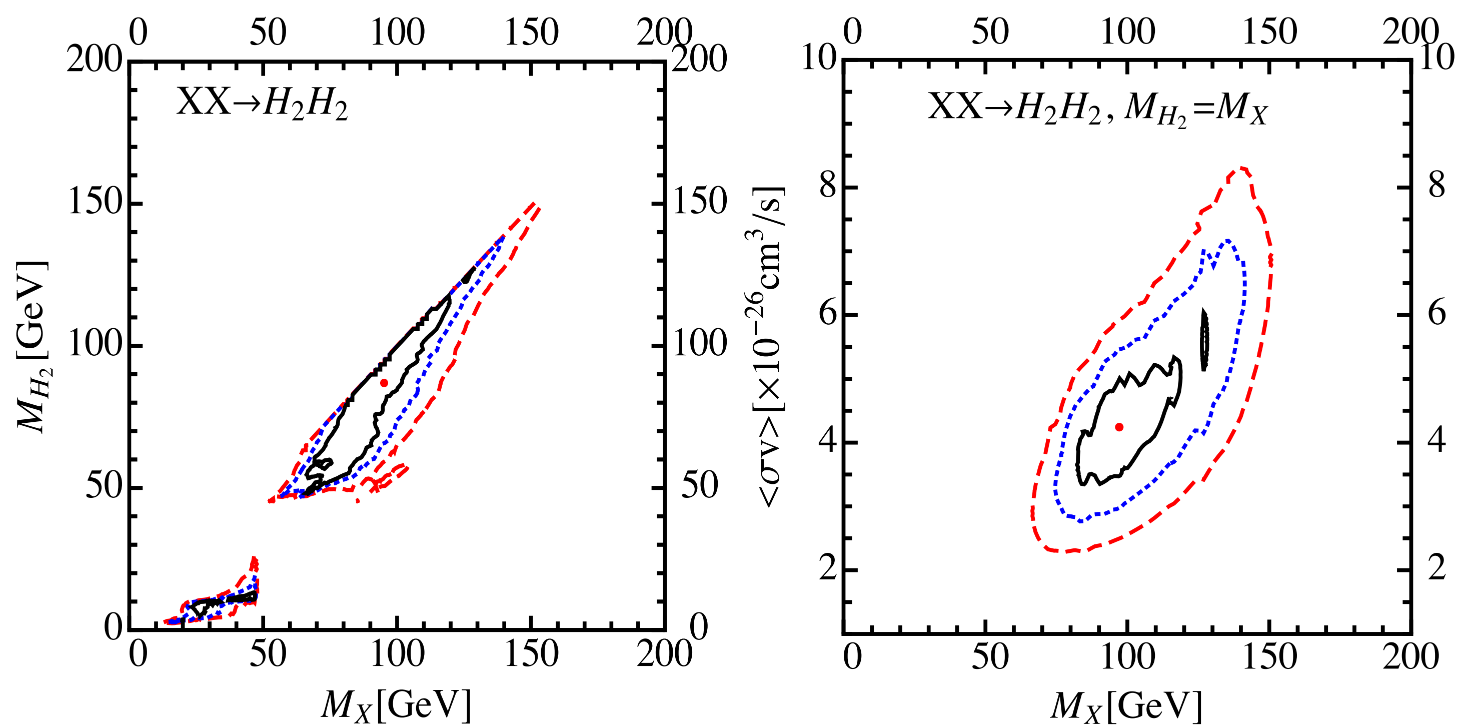

FIG. 3: The regions inside solid(black), dashed(blue) and long-dashed(red) contours correspond to 1σ, 2σ and 3σ, respectively. The red dots inside 1σ contours are the best-fit points. In the left panel, we vary freely M_X, M_{H_2} and $\langle\sigma v\rangle$. While in the right panel, we fix the mass of H_2, $M_{H_2} \simeq M_X$.

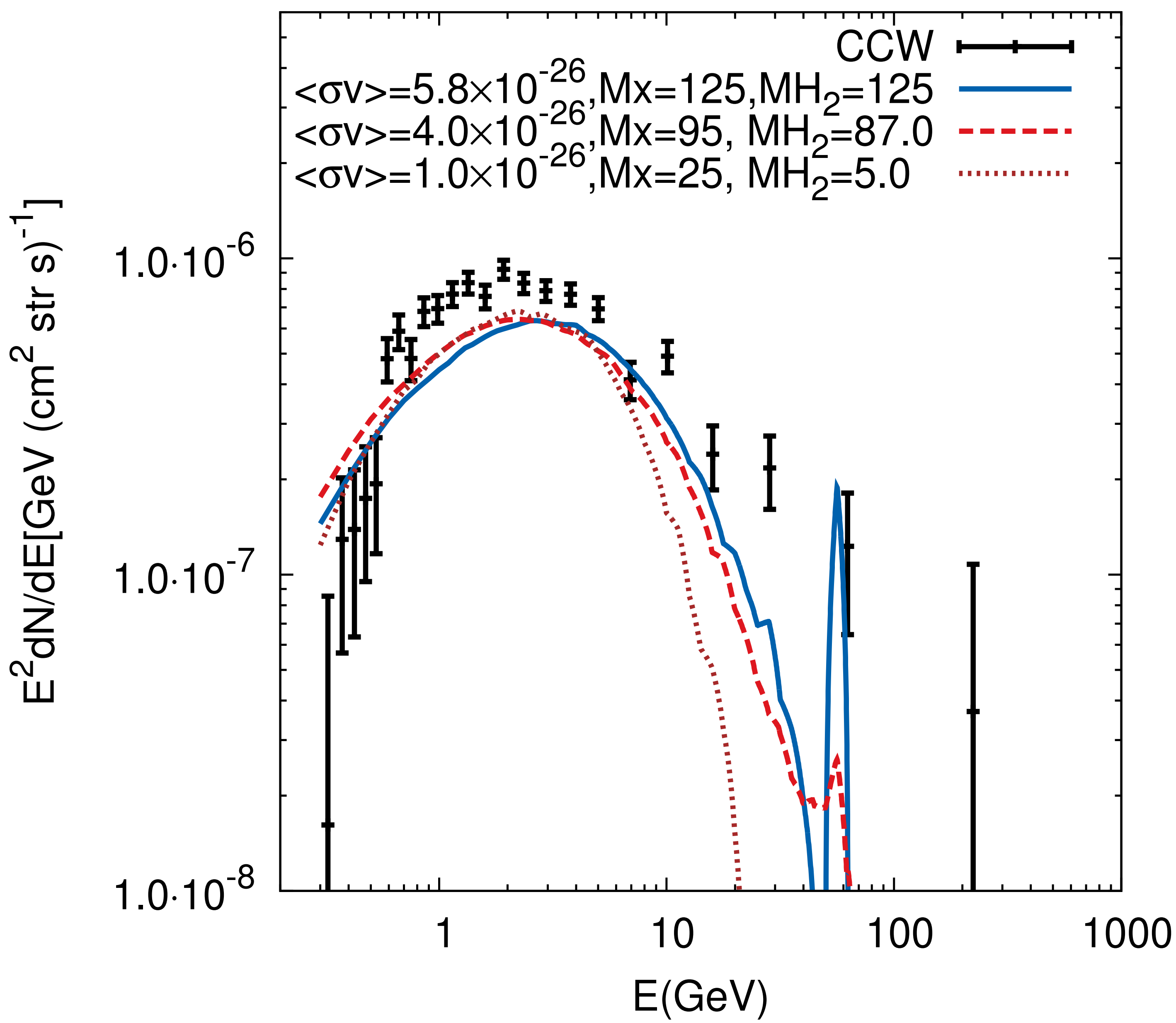

FIG. 2: Three illustrative cases for gamma-ray spectra in contrast with CCW data points [11]. All masses are in GeV unit and σv with cm^3/s. Line shape around $E \simeq M_{H_2}/2$ is due to decay modes, $H_2 \to \gamma\gamma, Z\gamma$.

This would have never been possible within the DM EFT

P.Ko, Yong Tang.
arXiv:1504.03908

Channels	Best-fit parameters	$\chi^2_{\rm min}/{\rm d.o.f.}$	p-value
$XX \to H_2H_2$ (with $M_{H_2} \neq M_X$)	$M_X \simeq 95.0{\rm GeV}, M_{H_2} \simeq 86.7{\rm GeV}$ $\langle\sigma v\rangle \simeq 4.0 \times 10^{-26}{\rm cm}^3/{\rm s}$	$22.0/21$	0.40
$XX \to H_2H_2$ (with $M_{H_2} = M_X$)	$M_X \simeq 97.1{\rm GeV}$ $\langle\sigma v\rangle \simeq 4.2 \times 10^{-26}{\rm cm}^3/{\rm s}$	$22.5/22$	0.43
$XX \to H_1H_1$ (with $M_{H_1} = 125{\rm GeV}$)	$M_X \simeq 125{\rm GeV}$ $\langle\sigma v\rangle \simeq 5.5 \times 10^{-26}{\rm cm}^3/{\rm s}$	$24.8/22$	0.30
$XX \to b\bar{b}$	$M_X \simeq 49.4{\rm GeV}$ $\langle\sigma v\rangle \simeq 1.75 \times 10^{-26}{\rm cm}^3/{\rm s}$	$24.4/22$	0.34

TABLE I: Summary table for the best fits with three different assumptions.

DM Production @ ILC

P Ko, H Yokoya, arXiv:1603.08802, JHEP

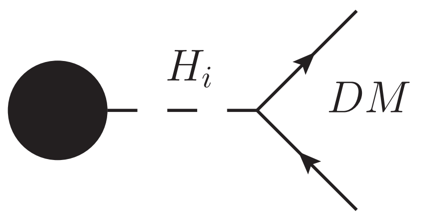

,

$$t \equiv m_{DD}^2$$

We consider $e^+e^- \to Z^* \to ZH_{i=1,2}$ followed by $H_i \to \bar{\chi}\chi$

$$\frac{d\sigma_{\rm SDM}}{dt} \propto \sigma^{h^*}_{\rm SDM} \times |\frac{1}{t - m_h^2 + i m_h \Gamma_h}|^2,$$

$$\frac{d\sigma_{\rm FDM}}{dt} \propto \sigma^{h^*}_{\rm FDM} \times |\frac{1}{t - m_{H_1}^2 + i m_{H_1}\Gamma_{H_1}} - \frac{1}{t - m_{H_2}^2 + i m_{H_2}\Gamma_{H_2}}|^2 \cdot \left(2t - 8m_\chi^2\right),$$

$$\frac{d\sigma_{\rm VDM}}{dt} \propto \sigma^{h^*}_{\rm VDM} \times |\frac{1}{t - m_{H_1}^2 + i m_{H_1}\Gamma_{H_1}} - \frac{1}{t - m_{H_2}^2 + i m_{H_2}\Gamma_{H_2}}|^2 \cdot \left(2 + \frac{(t - 2m_D^2)^2}{4m_V^4}\right).$$

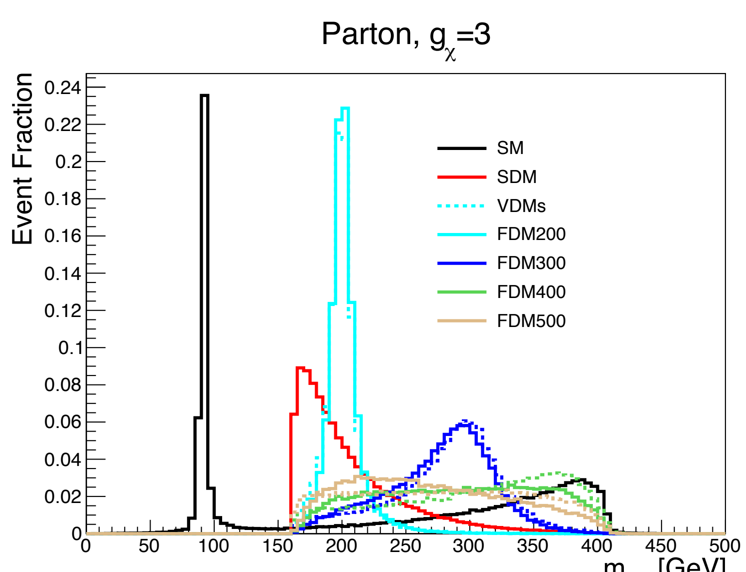

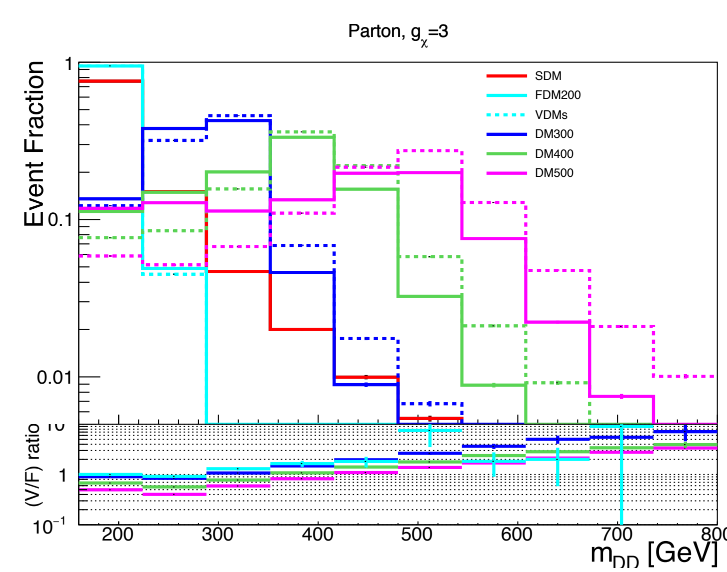

Fix DM mass = 80 GeV, sin(alpha) = 0.3, and vary H2 mass (200,300,400,500) GeV

Asymptotic behavior in the full theory ($t \equiv m_{\chi\chi}^2$)

$$\text{ScalarDM}: \quad G(t) \sim \frac{1}{(t-m_H^2)^2 + m_H^2\Gamma_H^2} \tag{5.7}$$

$$\text{SFDM}: \quad G(t) \sim \left| \frac{1}{t-m_1^2+im_1\Gamma_1} - \frac{1}{t-m_2^2+im_2\Gamma_2} \right|^2 \left(t-4m_\chi^2\right) \tag{5.8}$$

$$\rightarrow |\frac{1}{t^2}|^2 \times t \sim \frac{1}{t^3} \;(\text{as } t \rightarrow \infty) \tag{5.9}$$

$$\text{VDM}: \quad G(t) \sim \left| \frac{1}{t-m_1^2+im_1\Gamma_1} - \frac{1}{t-m_2^2+im_2\Gamma_2} \right|^2 \left[2 + \frac{(t-2m_V^2)^2}{4m_V^4}\right] \tag{5.10}$$

$$\rightarrow |\frac{1}{t^2}|^2 \times t^2 \sim \frac{1}{t^2} \;(\text{as } t \rightarrow \infty) \tag{5.11}$$

Asymptotic behavior w/o the 2nd Higgs (EFT)

$$\text{SFDM}: \quad G(t) \sim \frac{1}{(t-m_H^2)^2 + m_H^2\Gamma_H^2} \left(t-4m_\chi^2\right)$$

$$\rightarrow \frac{1}{t} \;(\text{as } t \rightarrow \infty)$$

$$\text{VDM}: \quad G(t) \sim \frac{1}{(t-m_H^2)^2 + m_H^2\Gamma_H^2} \left[2 + \frac{(t-2m_V^2)^2}{4m_V^4}\right]$$

$$\rightarrow \text{constant} \;(\text{as } t \rightarrow \infty)$$

Unitarity is violated in EFT!

Summary

- Phenomenology of HP VDM and Singlet FDM presented within EFT vs. UV completed models

- EFT approach has a number of drawbacks : non-renormalizable, unitarity violation at high energy colliders, and it applies only if $m_{DM}, m_{\rm SM} \ll m_\phi$ [But we don't know mass scales of dark particles !]

- In particular, one has $\Gamma_{\rm EFT}(H_{125} \to VV) \to \infty$, as $m_V \to 0$, whereas it is finite in UV completed models [Importance of gauge invariance, unitarity and renormalizability]

- The dark Higgs ϕ can play crucial roles in interpreting the DM signatures at colliders, explaining the GC γ-ray excess ($VV \to \phi\phi$), improving vacuum stability up to Planck scale, modifying the Higgs inflation [ϕ should be actively searched for !]

Inelastic DM and XENON1T Excess

We consider Both Scalar and Fermion IDM

arXiv:2006.16876, PLB 810 (2020) 135848
With Seungwon Baek, Jongkuk Kim

XENON1T Excess

- Excess between 1-7 keV
  - Expectated : 232 ± 15 , Observed : 285
  - Deviation ~ 3.5 σ
- Tritium contamination
  - Long half lifetime (12.3 years)
  - Abundant in atmosphere and cosmogenically produced in Xenon
- Solar axion
  - Produced in the Sun
  - Favored over bkgd @ 3.5 σ
- Neutrino magnetic dipole moment
  - Favored @ 3.2 σ

Electron recoil

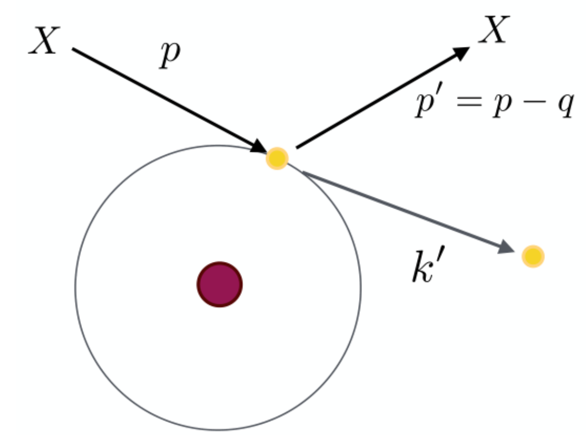

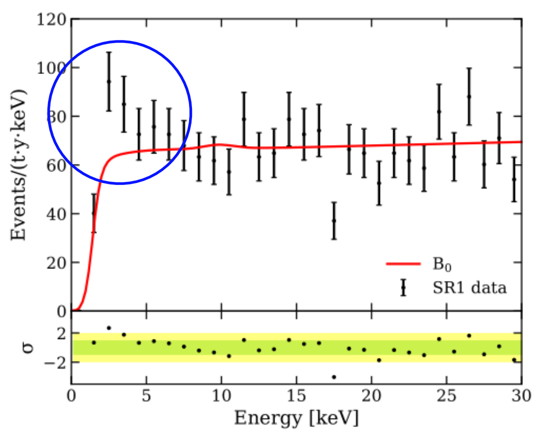

DD/CMB Constraints

- To evade stringent bounds from direct detection expt's : sub GeV DM

- CMB bound excludes thermal DM freeze-out determined by S-wave annihilation : DM annihiliation should be mainly in P-wave $\langle \sigma v \rangle \sim a + bv^2$

Planck 2018
R.K.Leane 35 al, PRD2018

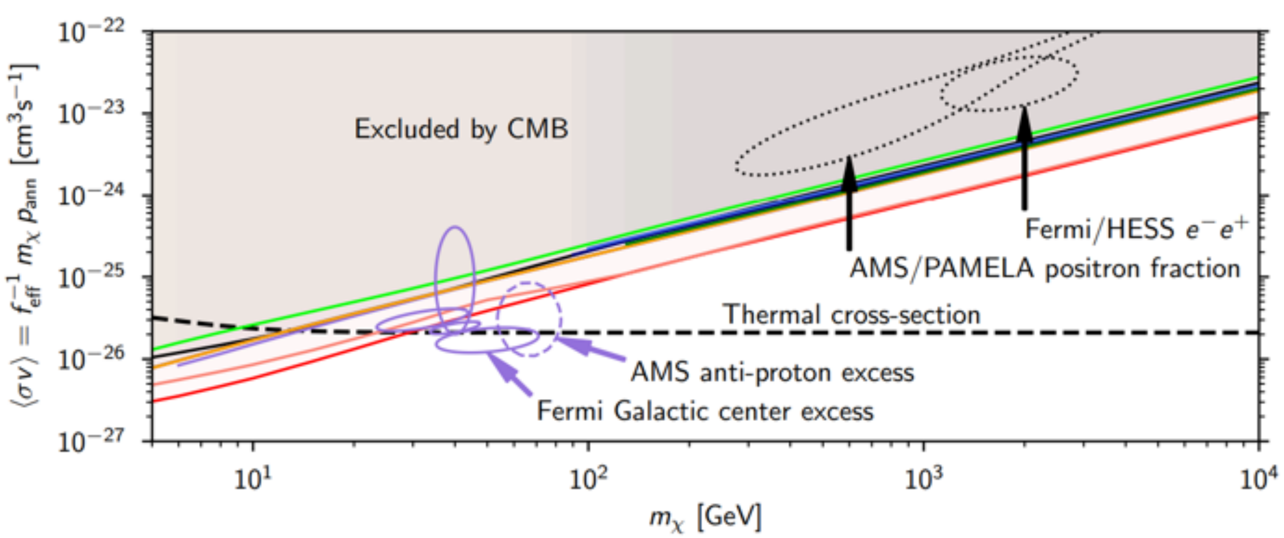

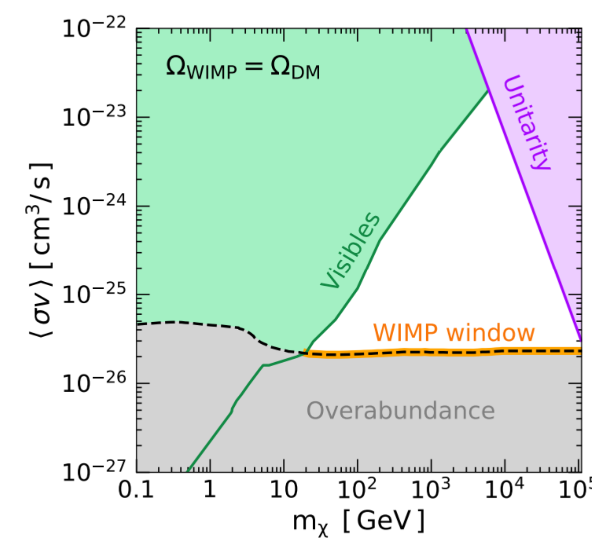

Exothermic DM

- Inelastic exothermic scattering of XDM
- $XDM + e_{\text{atomic}} \to DM + e_{\text{free}}$ by dark photon exchange + kinetic mixing
- Excess is determined by $E_R \sim \delta = m_{XDM} - m_{DM}$
- Most works are based on effective/toy models where δ is put in by hand, or ignored dark Higgs
- dim-2 op for scalar DM and dim-3 op for fermion DM : soft and explicit breaking of local gauge symmetry, and include massive dark photon as well → theoretically inconsistent !

Z_2 DM models with dark Higgs

- We solve this inconsistency and unitarity issue with Krauss-Wilczek mechanism
- By introducing a dark Higgs, we have many advantages:
  - Dark photon gets massive
  - Mass gap δ is generated by dark Higgs mechanism
  - We can have DM pair annihilation in P-wave involving dark Higgs in the final states, unlike in other works

Usual Approaches

For example, Harigaya, Nagai, Suzuki, arXiv:2006.11938

$$V(\phi) = m^2|\phi|^2 + \Delta^2\left(\phi^2 + \phi^{*2}\right), \qquad (1)$$

This term is problematic

$$\mathcal{L} = g_D A'^{\mu}\left(\chi_1 \partial_\mu \chi_2 - \chi_2 \partial_\mu \chi_1\right) + \epsilon e A'_\mu J^\mu_{\mathrm{EM}},$$

Similarly for the fermion DM case

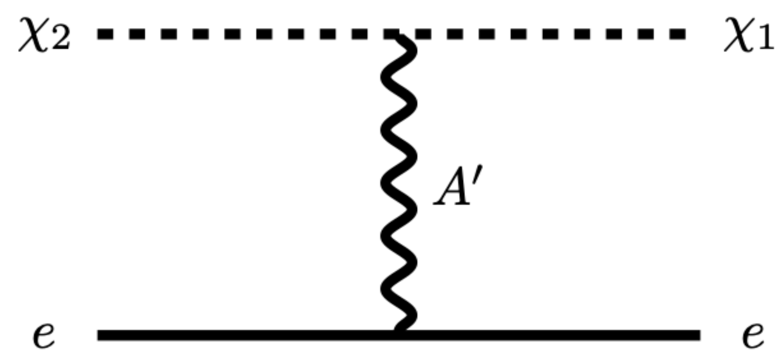

FIG. 1. Inelastic scattering of the heavier DM particle χ_2 off the electron e into the lighter particle χ_1, mediated by the dark photon A'.

- The model is not mathematically consistent, since there is no conserved current a dark photon can couple to in the massless limit
- The second term with Δ^2 breaks $U(1)_X$ explicitly, although softly

Relic Density from

$$XX^{\dagger} \to Z^{'\,*} \to f\bar{f}$$

(P-wave annihilation)

For example, Harigaya, Nagai, Suzuki, arXiv:2006.11938

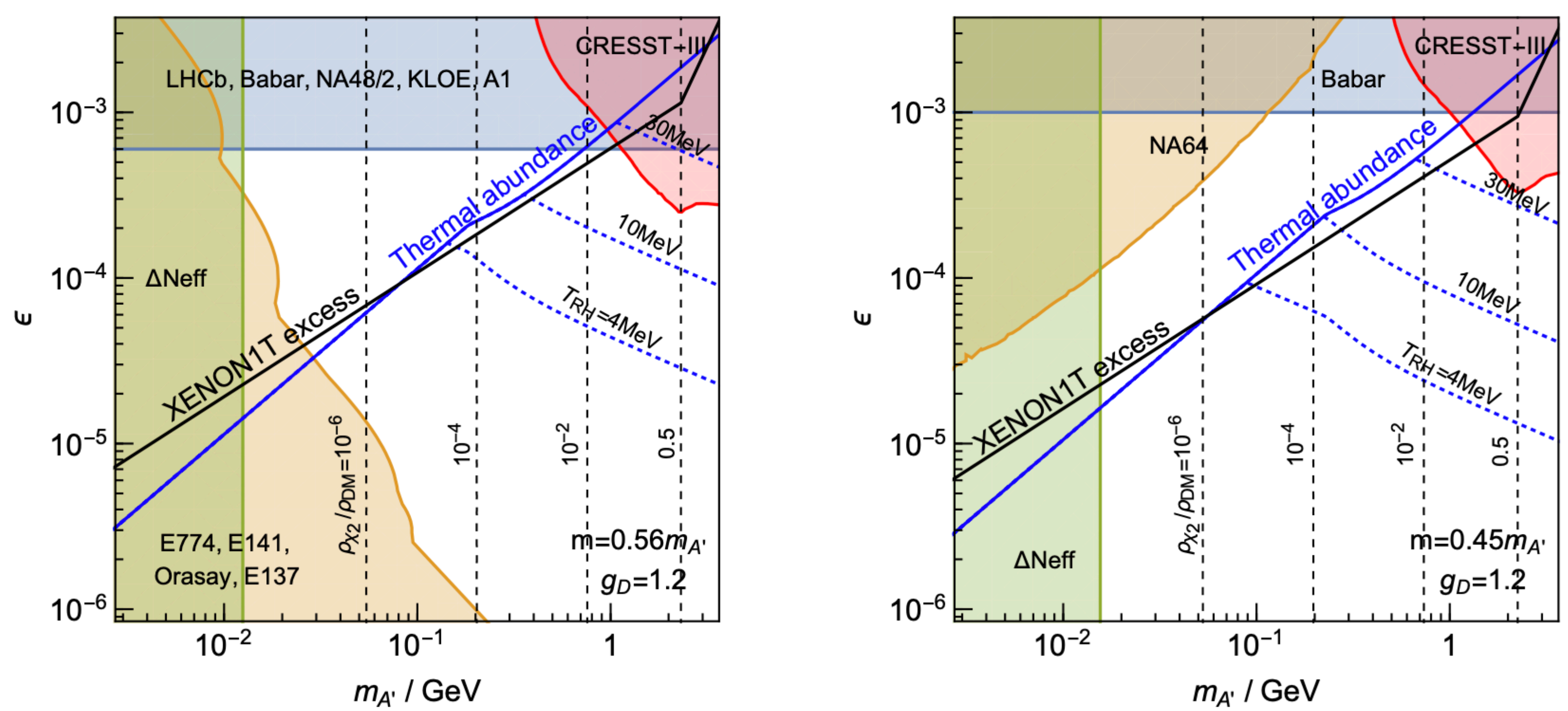

FIG. 4. The required value of ϵ to explain the observed excess of events at XENON1T in terms of the dark photon mass $m_{A'}$ (black solid lines). The left and right panels correspond to the cases of $m > m_{A'}/2$ and $m < m_{A'}/2$ respectively. We assume $g_D = 1.2$ in both cases. The blue lines denote the required value of ϵ to obtain the observed DM abundance by the thermal freeze-out process, discussed in Sec. IV. The solid lines correspond to the case without any entropy production. The dashed lines assume freeze-out during a matter dominated era and the subsequent reheating at $T_{\rm RH}$, which suppresses the DM abundance by a factor of $(T_{\rm RH}/T_{\rm FO})^3$. The black dashed lines denote the mass density of χ_2 normalized by the total DM density. The shaded regions show the constraints from dark radiation and various searches for the dark photon A' which are discussed in Sec. V.

Without dark Higgs, one can not consider light FDM, because of CMB bounds on the S-wave annihilation

Scalar XDM (X_R & X_I)

Field	ϕ	X	χ
U(1) charge	2	1	1

$$\mathcal{L} = \mathcal{L}_{\rm SM} - \frac{1}{4}\hat{X}_{\mu\nu}\hat{X}^{\mu\nu} - \frac{1}{2}\sin\epsilon \hat{X}_{\mu\nu}\hat{B}^{\mu\nu} + D^\mu\phi^\dagger D_\mu\phi + D^\mu X^\dagger D_\mu X - m_X^2 X^\dagger X + m_\phi^2\phi^\dagger\phi$$
$$-\lambda_\phi\left(\phi^\dagger\phi\right)^2 - \lambda_X\left(X^\dagger X\right)^2 - \lambda_{\phi X}X^\dagger X\phi^\dagger\phi - \lambda_{\phi H}\phi^\dagger\phi H^\dagger H - \lambda_{HX}X^\dagger X H^\dagger H$$
$$-\mu\left(X^2\phi^\dagger + H.c.\right), \qquad (1)$$

$$X = \frac{1}{\sqrt{2}}(X_R + iX_I),$$

$$H = \begin{pmatrix} 0 \\ \frac{1}{\sqrt{2}}(v_H + h_H) \end{pmatrix}, \quad \phi = \frac{1}{\sqrt{2}}(v_\phi + h_\phi),$$

$$\mathcal{L} \supset \epsilon g_X s_W Z^\mu (X_R\partial_\mu X_I - X_I\partial_\mu X_R) - \frac{g_Z}{2}Z_\mu\overline{\nu}_L\gamma^\mu\nu_L.$$

$$\mathcal{L} \supset g_X Z'^\mu (X_R\partial_\mu X_I - X_I\partial_\mu X_R) - \epsilon\, e c_W Z'_\mu\overline{e}\gamma^\mu e,$$

$U(1) \to Z_2$ by $v_\phi \neq 0 : X \to -X$

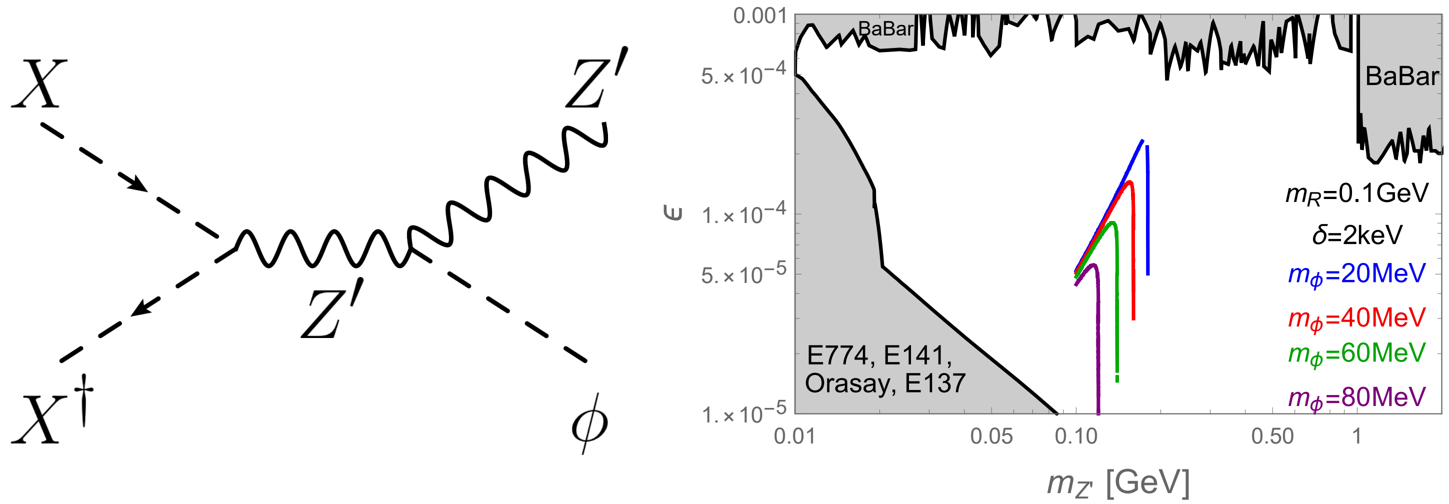

FIG. 1: (*left*) Feynman diagrams relevant for thermal relic density of DM: $XX^\dagger \to Z'\phi$ and (*right*) the region in the $(m_{Z'}, \epsilon)$ plane that is allowed for the XENON1T electron recoil excess and the correct thermal relic density for scalar DM case for $\delta = 2$ keV : (a) $m_{\rm DM} = 0.1$ GeV. Different colors represents $m_\phi = 20, 40, 60, 80$ MeV. The gray areas are excluded by various experiments, from BaBar [61], E774 [62], E141 [63], Orasay [64], and E137 [65], assuming $Z' \to X_R X_I$ is kinematically forbidden.

P-wave annihilation x-sections

Scalar DM : $XX^{\dagger} \to Z^{'*} \to Z^{'}\phi$

$$\sigma v \simeq \frac{g_X^4 v^2}{384\pi\, m_X^4 (4m_X^2 - m_{Z'}^2)^2} \left(16 m_X^4 + m_{Z'}^4 + m_\phi^4 + 40 m_X^2 m_{Z'}^2 - 8 m_X^2 m_\phi^2 - 2 m_{Z'}^2 m_\phi^2\right)$$
$$\times \left[\left\{4m_X^2 - (m_{Z'} + m_\phi)^2\right\} \left\{4m_X^2 - (m_{Z'} - m_\phi)^2\right\} \right]^{1/2} + \mathcal{O}(v^4), \qquad (10)$$

Fermion XDM (χ_R & χ_I)

$$\begin{aligned}\mathcal{L} &= -\frac{1}{4}\hat{X}^{\mu\nu}\hat{X}_{\mu\nu} - \frac{1}{2}\sin\epsilon \hat{X}_{\mu\nu}B^{\mu\nu} + \overline{\chi}\left(i\not{D} - m_\chi\right)\chi + D_\mu\phi^\dagger D^\mu\phi \\ &- \mu^2\phi^\dagger\phi - \lambda_\phi|\phi|^4 - \frac{1}{\sqrt{2}}\left(y\phi^\dagger\overline{\chi^C}\chi + \text{h.c.}\right) - \lambda_{\phi H}\phi^\dagger\phi H^\dagger H\end{aligned}$$

$$\begin{aligned}\chi &= \frac{1}{\sqrt{2}}(\chi_R + i\chi_I), \\ \chi^c &= \frac{1}{\sqrt{2}}(\chi_R - i\chi_I), \\ \chi_R^c &= \chi_R, \quad \chi_I^c = \chi_I,\end{aligned}$$

$$\begin{aligned}\mathcal{L} &= \frac{1}{2}\sum_{i=R,I}\overline{\chi_i}\left(i\not{\partial} - m_i\right)\chi_i - i\frac{g_X}{2}(Z'_\mu + \epsilon s_W Z_\mu)\left(\overline{\chi_R}\gamma^\mu\chi_I - \overline{\chi_I}\gamma^\mu\chi_R\right) \\ &- \frac{1}{2}yh_\phi\left(\overline{\chi_R}\chi_R - \overline{\chi_I}\chi_I\right),\end{aligned}$$

$U(1) \to Z_2$ by $v_\phi \neq 0 : \chi \to -\chi$

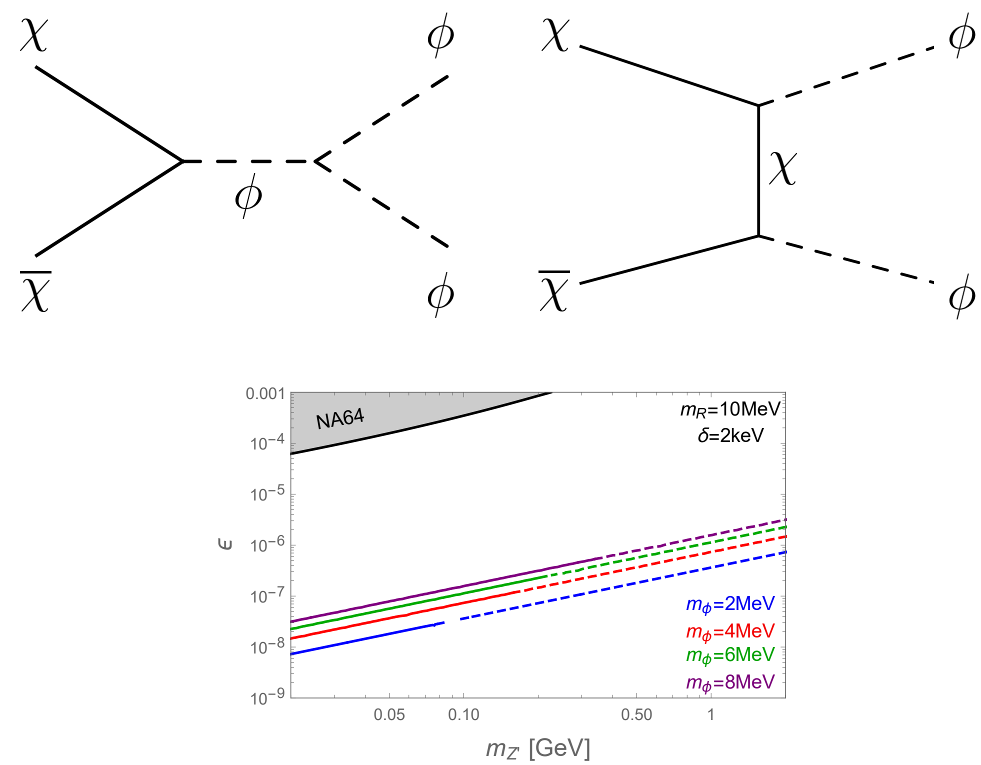

FIG. 2: (*top*) Feyman diagrams for $\chi\bar{\chi} \to \phi\phi$. (*bottom*) the region in the $(m_{Z'}, \epsilon)$ plane that is allowed for the XENON1T electron recoil excess and the correct thermal relic density for fermion DM case for $\delta = 2$ keV and the fermion DM mass to be $m_R = 10$ MeV. Different colors represents $m_\phi = 2, 4, 6, 8$ MeV. The gray areas are excluded by various experiments, assuming $Z' \to \chi_R \chi_I$ is kinematically allowed, and the experimental constraint is weaker in the ϵ we are interested in, compared with the scalar DM case in Fig. 1 (right). We also show the current experimental bounds by NA64 [66].

P-wave annihilation x-sections

Scalar DM : $XX^{\dagger} \to Z'^{*} \to Z'\phi$

$$\sigma v \simeq \frac{g_X^4 v^2}{384\pi\, m_X^4 (4m_X^2 - m_{Z'}^2)^2} \left(16 m_X^4 + m_{Z'}^4 + m_\phi^4 + 40 m_X^2 m_{Z'}^2 - 8 m_X^2 m_\phi^2 - 2 m_{Z'}^2 m_\phi^2\right) \times \left[\left\{4m_X^2 - (m_{Z'} + m_\phi)^2\right\}\left\{4m_X^2 - (m_{Z'} - m_\phi)^2\right\}\right]^{1/2} + \mathcal{O}(v^4), \quad (10)$$

Fermion DM : $\chi\bar{\chi} \to \phi\phi$

$$\sigma v = \frac{y^2 v^2 \sqrt{m_\chi^2 - m_\phi^2}}{96\pi m_\chi} \left[\frac{27\lambda_\phi^2 v_\phi^2}{(4m_\chi^2 - m_\phi^2)^2} + \frac{4y^2 m_\chi^2 (9m_\chi^4 - 8m_\chi^2 m_\phi^2 + 2m_\phi^4)}{(2m_\chi^2 - m_\phi^2)^4}\right] + \mathcal{O}(v^4), \quad (28)$$

Crucial to include "dark Higgs" to have Light DM pair annihilation in P-wave

Summary

- Local Z_2 scalar/fermion DM : theoretically well defined & mathematically consistent models for XDM
- Can explain a number of phenomena including the recent XENON1T data
- One can discriminate the spin of (X)DM at Belle2 from the polar angle distributions of the decaying points
- DM mass and the Δm can be determined with the focus point method
- Similar studies at ILC, CEPC, HL-LHC and FCC-hh in progress (The current version of FCC CDR does not include this interesting case.)

$U(1)_{L_\mu - L_\tau}$ -charged DM

: Z' only vs. $Z' + \phi$

arXiv:2204.04889 [hep-ph]
With Seungwon Baek, Jongkuk Kim

SM+$U(1)_{L_\mu - L_\tau}$ gauge sym

- He, Josh, Lew, Volkas, PRD 43, 22; PRD 44, 2118 (1991)

- One of the anomaly free gauge groups without extension of fermion contents

- The simplest anomaly free U(1) extensions that couple to the SM fermions directly

- Can affect the muon g-2, PAMELA e^+ excess, (and B anomalies with extra fermions : Not covered in this talk)

Muon g-2

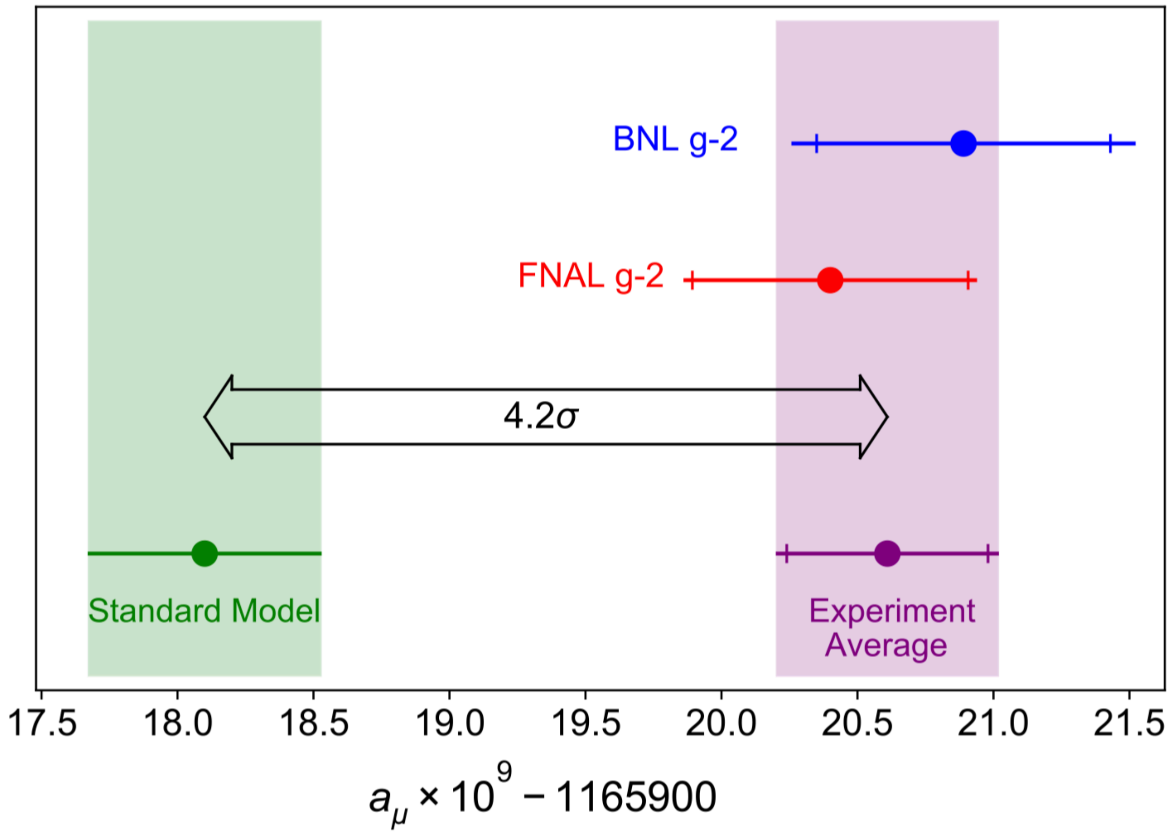

The Muon g-2 Collaboration, 2104.03281

Excellent example for graduate students

- Relativistic E&M (spinning particle in EM fields)
- Special relativity (time dilation)
- (V-A) structure of charged weak interaction

Muon (g-2) in $U(1)_{\mu-\tau}$ Model

Baek, Deshpande, He, Ko : hep-ph/0104141
Baek, Ko : arXiv:0811.1646 [hep-ph]

$$
\begin{array}{llll}
L_L^e: & (1,2,-1)(0) & e_R: & (1,1,-2)(0) \\
L_L^\mu: & (1,2,-1)(2a) & \mu_R: & (1,1,-2)(2a) \\
L_L^\tau: & (1,2,-1)(-2a) & \mu_R: & (1,1,-2)(-2a).
\end{array}
$$

$$\Delta a_\mu = \frac{\alpha'}{2\pi} \int_0^1 dx \frac{2m_\mu^2 x^2(1-x)}{x^2 m_\mu^2 + (1-x)M_{Z'}^2} \approx \frac{\alpha'}{2\pi}\frac{2m_\mu^2}{3M_{Z'}^2}$$

$$Z' \to \mu^+\mu^-, \tau^+\tau^-, \nu_\alpha\bar{\nu}_\alpha \text{ (with } \alpha = \mu \text{ or } \tau), \ \psi_D\overline{\psi}_D$$

$$\Gamma(Z' \to \mu^+\mu^-) = \Gamma(Z' \to \tau^+\tau^-) = 2\Gamma(Z' \to \nu_\mu\bar{\nu}_\mu) = 2\Gamma(Z' \to \nu_\tau\bar{\nu}_\tau) = \Gamma(Z' \to \psi_D\bar{\psi}_D)$$

if $M_{Z'} \gg m_\mu, m_\tau, M_{\rm DM}$. The total decay rate of Z' is approximately given by

$$\Gamma_{\rm tot}(Z') = \frac{\alpha'}{3} M_{Z'} \times 4(3) \approx \frac{4(\text{or } 3)}{3} \text{ GeV} \left(\frac{\alpha'}{10^{-2}}\right)\left(\frac{M_{Z'}}{100\text{GeV}}\right)$$

$$q\bar{q} \text{ (or } e^+e^-) \to \gamma^*, Z^* \to \mu^+\mu^- Z', \tau^+\tau^- Z'$$
$$\to Z^* \to \nu_\mu\bar{\nu}_\mu Z', \nu_\tau\bar{\nu}_\tau Z'$$

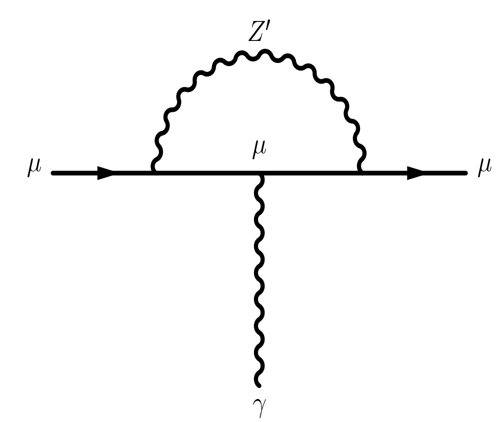

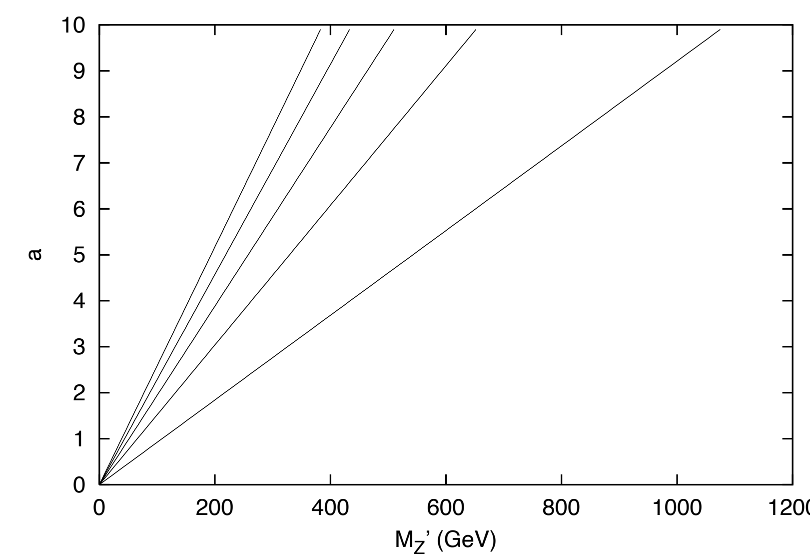

FIG. 2. Δa_μ on the a vs. $m_{Z'}$ plane in case b). The lines from left to right are for Δa_μ away from its central value at $+2\sigma, +1\sigma, 0, -1\sigma$ and -2σ, respectively.

Baek and Ko, arXiv:0811.1646, for PAMELA e^+ excess

$$\mathcal{L}_{\rm Model} = \mathcal{L}_{\rm SM} + \mathcal{L}_{\rm New}$$

$$\mathcal{L}_{\rm New} = -\frac{1}{4} Z'_{\mu\nu} Z'^{\mu\nu} + \overline{\psi_D} i D \cdot \gamma \psi_D - M_{\psi_D} \overline{\psi_D} \psi_D + D_\mu \phi^* D^\mu \phi - \lambda_\phi (\phi^* \phi)^2 - \mu_\phi^2 \phi^* \phi - \lambda_{H\phi} \phi^* \phi H^\dagger H.$$

Here we ignored kinetic mixing for simplicity

$$D_\mu = \partial_\mu + ieQA_\mu + i\frac{e}{s_W c_S}(I_3 - s_W^2 Q) Z_\mu + ig' Y' Z'_\mu$$

muon g-2, Leptophilc DM, Collider Signature

Muon (g-2)

$$\Delta a_\mu = a_\mu^{\rm exp} - a_\mu^{\rm SM} = (302 \pm 88) \times 10^{-11}.$$

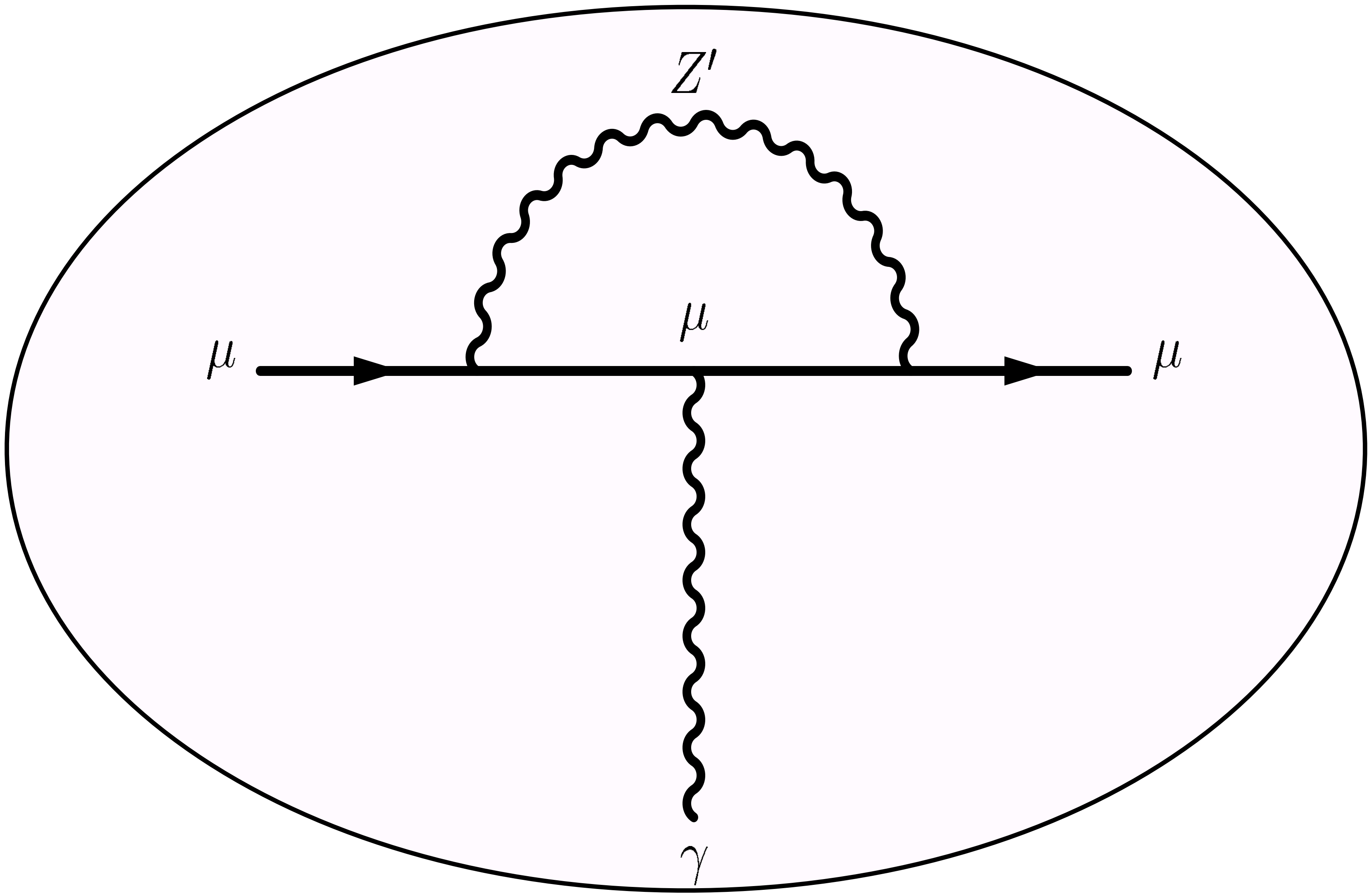

$$\Delta a_\mu = \frac{\alpha'}{2\pi} \int_0^1 dx \frac{2m_\mu^2 x^2(1-x)}{x^2 m_\mu^2 + (1-x)M_{Z'}^2} \approx \frac{\alpha'}{2\pi}\frac{2m_\mu^2}{3M_{Z'}^2}$$

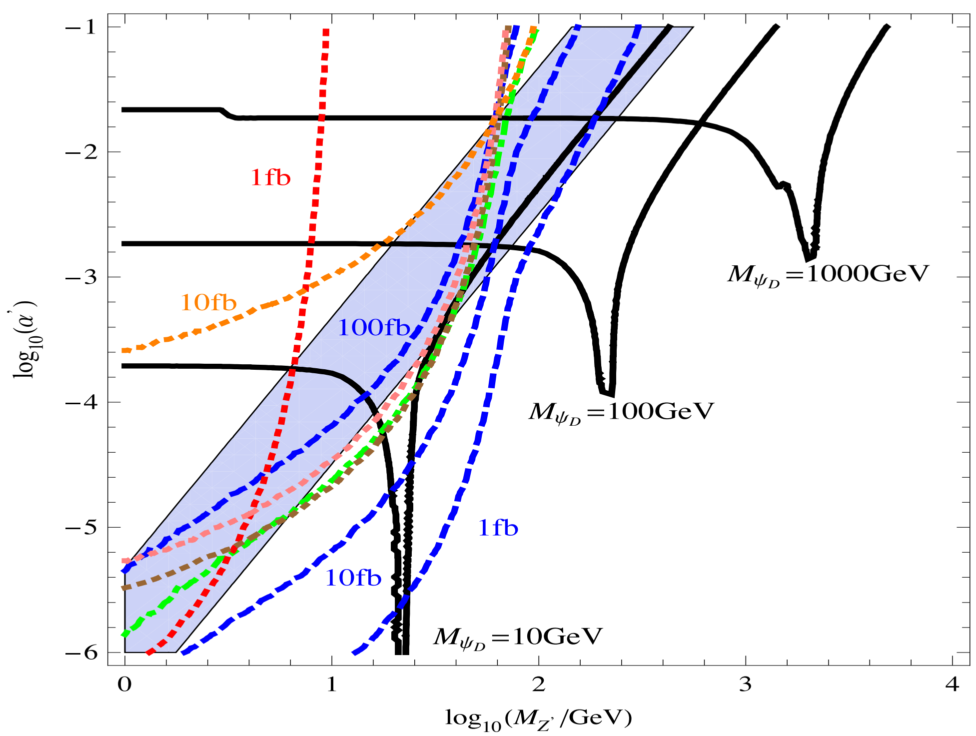

Figure 1: The relic density of CDM (black), the muon $(g-2)_\mu$ (blue band), the production cross section at B factories (1 fb, red dotted), Tevatron (10 fb, green dotdashed), LEP (10 fb, pink dotted), LEP2 (10 fb, orange dotted), LHC (1 fb, 10 fb, 100 fb, blue dashed) and the Z^0 decay width (2.5×10^{-6} GeV, brown dotted) in the $(\log_{10}\alpha', \log_{10} M_{Z'})$ plane. For the relic density, we show three contours with $\Omega h^2 = 0.106$ for $M_{\psi_D} = 10$ GeV, 100 GeV and 1000 GeV. The blue band is allowed by $\Delta a_\mu = (302 \pm 88)\times 10^{-11}$ within 3 σ.

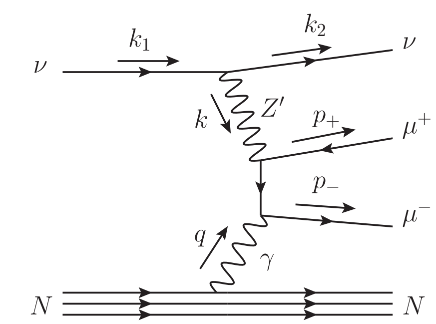

FIG. 1. The leading order contribution of the Z′ to neutrino trident production (another diagram with μ^+ and μ^- reversed
i ... in g'

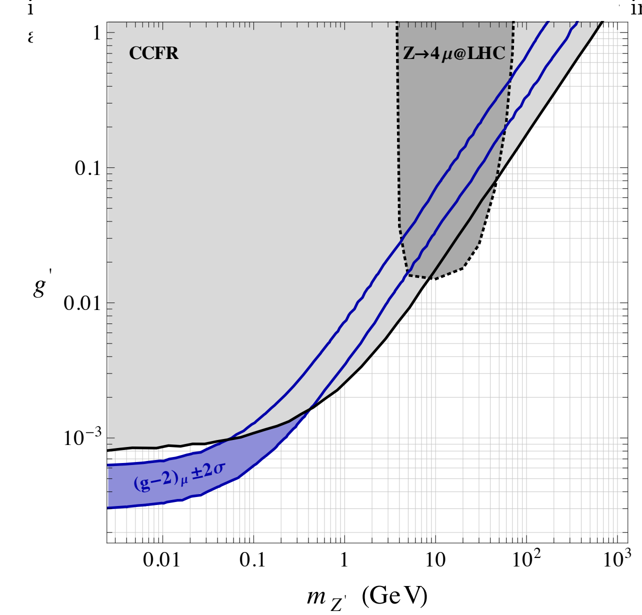

FIG. 2. Parameter space for the Z′ gauge boson. The light-grey area is excluded at 95% C.L. by the CCFR measurement of the neutrino trident cross-section. The grey region with the dotted contour is excluded by measurements of the SM

Seungwon Baek, Pyungwon Ko, arXiv:0811.1646, JCAP(2009) about PAMELA e^+ excess

Altmannshofer et al. arXiv:1406.2332 [hep-ph]

Neutrino trident puts strong constraints on this model

One can evade the neutrino trident constraint, if one introduces New fermions and generate muon g-2 at loop level w/ new fermions !

Z’ Only

- Consider light Z’ and $g_X \sim (\text{a few}) \times 10^{-4}$ for the muon g-2. Then

- $\chi\bar{\chi} \to Z'^{*} \to f_{\rm SM}\bar{f}_{\rm SM}$: dominant annihilation channel

- $g_X \sim 10^{-4}$ is too small for $\chi\bar{\chi} \to Z'Z'$ to be effective for $\Omega_\chi h^2$

- $m_{Z'} \sim 2m_{\rm DM}$ with the s-channel Z' resonance for the correct relic density

- Many recent studies on this case:

  - Asai, Okawa, Tsumura, 2011.03165
  - Holst, Hooper, Krnjaic, 2107.09067
  - Drees and Zhao, arXiv:2107.14528
  - And some earlier papers

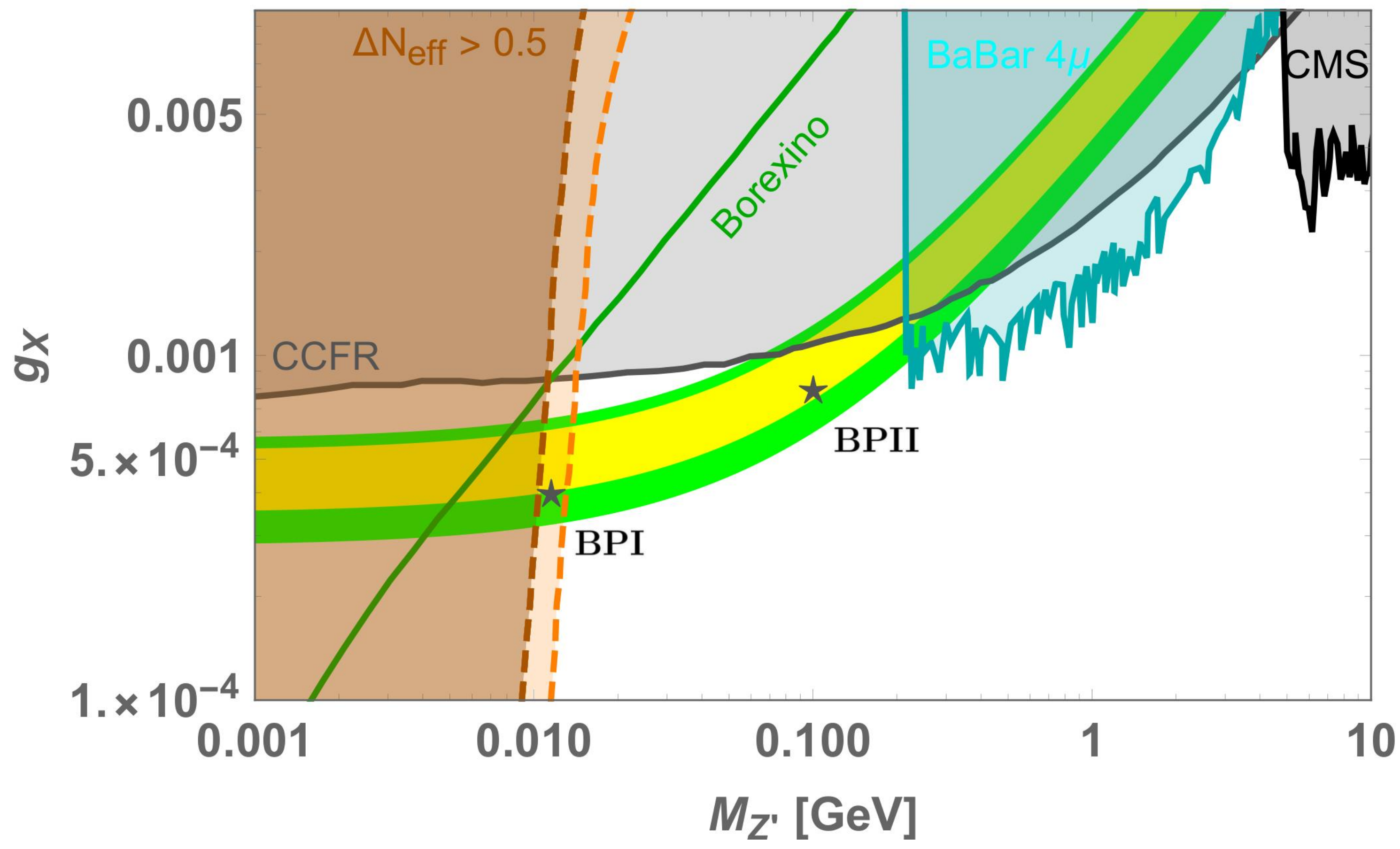

FIG. 1. Regions inside the yellow and Green shaded areas by the Δa_μ are allowed at 1σ and 2σ C.L.. Cyan, black, and orange regions are excluded by other experimental bounds. Above green solid line is ruled out by the Borexino experiment. Region inside the orange area can resolve the Hubble tension. We take two Benchmark Points (BP) $(M_{Z'}, g_X)$ as **BPI** $=(11.5\,\text{MeV}, 4\times10^{-4})$ and **BPII** $=(100\,\text{MeV}, 8\times10^{-4})$.

$U(1)_{L_\mu - L_\tau}$ -charged DM

: Z' only vs. $Z' + \phi$

cf: Let me call Z' , $U(1)_{L_\mu - L_\tau}$ gauge boson,
"dark photon", since it couples to DM

Models with Φ

TABLE I: $U(1)$ charge assignments of newly introduced particles and SM particles. The other SM particles are singlet.

Field	Z'_μ	$X(\chi)$	Φ	$L_\mu = (\nu_{L\mu}, \mu_L), \mu_R$	$L_\tau = (\nu_{L\tau}, \tau_L), \tau_R$
spin	1	0 (1/2)	0	1/2	1/2
$U(1)$ charge	0	$Q_X(Q_\chi)$	Q_Φ	+1	-1

We Consider Both Complex Scalar (X) and Dirac Fermion DM (χ)

- Physics depends on Q_Φ , Q_X and Q_χ
- $Q_\Phi = 2Q_{X(\chi)}$ and $3Q_X$ need special cares, since there are extra gauge invariant op's that break $U(1) \to Z_2$, Z_3 after $U(1)$ is spontaneously broken by nonzero VEV of Φ

Complex Scalar DM (generic with $Q_\Phi \neq Q_X, etc$)

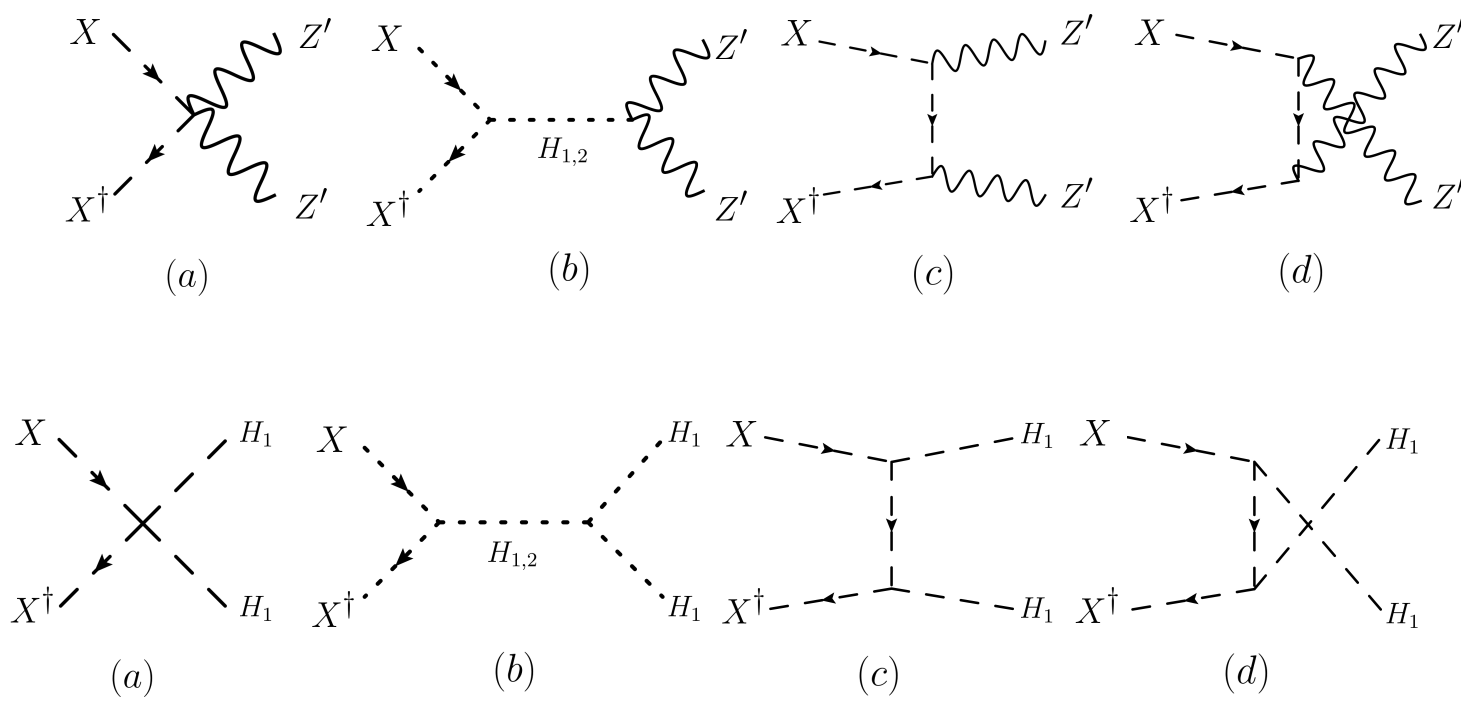

FIG. 2. (*Top*) Feynman diagrams for Complex scalar DM annihilating to a pair of Z' bosons. (*Bottom*) Feynman diagrams for Complex scalar DM annihilating to a pair of H_1 bosons.

$H_2 \simeq H_{125}$ and $H_1 \simeq \phi$ (dark Higgs)

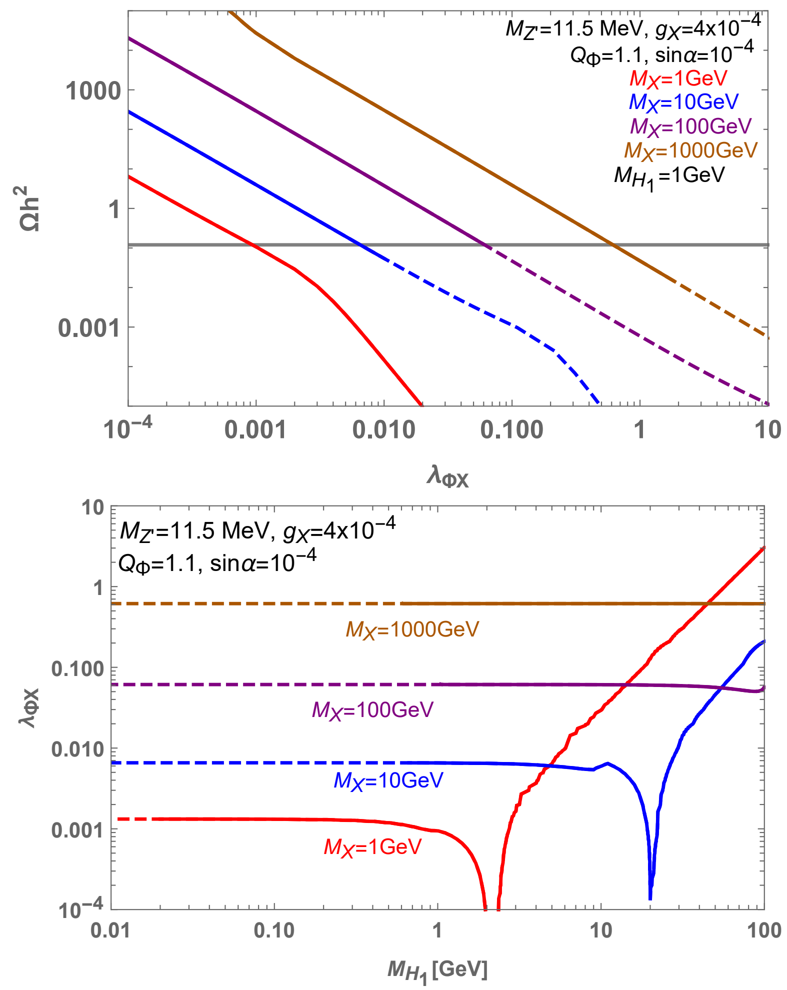

FIG. 3. *Top*: relic abundance of complex scalar DM as functions of $\lambda_{\Phi X}$ for [**BPI**] for $M_X = 1,\ 10, 100,\ 1000$GeV, respectively. We assumed $Q_\Phi = 1.1$, $M_{H_1} = 1$GeV, and $\sin\alpha = 10^{-4}$. Solid (Dashed) lines represent the region where bounds on DM direct detection are satisfied (ruled out). *Bottom*: the preferred parameter space in the $(M_{H_1}, \lambda_{\Phi X})$ plane for $\lambda_{HX} = 0$.

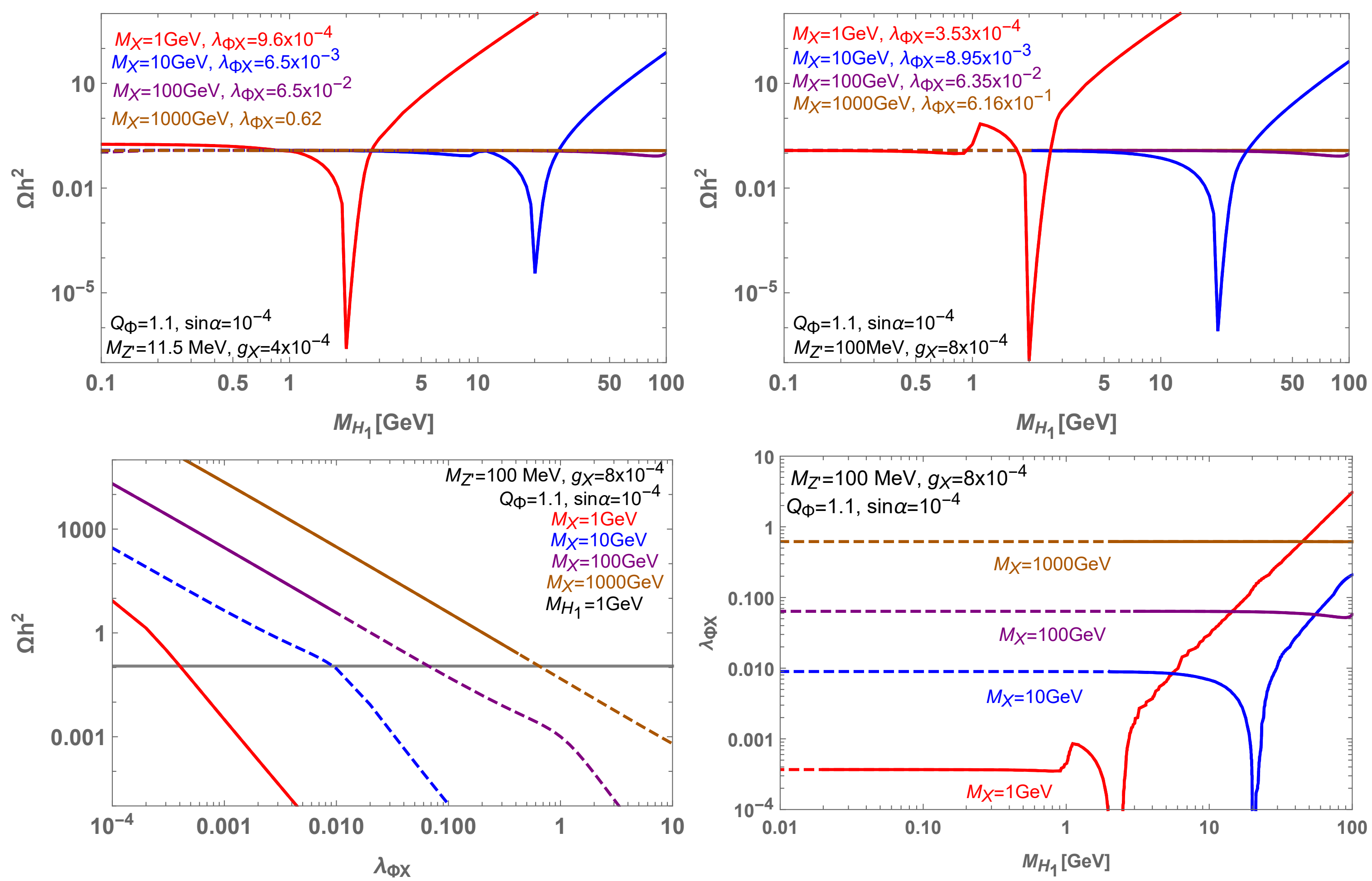

FIG. 7. The (*Top*) plots show the relic abundance of complex scalar DM for $Q_\Phi = 1.1$ as functions of dark Higgs mass M_{H_1} for [**BPI**] (*Left*) and [**BPII**] (*Right*). The (*Bottom*) plots show the relic density as functions of $\lambda_{\Phi X}$ (*Left*) and the preferred parameter space in the $(M_{H_1}, \lambda_{\Phi X})$ plane for $\lambda_{HX} = 0$ (*Right*) for [**BPII**] . We take four different DM masses, $M_X = 1,\ 10, 100,\ 1000$GeV, respectively. Solid (Dashed) lines represent the region where bounds on DM direct detection are satisfied (ruled out).

DM mass : much wider range than $m_{Z'} \sim 2 m_{\rm DM}$
due to dark Higgs boson contributions

Complex Scalar DM: $U(1)_{L_\mu - L_\tau} \to Z_2\ (Q_\Phi = 2Q_X)$

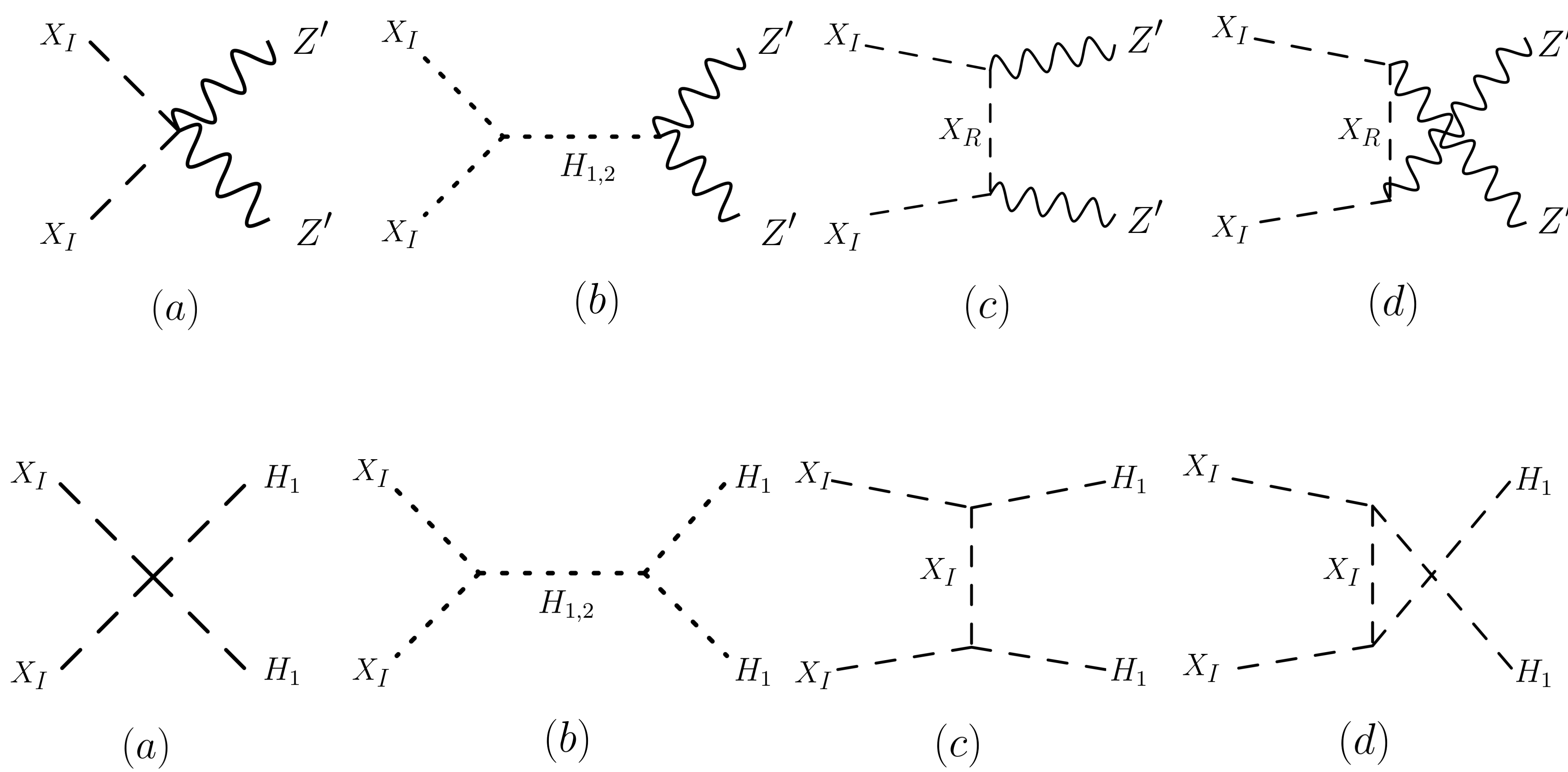

FIG. 8. (*Top*) Feynman diagrams for local Z_2 scalar DM annihilatiing to a pair of Z' bosons. (*Bottom*) Feynman diagrams for local Z_2 scalar DM annihilatiing to a pair of H_1 bosons, which is mostly dark Higgs-like.

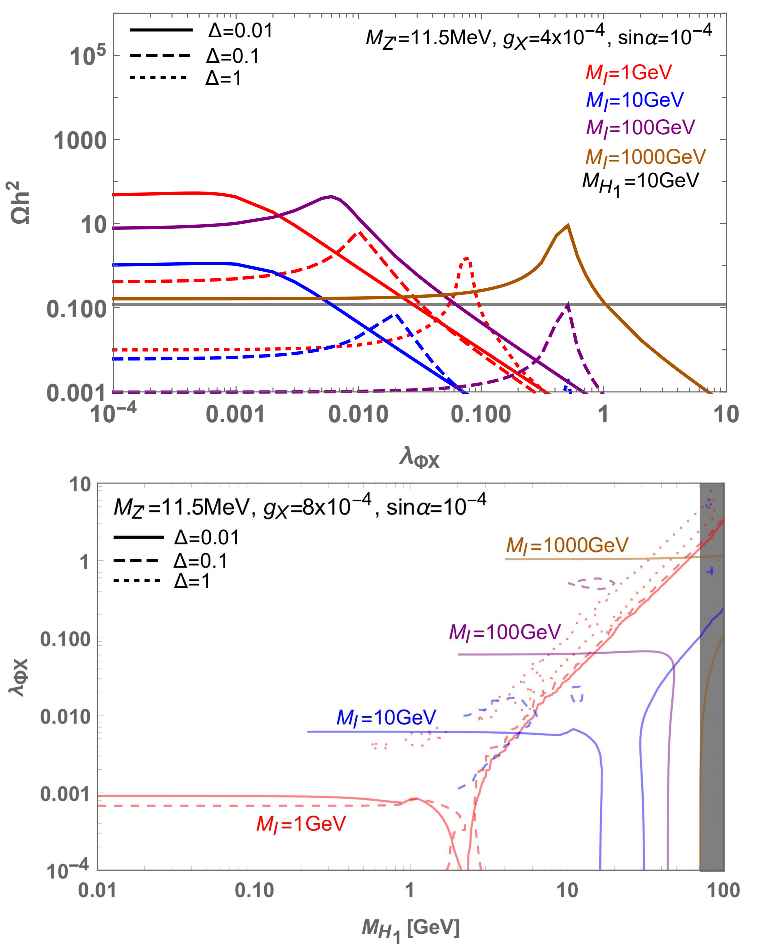

FIG. 4. *Top*: Relic abundance of local Z_2 scalar DM as functions of $\lambda_{\Phi X}$ for [**BPI**] and different values of mass splittings (Δ). We take $\lambda_{HX} = 0$, $M_{H_1} = 10\text{GeV}$, and $s_\alpha = 10^{-4}$. All the curves satisfy the DM direct detection bound. *Bottom*: The preferred parameter space in the $(M_{H_1}, \lambda_{\Phi X})$ plane for different values of Δ. The gray area is excluded by the perturbative condition.

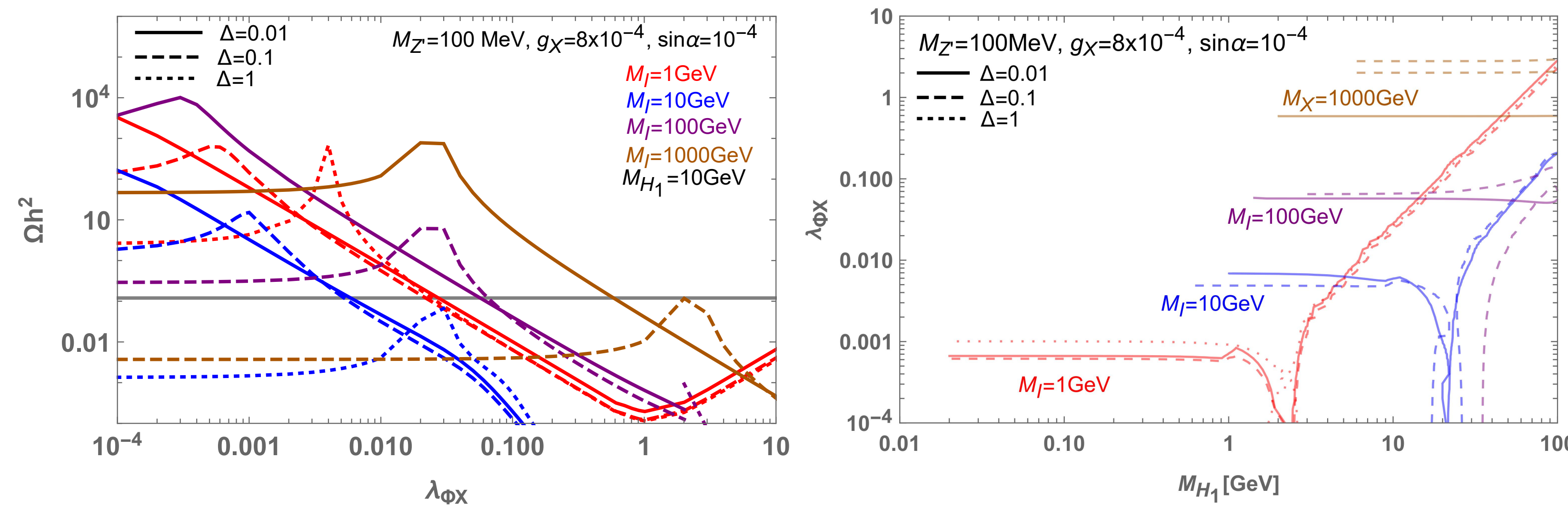

FIG. 9. (*Left*) Relic abundance of local Z_2 scalar DM in case of [**BPII**]. We take $\lambda_{HX} = 0$, $M_{H_1} = 10\text{GeV}$, and $s_\alpha = 10^{-4}$. All the lines satisfy the DM direct detection bound. (*Right*) Relic abundance of local Z_2 scalar DM in the $(M_{H_1}, \lambda_{\Phi X})$ plane.

DM mass : much wider range than $m_{Z'} \sim 2m_{\rm DM}$ due to dark Higgs boson contributions

Complex Scalar DM: $U(1)_{L_\mu - L_\tau} \to Z_3 \; (Q_\Phi = 3Q_X)$

Local Z_3 DM Model : first considered by Ko, Tang:
arXiv:1402.6449 (SIDM), 1407.5492 (GC γ-ray excess)

$$V = -\mu_H^2 H^\dagger H + \lambda_H \left(H^\dagger H\right)^2 - \mu_\phi^2 \phi_X^\dagger \phi_X + \lambda_\phi \left(\phi_X^\dagger \phi_X\right)^2 + \mu_X^2 X^\dagger X + \lambda_X \left(X^\dagger X\right)^2 + \lambda_{\phi H} \phi_X^\dagger \phi_X H^\dagger H + \lambda_{\phi X} X^\dagger X \phi_X^\dagger \phi_X + \lambda_{HX} X^\dagger X H^\dagger H + \left(\lambda_3 X^3 \phi_X^\dagger + H.c.\right) \quad (2.1)$$

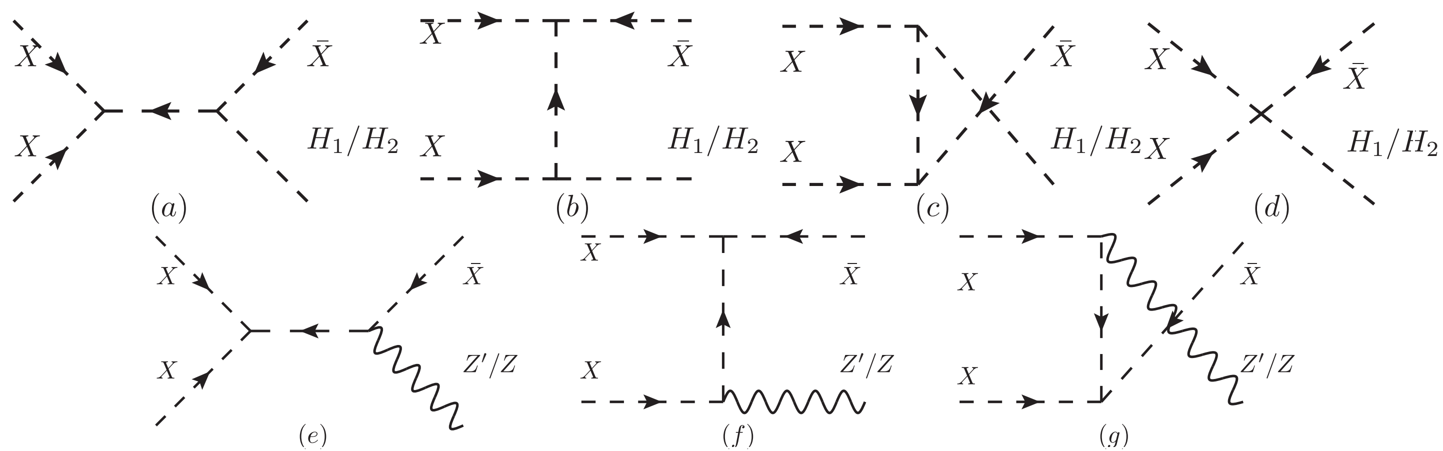

FIG. 1: Feynman diagrams for dark matter semi-annihilation. Only (a), (b), and (c) with H_1 as final state appear in the global Z_3 model, while all diagrams could contribute in local Z_3 model.

ϕ and Z' : present only in models with dark gauge symmetries,
And not in models with global dark symmetries

Dark $U(1) \to Z_3$

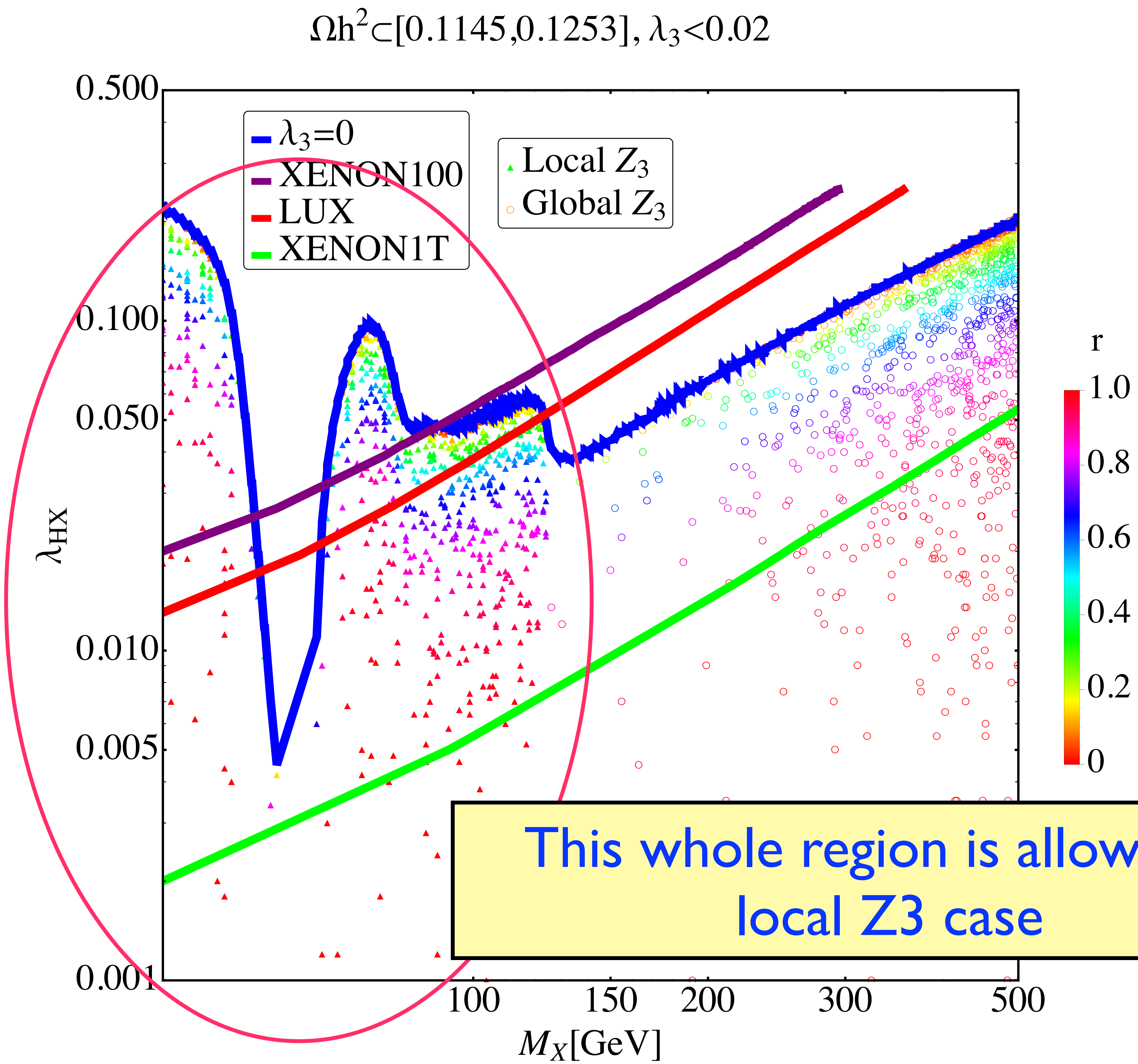

- Blue band marks the upper bound,
- All points are allowed in our local Z3 model,1402.6449
- only circles are allowed in global Z3 model,1211.1014

$$r \equiv \frac{1}{2} \frac{v\sigma^{XX \to X^* Y}}{v\sigma^{XX^* \to YY} + \frac{1}{2} v\sigma^{XX \to X^* Y}}.$$

$U(1)_{L_\mu - L_\tau} \to Z_3$

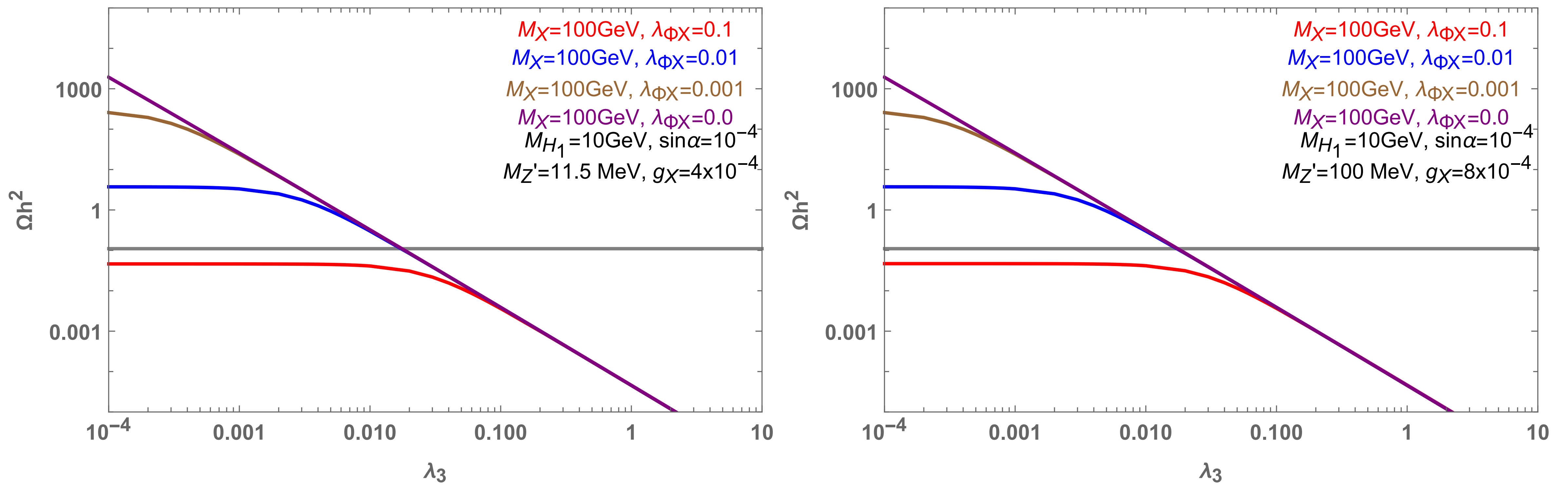

FIG. 10. Relic abundance of Z_3 scalar DM for the [**BPI**] (*Left*) and the [**BPII**] (*Right*), respectively. Here we fixed $\lambda_{HX} = 0$ for simplicity.

- $g_X \sim O(10^{-4})$: very small, $XX \to X^\dagger Z'$ is not important

DM mass : much wider range than $m_{Z'} \sim 2m_{\rm DM}$
due to dark Higgs boson contributions

- λ_3 controlling $XX \to X^\dagger H_1$ is an important parameter

Dirac fermion DM: $U(1)_{L_\mu - L_\tau} \to Z_2$ $(Q_\Phi = 2Q_\chi)$

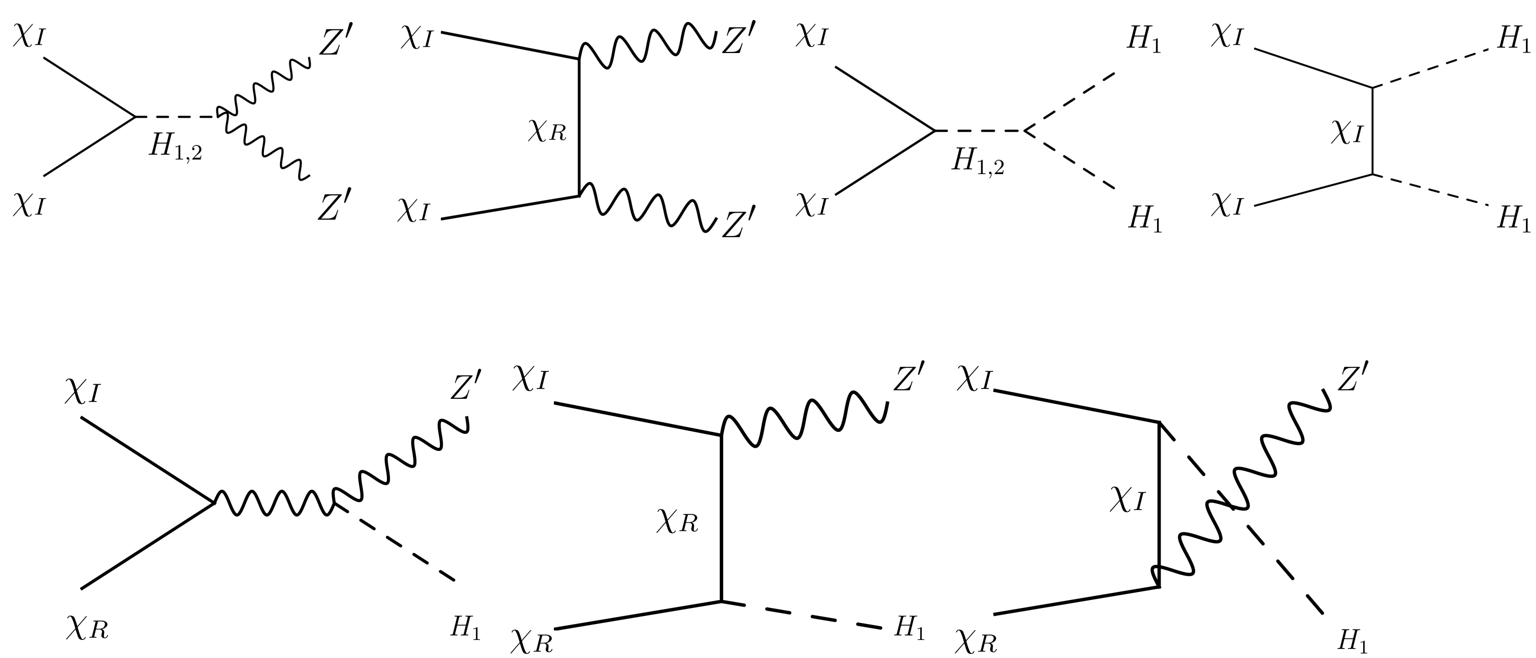

FIG. 5. Feynman diagrams of local Z_2 fermion DM (co-)annihilating into a pair of Z' bosons and H_1 bosons (*Top*), and $Z' + H_1$ (*Bottom*).

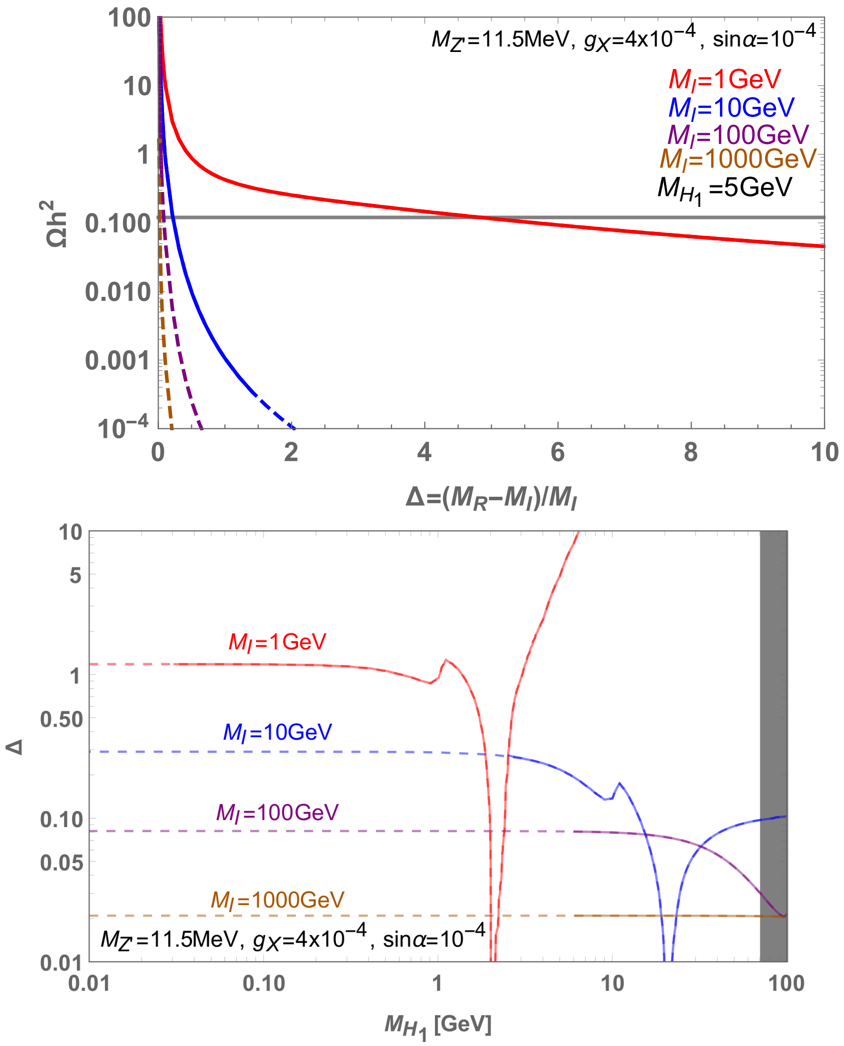

FIG. 6. *Top*: Dark matter relic density as functions of mass splitting Δ for [**BPI**] and for different values of DM mass, $M_I = 1, 10, 100, 1000$GeV. Solid (Dashed) lines denote the region where bounds on DM direct detection are satisfied (ruled out). *Bottom*: Preferred parameter space in the (M_{H_1}, Δ) plane for different DM masses. The gray region is ruled out by the perturbativity condition on λ_Φ.

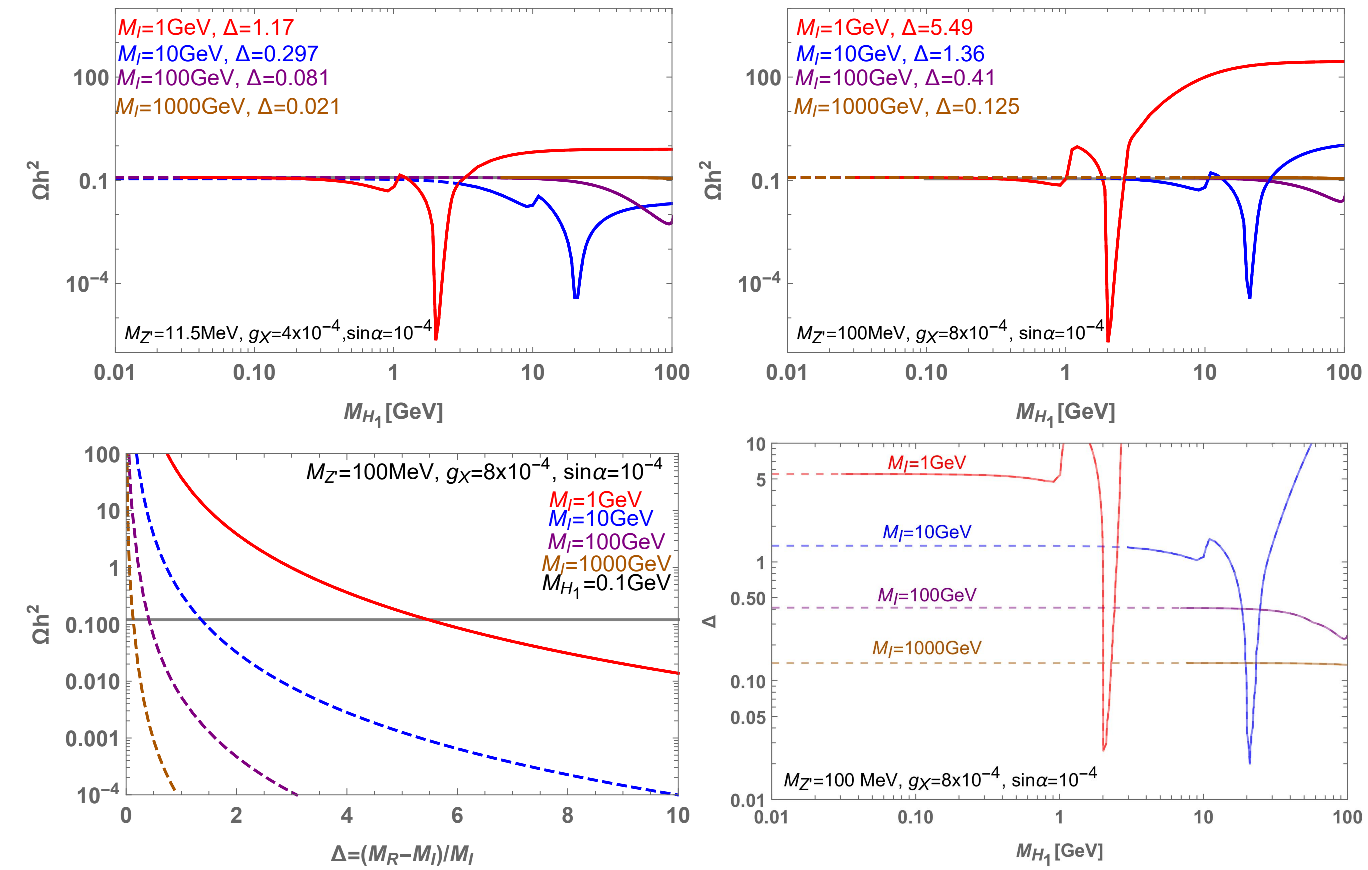

FIG. 11. (*Top*) Dark matter relic density as functions of dark Higgs mass M_{H_1} for [**BPI**] (*Left*) and [**BPII**] (*Right*) (*Bottom-Left*) Dark matter relic density as functions of Δ for [**BPII**], and *(Bottom-right)* Preferred parameter region in the (Δ, M_{H_1}) plane. Solid (Dashed) lines denote the region where bounds on DM direct detection are satisfied (ruled out).

DM mass : much wider range than $m_{Z'} \sim 2m_{\rm DM}$
due to dark Higgs boson contributions

Conclusion

- DM physics with massive dark photon can not be complete without including dark gauge symmetry breaking mechanism, e.g. dark Higgs field ϕ, which have been largely ignored by DM community (or some ways other than dark Higgs to provide dark photon mass)

- Many examples show the importance of ϕ in DM phenomenology, astroparticle physics and cosmology

- Once ϕ is included, can accommodate the muon g-2 and thermal DM without the s-channel resonance condition $m_{Z'} \sim 2m_{\rm DM}$

- $m_{\rm DM}$: essentially free, whereas $m_{Z'} \sim O(10-100)$ MeV and $g_X \sim O(10^{-4})$ can explain the muon (g-2)

Higgs-Portal Assisted Higgs Inflation

arXiv:1405.1635 [hep-ph], JCAP02 (2017) 003
With Jinsu Kim, Wan-Il Park

Higgs Inflation

- Inflation : the main paradigm for very early Universe
- But no very compelling inflation scenarios based on high energy physics
- SM Higgs boson can play a role of inflaton if it has large non minimal coupling [Bezrukov, Shaposhnikov (2007)] or non canonical kinetic term
- Merits: Minimal model, Consistent with Planck data, Can connect low energy ($m_{\rm EW}$) scale to high energy (inflation) scale

Higgs Inflation in SM

(before BICEP2) [Bezrukov and Shaposhnikov, 0710.3755]

$$\frac{\mathcal{L}}{\sqrt{-g}} = -\frac{1}{2\kappa}\left(1+\xi\frac{h^2}{M_{\rm Pl}^2}\right)R + \mathcal{L}_h$$

Nonminimal coupling

$$\epsilon = \frac{M_P^2}{2}\left(\frac{dU/d\chi}{U}\right)^2 \simeq \frac{4M_P^4}{3\xi^2 h^4}$$

$$\eta = M_P^2\frac{d^2U/d\chi^2}{U} \simeq -\frac{4M_P^2}{3\xi h^2},$$

$$\Rightarrow \epsilon \simeq \frac{3}{4}\eta^2$$

$$n_s = 1 - 6\epsilon + 2\eta \sim 0.96$$

$$\Rightarrow \eta \simeq \frac{1}{2}(n_s - 1)$$

$$\Rightarrow \epsilon \simeq \frac{3}{16}(n_s - 1)^2$$

$$\Rightarrow r \simeq 16\epsilon \simeq 3(n_s-1)^2 \sim 5\times 10^{-3}$$

$$U(\chi) = \frac{1}{\Omega(\chi)^4}\frac{\lambda}{4}\left(h(\chi)^2 - v^2\right)^2$$

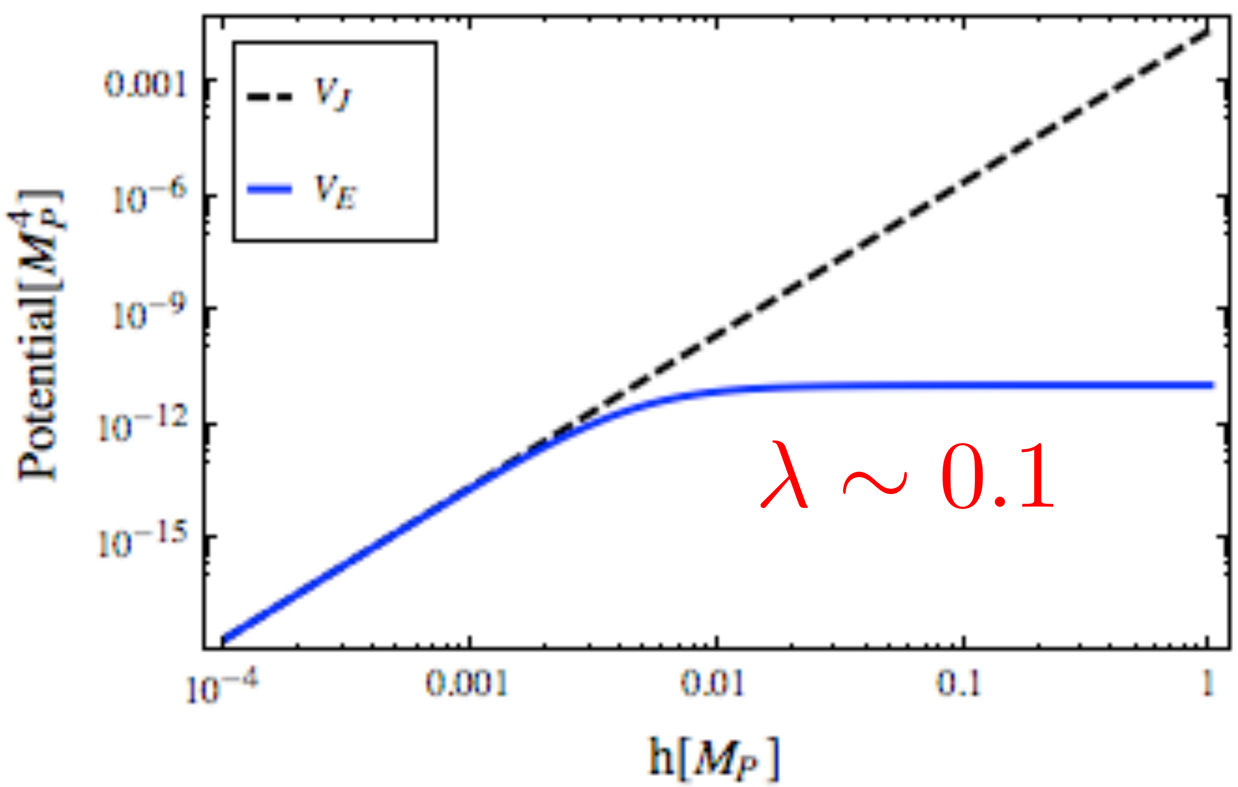

Higgs Inflation in SM

(after BICEP2)

$r_{\rm BICEP2} \sim 0.1$ ⇨ Is Higgs inflation ruled out? No!

$$U(h) = \frac{\lambda}{4\Omega^4}\left(h^2 - v_H^2\right) \to \frac{\lambda(\mu)}{4\Omega^4}\left(h^2 - v_H^2\right)$$

[Hamada, Kawai, Oda and Park, 1403.5043; Bezrukov and Shposhnikov, 1403.6078]

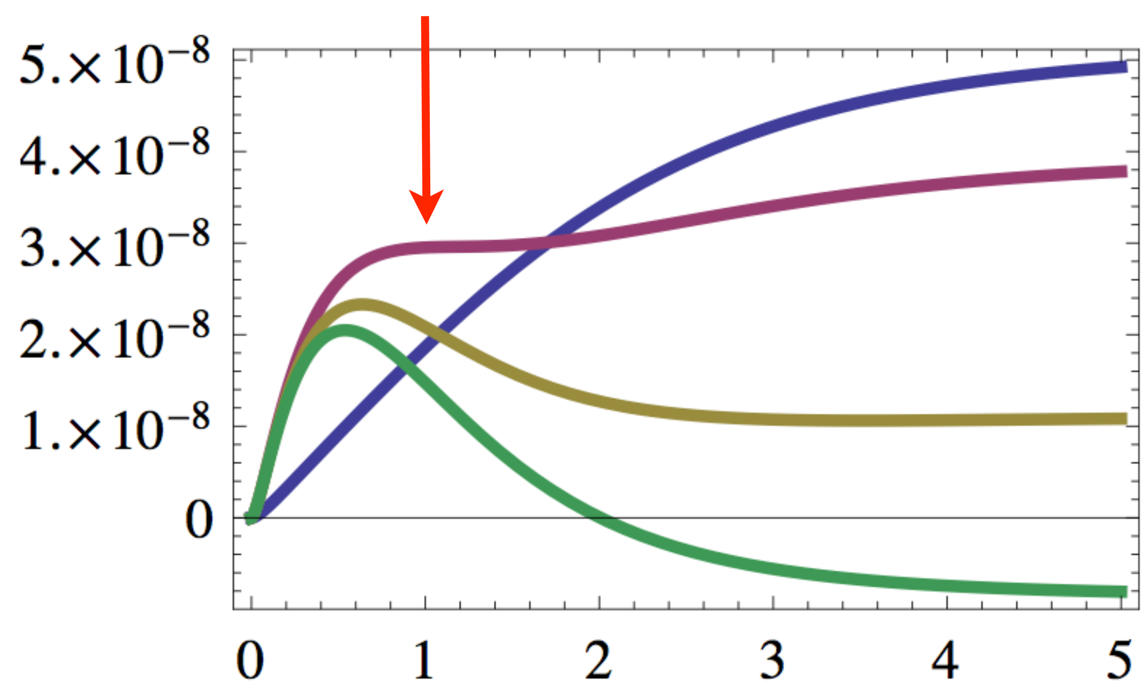

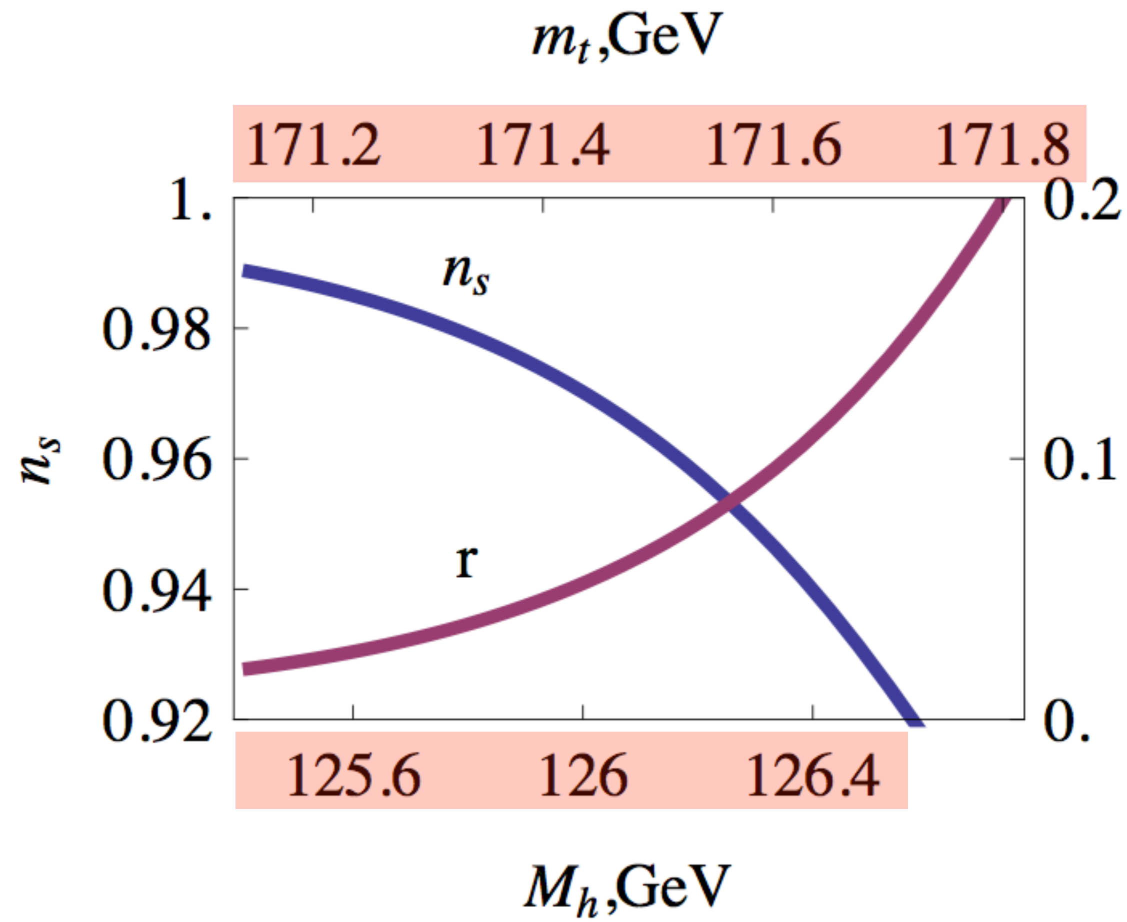

Effects of running on slow-roll parameters

$$\epsilon = \frac{M_{\rm Pl}^2}{2}\left(\frac{dh}{d\chi}\frac{dU}{dh}\right)^2 = \frac{1}{2}\left(4+\frac{\beta_\lambda}{\lambda_H}\right)^2 \frac{M_{\rm Pl}^2/h^2}{\sqrt{\Omega^2+6\xi^2h^2/M_{\rm Pl}^2}} \approx \frac{1}{12}\left(4+\frac{\beta_\lambda}{\lambda_H}\right)^2\frac{M_{\rm Pl}^4}{\xi^2h^4} \quad (17)$$

$$\begin{aligned}\eta &= \frac{M_{\rm Pl}^2}{U}\frac{dh}{d\chi}\frac{d}{dh}\left(\frac{dh}{d\chi}\frac{dU}{dh}\right)\\ &= \left(4+\frac{\beta_\lambda}{\lambda_H}\right)\frac{M_{\rm Pl}^2}{h^2}\frac{\Omega^2}{\Omega^2+6\xi^2h^2/M_{\rm Pl}^2}\left\{\frac{1}{\Omega^2}\frac{\beta_\lambda}{\lambda_H}\left[1+\frac{d\ln\left(\beta_\lambda/\lambda_H\right)/d\ln\varphi}{4+\beta_\lambda/\lambda_H}\right]+3-2\frac{d\ln\Omega^2}{d\ln h}-\frac{\xi\left(1+6\xi\right)h^2/M_{\rm Pl}^2}{1+\xi\left(1+6\xi\right)h^2/M_{\rm Pl}^2}\right\}\\ &\simeq -\frac{1}{3}\left(4+\frac{\beta_\lambda}{\lambda_H}\right)\frac{M_{\rm Pl}^2}{\xi h^2}\left\{1-\frac{M_{\rm Pl}^2}{2\xi h^2}\frac{\beta_\lambda}{\lambda_H}\left[1+\frac{d\ln\beta_\lambda/d\ln\varphi-\beta_\lambda/\lambda_H}{4+\beta_\lambda/\lambda_H}\right]\right\} \quad (18)\end{aligned}$$

ϵ & η are independent

However m_t and m_h are tightly constrained!

[CMS PAS HIG-13-001]

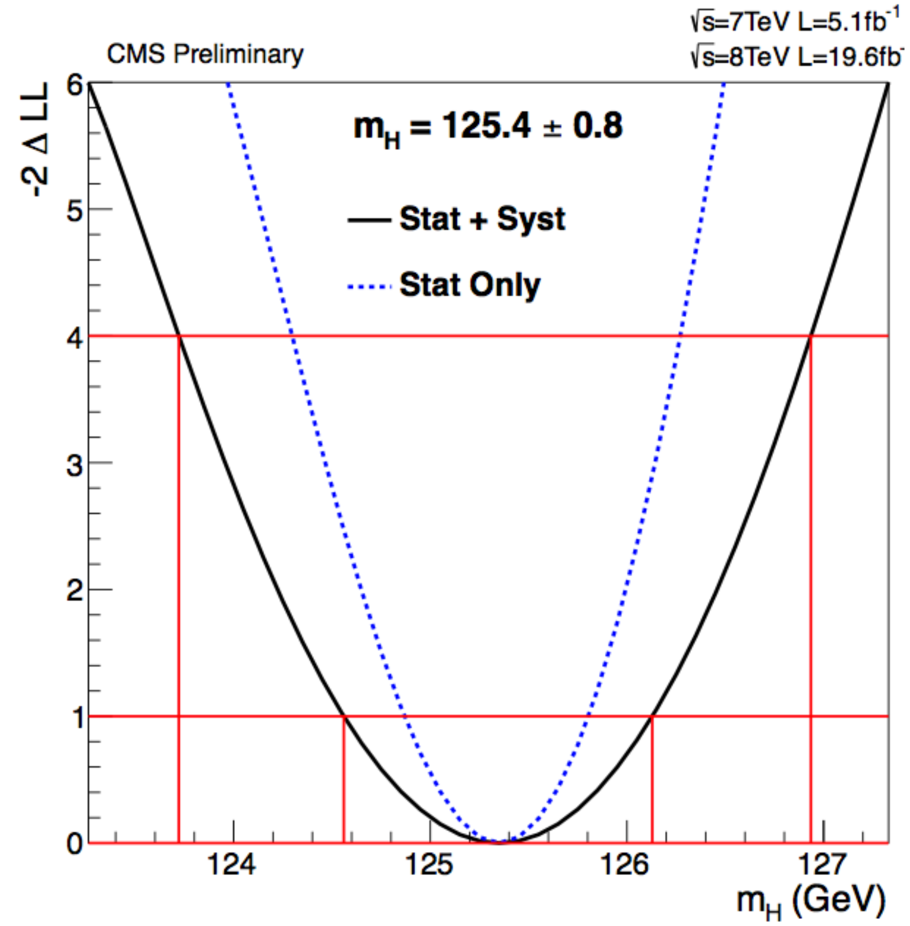

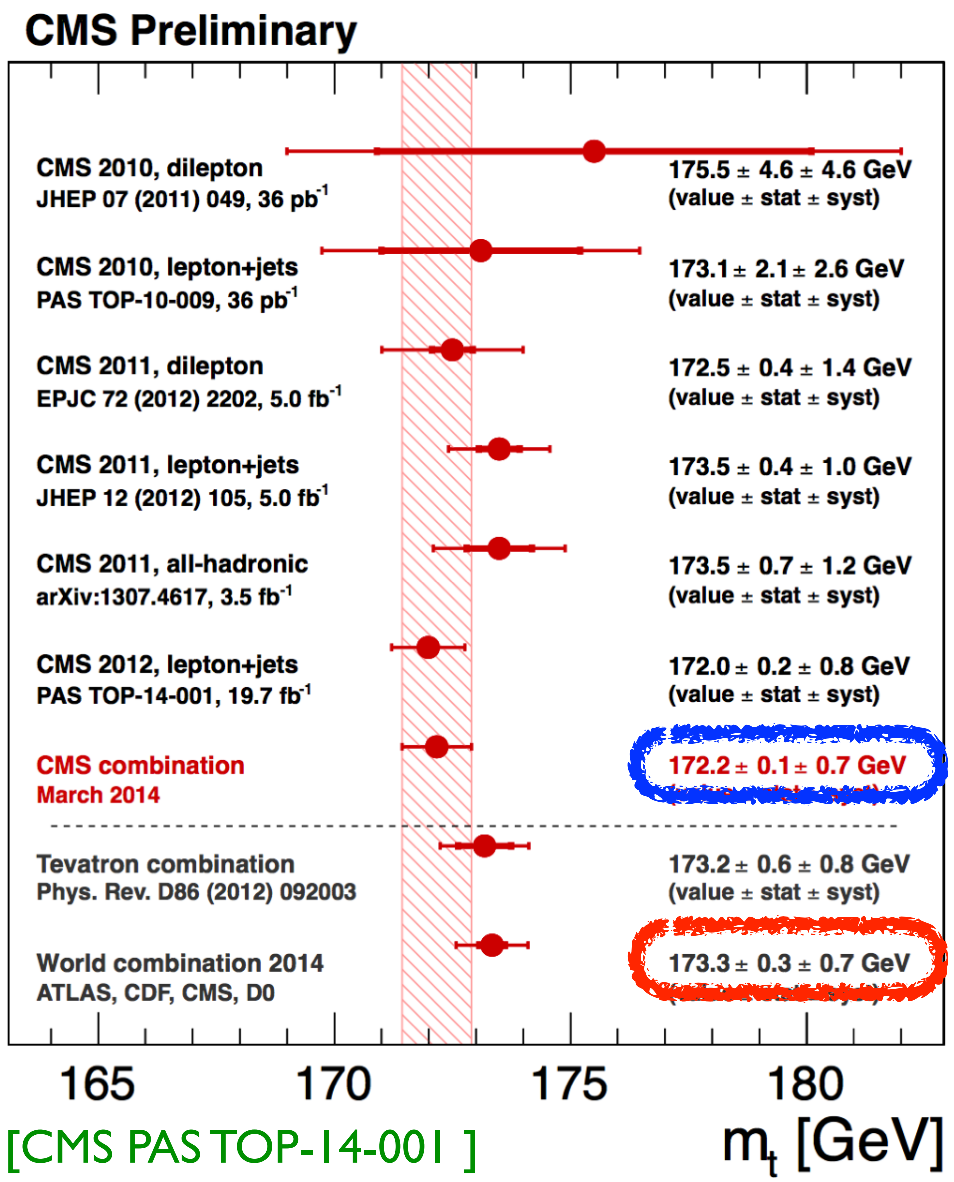

[CMS PAS TOP-14-001]

[1406.3827]

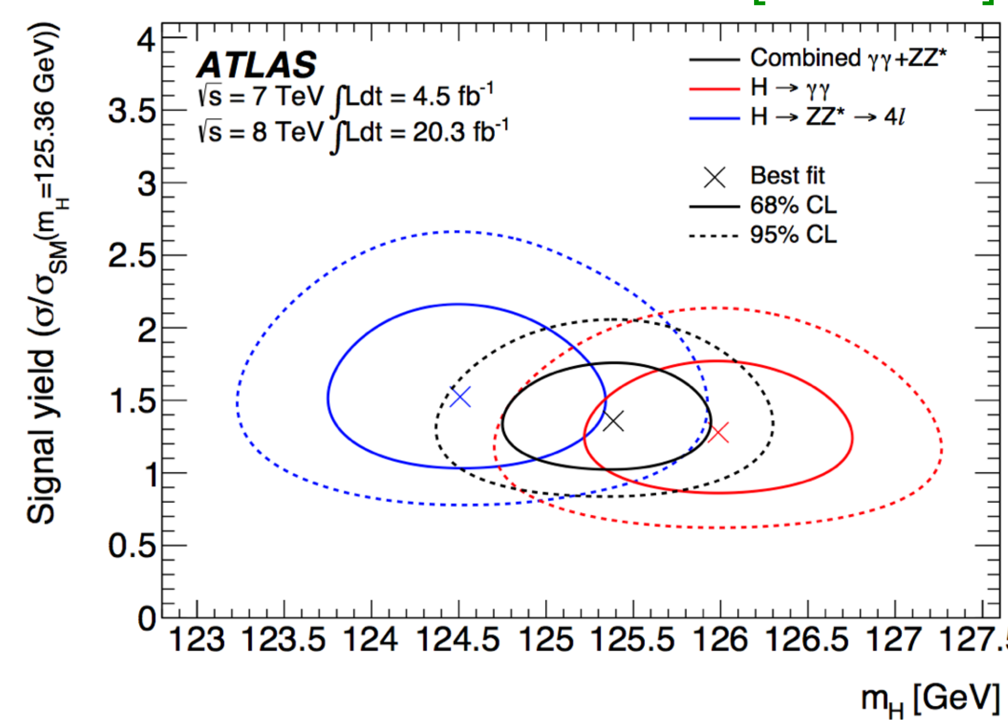

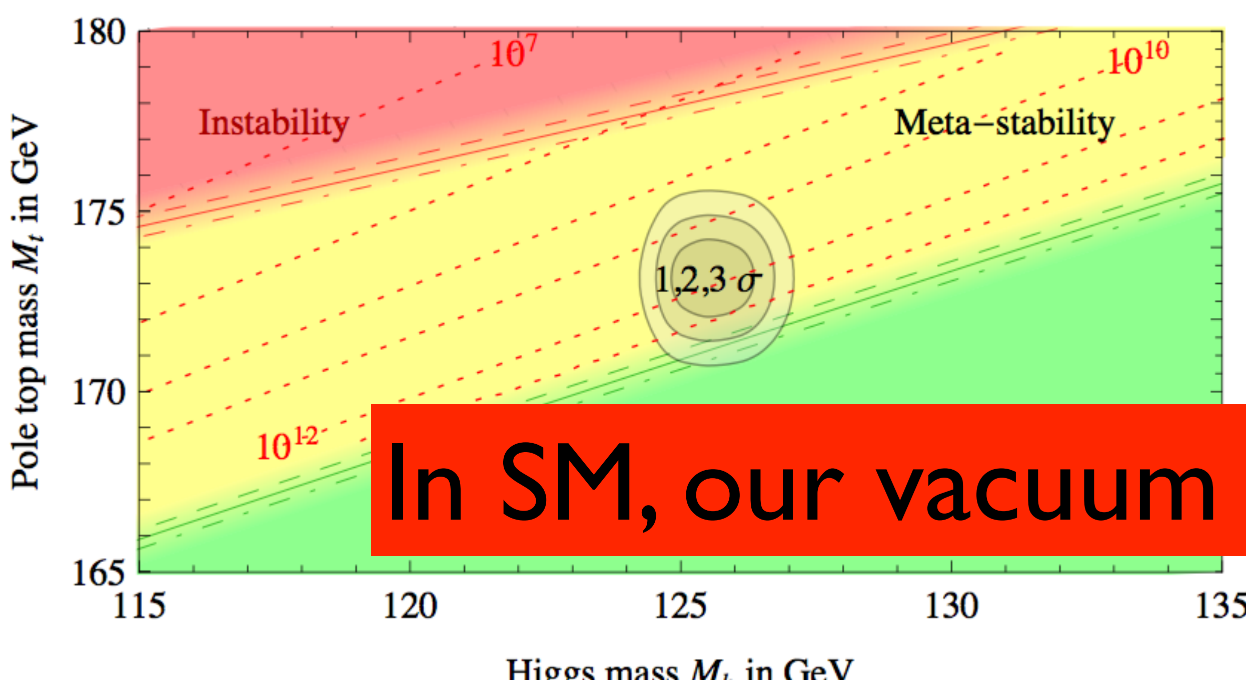

In SM, our vacuum is likely to be meta-stable.

Higgs portal interaction

$$V \supset \lambda_{\Phi H} |\Phi|^2 H^\dagger H$$

Scalar mixing

$$\lambda_H = \left[1 - \left(1 - \frac{m_\phi^2}{m_h^2}\right) \sin^2\alpha\right] \lambda_H^{\mathrm{SM}}$$

$$\Rightarrow \lambda_H > \lambda_H^{\mathrm{SM}} \text{ for } m_\phi > m_h \ \& \ \alpha \neq 0$$

⇒ Vacuum instability along the Higgs direction is easily removed.

⇒ Higgs inflation consistent with BICEP2 is possible for a wide range of m_t and M_h

Higgs portal interaction disconnect m_t and M_h from inflationary observables.

Higgs-portal Higgs inflation

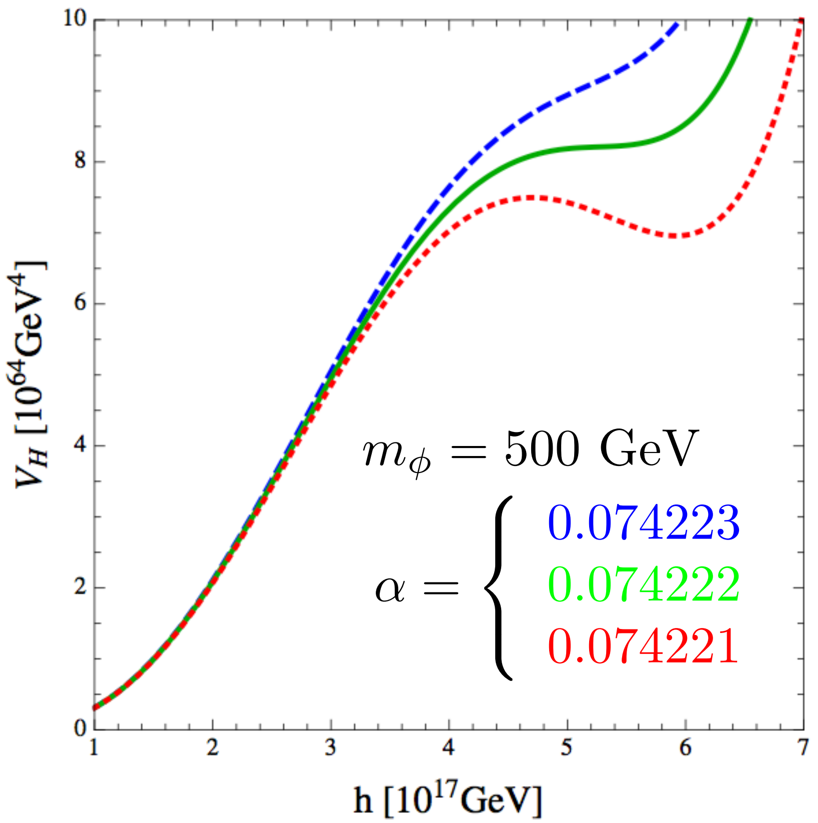

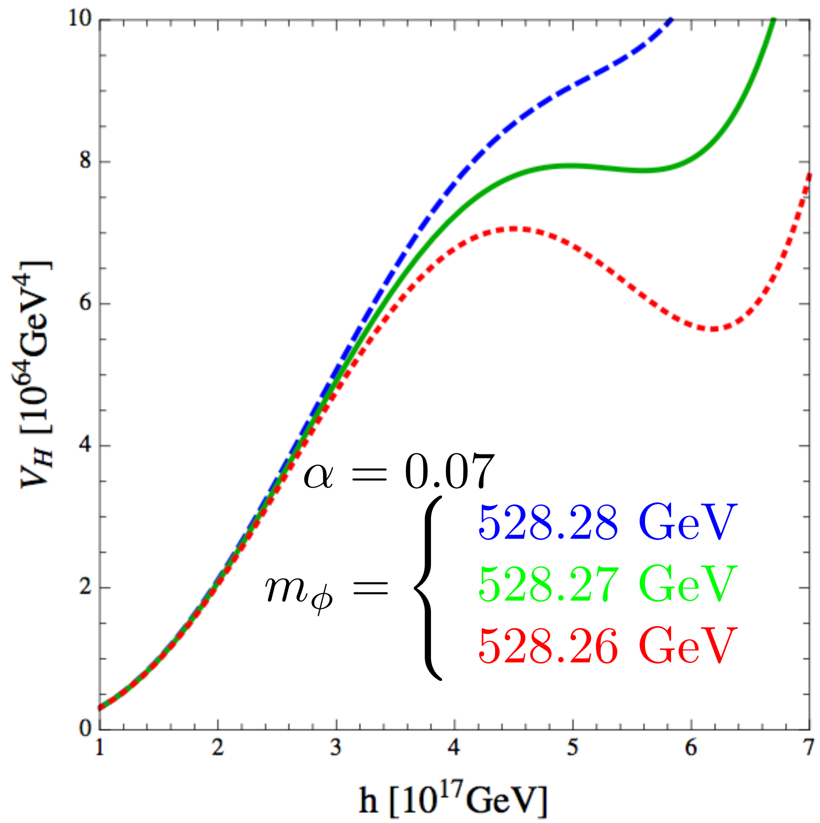

$m_t = 173.2$ GeV
$M_h = 125.5$ GeV

* Inflection point control

(α, m_ϕ) & $\lambda_{\Phi H}$

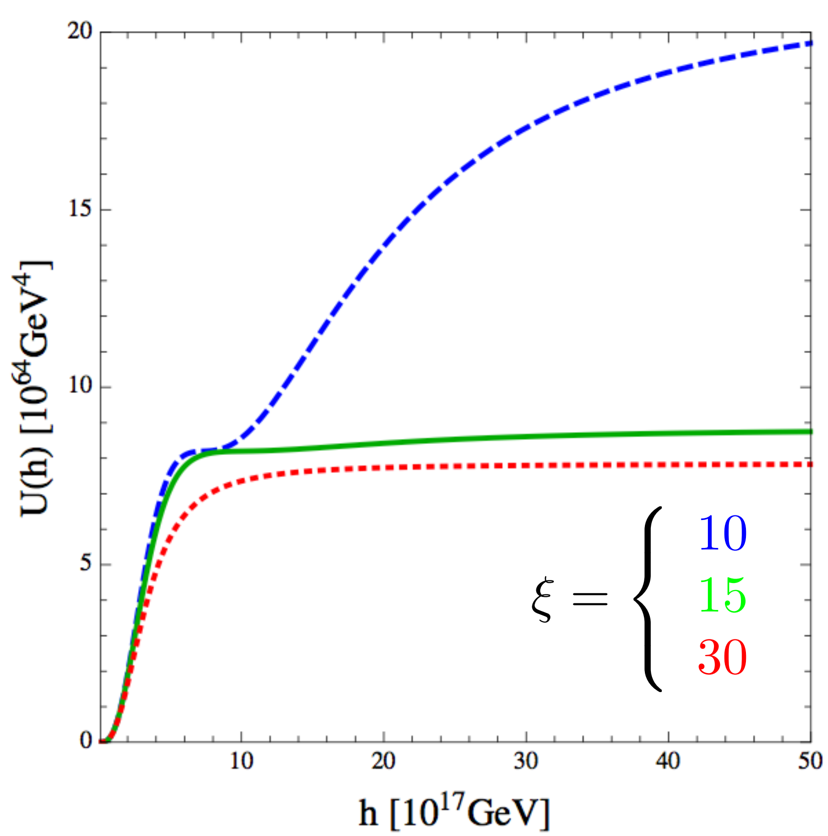

Result of numerical analysis

$k_* \times$ Mpc	N_e	$h_*/M_{\rm Pl}$	ϵ_*	η_*	$10^9 P_S$	n_s	r
0.002	59	0.83	0.00448	-0.02465	2.2639	0.9238	0.0717
0.05	56	0.72	0.00525	-0.00190	2.1777	0.9647	0.0840

- Result depends very sensitively on α, m_Φ and $\lambda_{\Phi H}$ -

Higgs Portal Higgs Inflation can have $r \lesssim O(0.1)$ without resorting to m_t and M_h.

Singlet fermion CDM

Baek, Ko, Park, arXiv:1112.1847

$$
\begin{aligned}
\mathcal{L} &= \mathcal{L}_{\rm SM} - \mu_{HS} S H^\dagger H - \frac{\lambda_{HS}}{2} S^2 H^\dagger H \\
&+ \frac{1}{2}(\partial_\mu S \partial^\mu S - m_S^2 S^2) - \mu_S^3 S - \frac{\mu'_S}{3} S^3 - \frac{\lambda_S}{4} S^4 \\
&+ \overline{\psi}(i \not\partial - m_{\psi_0})\psi - \lambda S \overline{\psi}\psi
\end{aligned}
$$

mixing

invisible decay

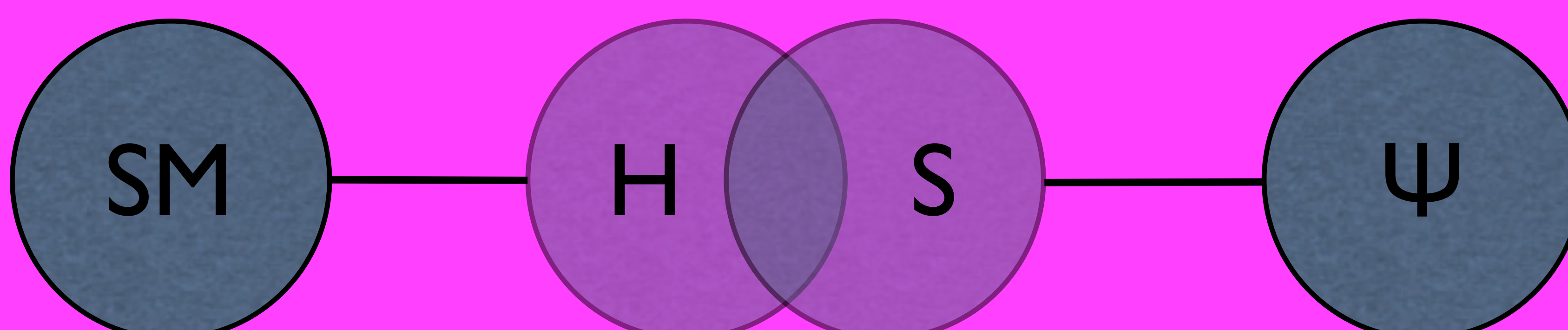

Production and decay rates are suppressed relative to SM.

This simple model has not been studied properly !!

HP assisted HI w/ SFDM

$$\mathcal{L} \supset \frac{1}{2}\xi_s S^2 R$$

ξ_s term is generated by RG, even if $\xi_s = 0$ at $\mu = m_t$ scale.

We assume $S = 0$ during inflation : Inflation along the Higgs direction.

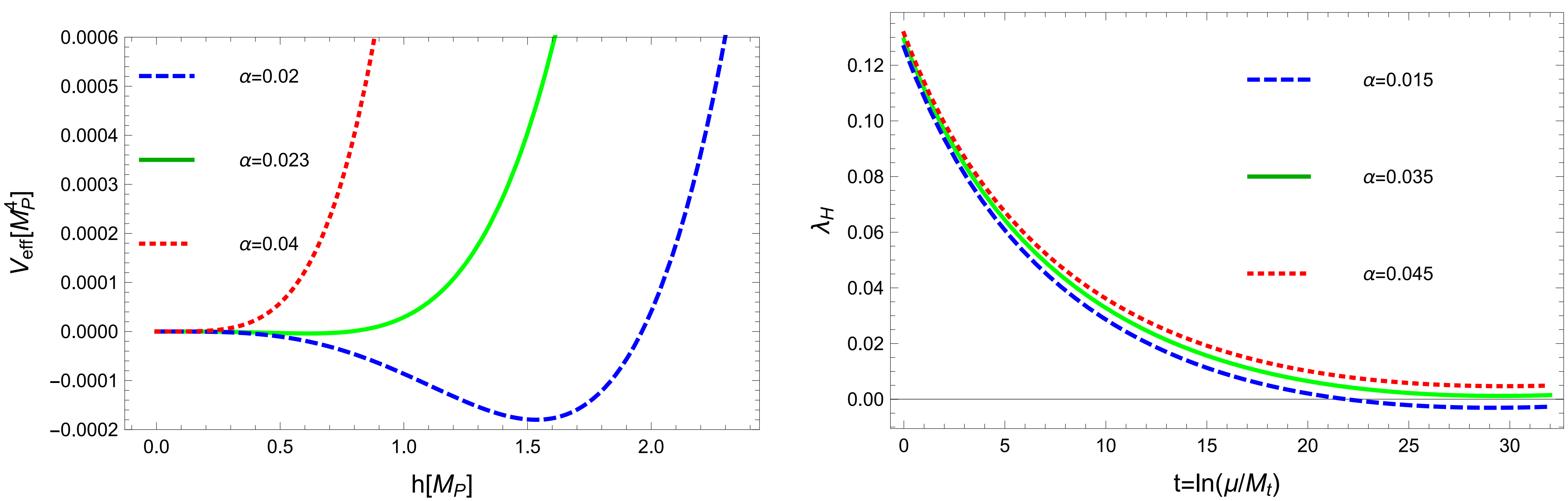

Figure 3. Jordan-frame Higgs potential $V_{\rm eff}$ (left panel) and the running of λ_H (right panel) in SFDM for $\xi_h = 440$, $\xi_s = 0$, $m_s = 600\,\text{GeV}$, $\lambda_{SH} = 0.1$, $\lambda_S = 0.2$, and $\lambda_\psi = 0.3$ chosen at M_t scale.

HP assisted HI w/ SFDM

α	m_s	λ_{SH}	λ_S	λ_ψ	ξ_h	N_e	$10^9 P_S$	n_s	r	α_s
0.036	500	0.1	0.2	0.3	433	57.3	2.2	0.9758	0.0926	−0.0003
0.03885	500	0.1	0.1	0.1	396	57.3	2.2	0.9775	0.0878	−0.0003

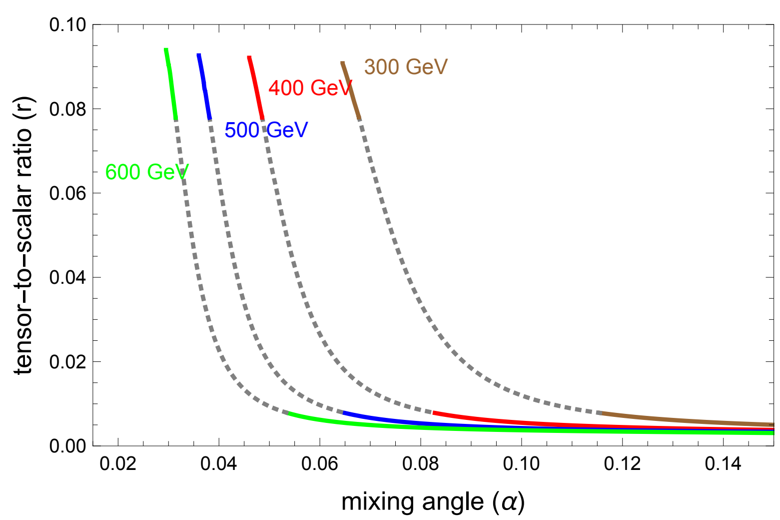

Figure 4. Tensor-to-scalar ratio as a function of the mixing angle α for $m_s = 300\,\mathrm{GeV}$, $400\,\mathrm{GeV}$, $500\,\mathrm{GeV}$ and $600\,\mathrm{GeV}$ at the pivot scale $k_* = 0.05\,\mathrm{Mpc}^{-1}$. Here $\xi_s = 0$, $\lambda_{SH} = 0.1$, $\lambda_S = 0.2$, and $\lambda_\psi = 0.3$ at M_t scale are used. The nonminimal coupling of the SM Higgs to gravity, ξ_h, is chosen in such a way that the Planck normalization (3.8) is satisfied. The grey-dotted lines indicate the parameter region where the spectral index n_s becomes larger than 2σ Planck bound, $n_s \gtrsim 0.98$. Similar behaviors are found for different sets of model parameters.

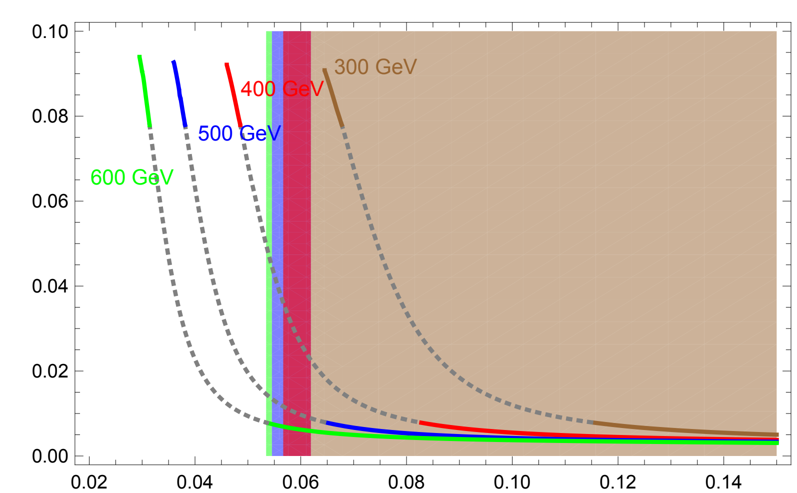

Figure 6. Tensor-to-scalar ratio as a function of the mixing angle α for m_s = 300 GeV, 400 GeV, 500 GeV and 600 GeV, with the constraints discussed in the main text. The stringent upper bounds for a given m_s comes from the DM physics. The values of the other parameters are the same as in figure 4. Color-shaded regions (following the scheme of colored lines) are the excluded regions from the latest LUX experiment, corresponding to different dark Higgs masses.

Large $r \sim O(0.1)$ is possible in HP assisted HI, without tight connection to m_t, m_h

Summary

Message to take home

- DM interacting with massive dark photon is a typical scenario in DM physics
- Very often, dark Higgs boson (or some mechanism to generate dark photon mass) has been ignored
- However, there are many examples that show importance of dark Higgs boson
- In this talk, I discussed the following examples:

- HP VDM: $\Gamma_{\rm inv}(H \to VV)$ and GC γ-ray excesss

- XENON1T excess in terms of exothermic scattering of inelastic DM (both scalar and fermion DM)

- $U(1)_{L_\mu - L_\tau}$-charged scalar/fermion DM outside the $m_{Z'} \sim 2m_{\rm DM}$ window

- Higgs-portal assisted Higgs inflation with large $r \sim O(0.1)$
    - Additional dark Higgs (singlet-like scalar) : generic (in DM models with dark gauge symmetry), improves EW vac stability, helps Higgs inflation with larger tensor/scalar ratio >> Should be actively searched for @ LHC & other future colliders !

BACKUP SLIDES

Determination of (M,spin) @ Belle2

Work in preparation with
DongWoo Kang, Chih-Ting Lu

Search for long-lived particles in inelastic DM models at Belle II

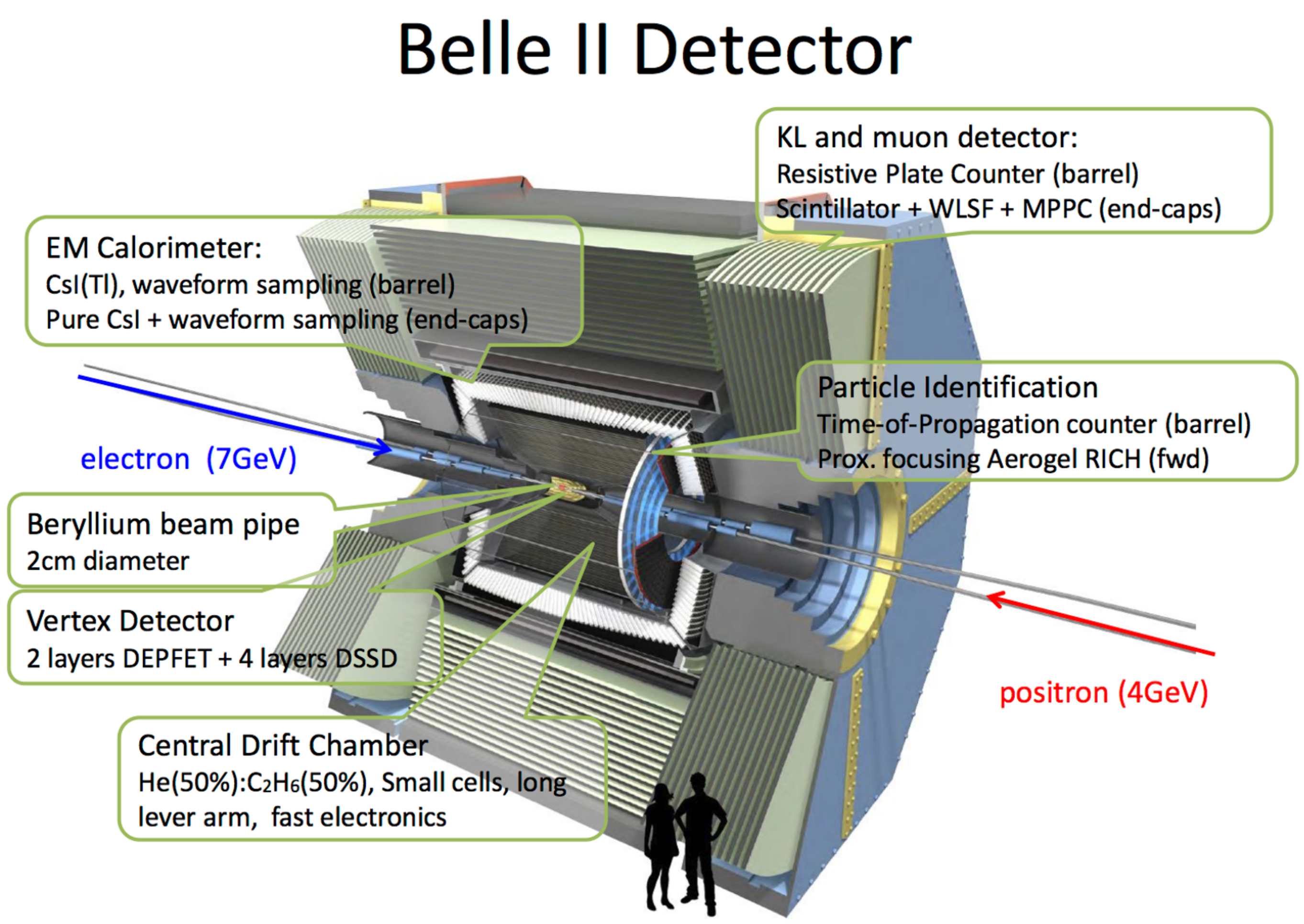

The tracking resolution of electron/muon momenta in the drift chamber detector is given by

$$\sigma_{p_{l^\pm}}/p_{l^\pm} = 0.0011 p_{l^\pm}[GeV] \oplus 0.0025/\beta$$

The resolution of photon momenta in the calorimeter

$$\sigma_{E_\gamma}/E_\gamma = 2\%$$

The resolution for the displaced vertex of lepton pair

$$\sigma_{r_{DV}} = 26\mu m$$

Displaced signature examples in Belle II detector (xy-plane)

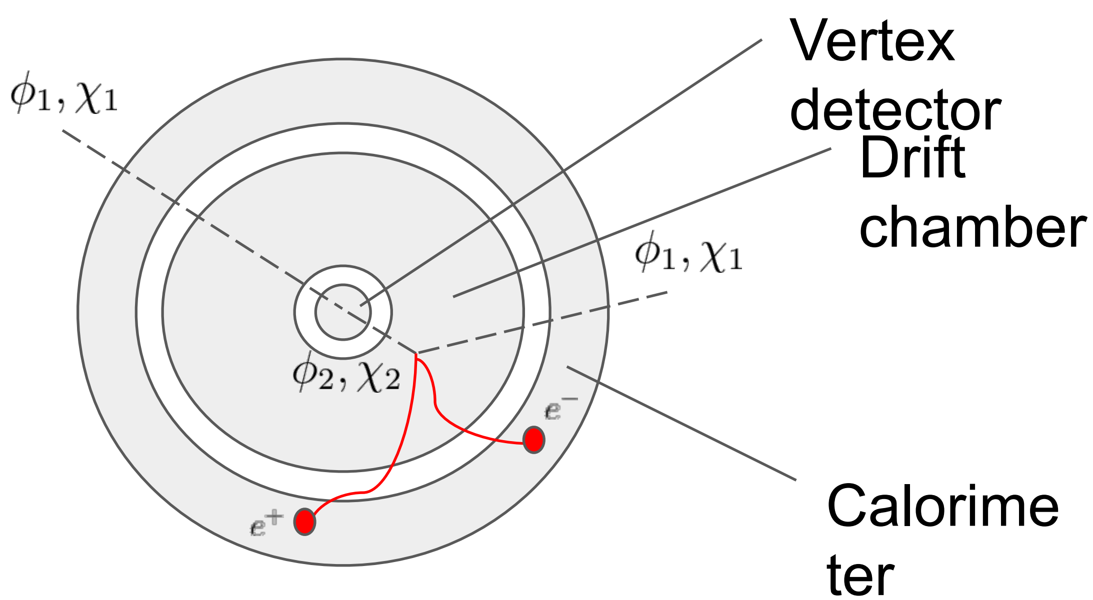

$$e^+e^- \to \phi_1\phi_2 \to \phi_1\phi_1 e^+e^-$$
$$e^+e^- \to \chi_1\chi_2 \to \chi_1\chi_1 e^+e^-$$

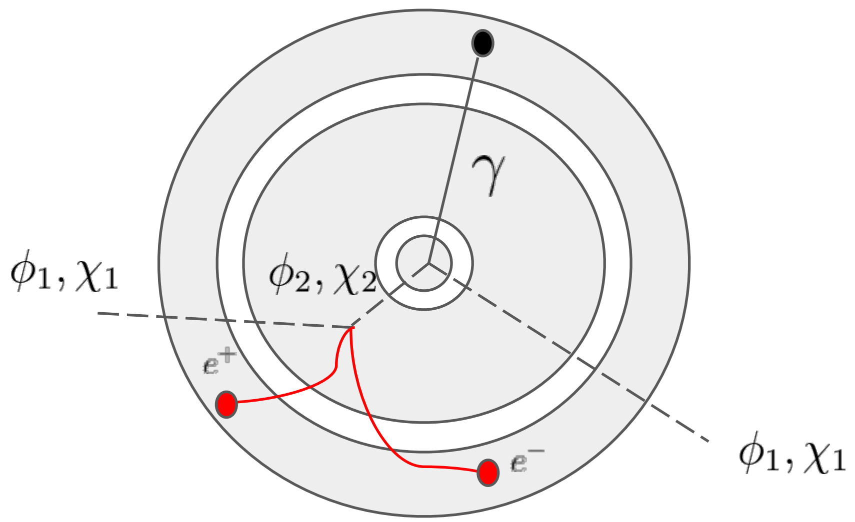

$$e^+e^- \to \phi_1\phi_2\gamma \to \phi_1\phi_1 e^+e^-\gamma$$
$$e^+e^- \to \chi_1\chi_2\gamma \to \chi_1\chi_1 e^+e^-\gamma$$

Any difference for fermion and scalar boson pair productions @ colliders ?

1. The cross sections for fermion and scalar boson pair productions are scaled by $\beta^{1/2}$ and $\beta^{3/2}$ respectively, where β is the velocity of the final state particle in the center-of-mass frame.

2. Hence, one can expect the production of the scalar pair is suppressed by an extra factor of β compared with the fermionic case.

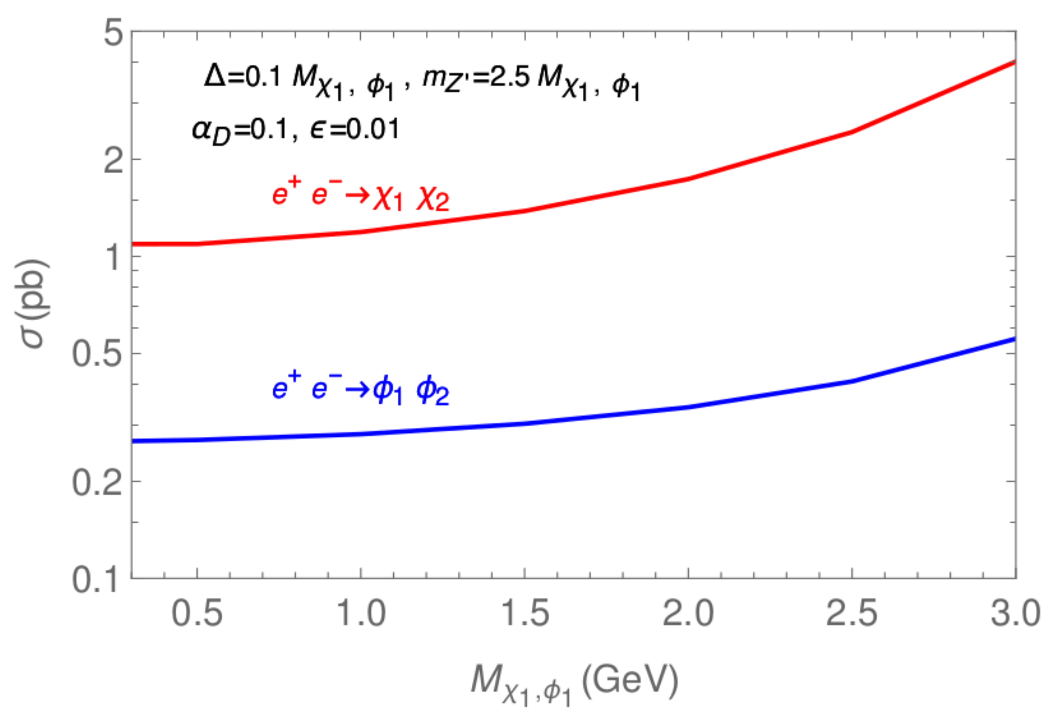

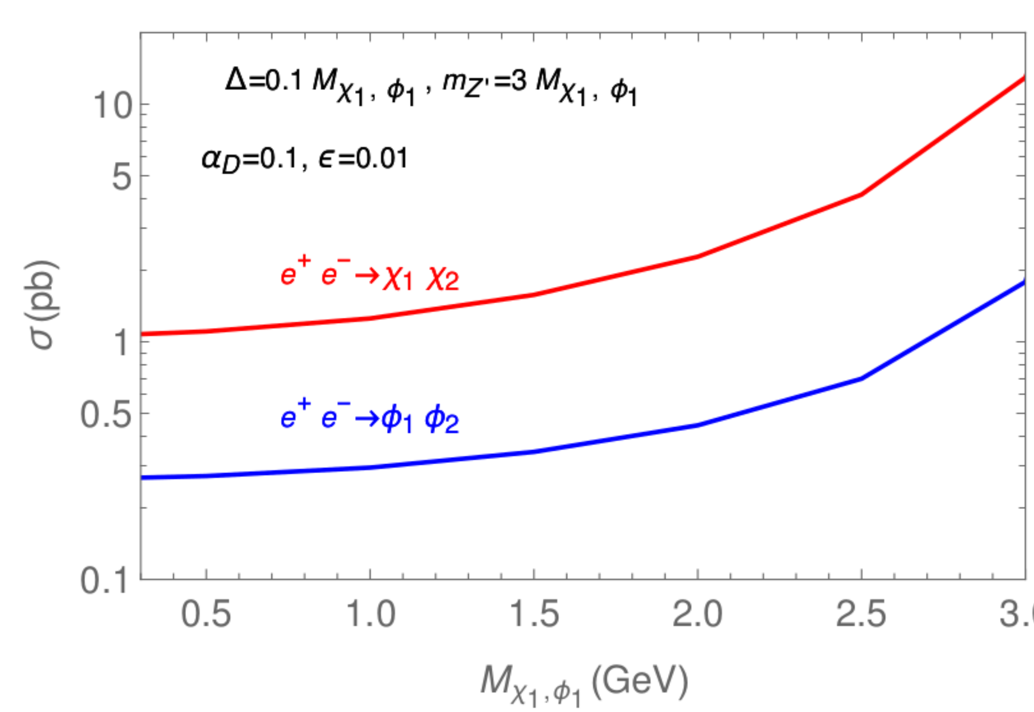

If ϕ_2, χ_2 are long-lived, can we determine their spins at colliders ?

In the center of mass (CM) frame, the normalized differential cross section can be written as

$$\frac{1}{\sigma}\frac{d\sigma}{dcos\theta} = \frac{3}{4}(1 - cos^2\theta)$$

for the scalar case $(e^+e^- \rightarrow \phi_2\phi_1)$

$$\frac{1}{\sigma}\frac{d\sigma}{dcos\theta} = \frac{(1 - \frac{(M_{\chi 2}^2 - M_{\chi 1}^2)^2}{s^2} + \frac{4M_{\chi 1}M_{\chi 2}}{s})\xi + \xi^{3/2}cos^2\theta}{2(1 - \frac{(M_{\chi 2}^2 - M_{\chi 1}^2)^2}{s^2} + \frac{4M_{\chi 1}M_{\chi 2}}{s})\xi + \frac{2}{3}\xi^{3/2}}$$

for the fermion case $(e^+e^- \rightarrow \chi_2\chi_1)$

where $\xi = \sqrt{1 - \frac{2(M_{\chi 2}^2 + M_{\chi 1}^2)}{s} + \frac{(M_{\chi 2}^2 - M_{\chi 1}^2)^2}{s^2}}$

We need to know the direction of the displaced vertex

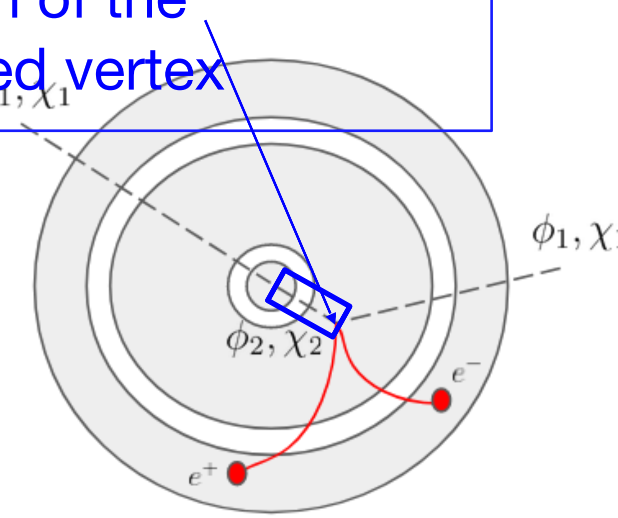

Note θ is the direction of ϕ_2 , χ_2 relative to the beam direction.

If ϕ_2, χ_2 are long-lived, can we determine their spins at colliders ?

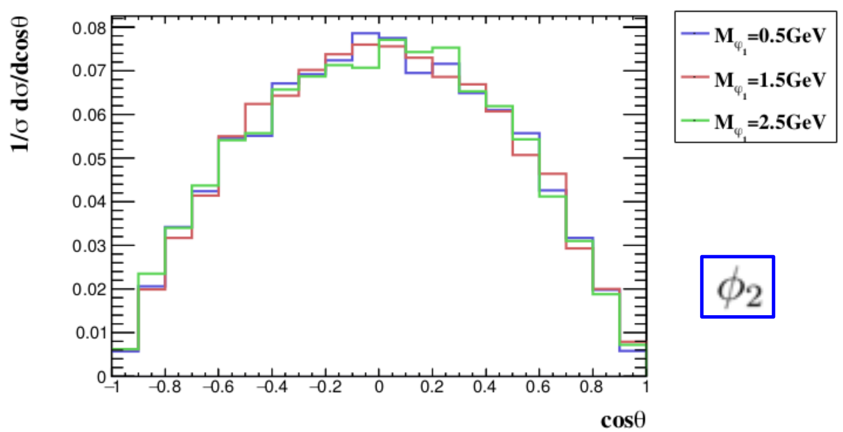

ϕ_2

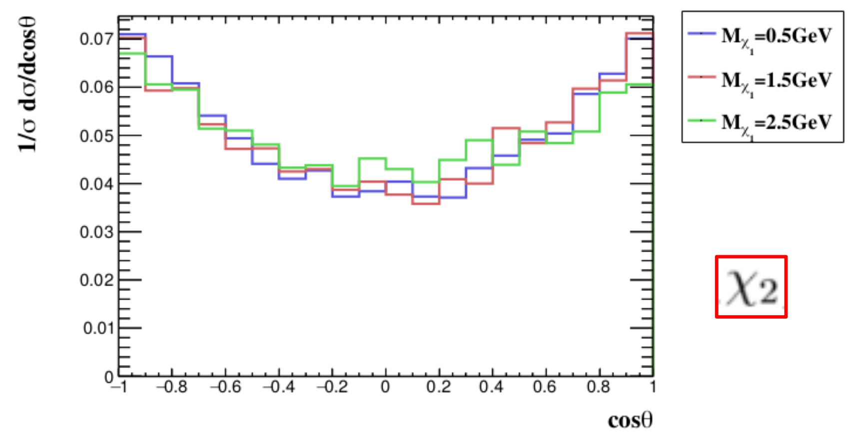

χ_2

Fix $\alpha_D = 0.1$, $\epsilon = 0.01$, $\Delta = 0.1 M_{\phi_1,\chi_1}$, and $m_{Z'} = 3.0 M_{\phi_1,\chi_1}$

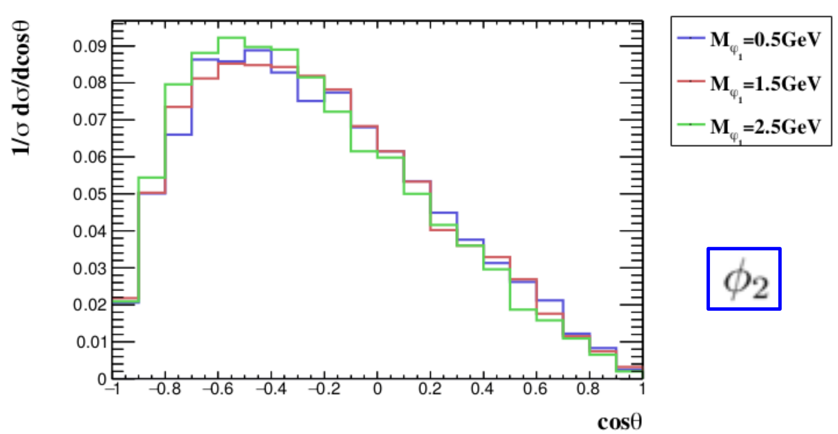

ϕ_2

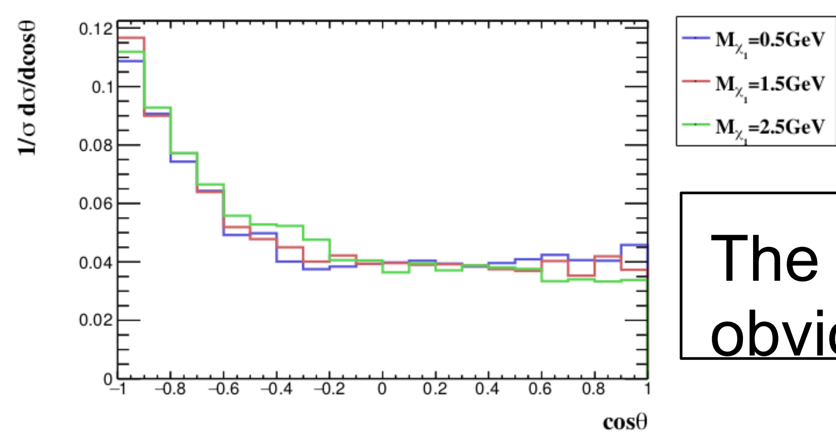

χ_2

The differences are still obvious in the LAB frame!

If the excited DM is long-lived, can we determine its mass at colliders ?

In the center of mass (CM) frame for the process $e^+e^- \to \chi_1\chi_2 \to \chi_1\chi_1 e^+e^-$

There are 8 unknown values from four-momentum of two dark matters in the final states.

However, we have 7 constraints for this process :

1. four-momentum conservation (4)
2. two dark matters with the same mass (1)
3. because of the charge neutrality of the excited DM, a three-momentum vector is proportional to the displaced vertex (2) : $\overrightarrow{p_{\chi_2}} = |\overrightarrow{p_{\chi_2}}|\hat{r}_{DV}$

Therefore, we cannot get the unique solution for 8 unknown values. We need to find other ways to determine the mass of DM and mass splitting !

If the excited DM is long-lived, can we determine its mass at colliders ?

In the center of mass (CM) frame for the process $e^+e^- \to \chi_1\chi_2 \to \chi_1\chi_1 e^+e^-$

We can first write down the following equation with the help of four-momentum conservation,

$$m_{\chi_2}^2 - m_{\chi_1}^2 - 2E(1+\alpha)E_{V'} + E_{V'}^2 - |\overrightarrow{p_{V'}}|^2 + 2\sqrt{(E(1+\alpha))^2 - m_{\chi_2}^2}(\hat{r_{DV}} \cdot \overrightarrow{p_{V'}}) = 0$$

where $\hat{r_{DV}}$ is the direction of displaced vertex, E is half of the center of mass energy,

$E_{V'}$, $\overrightarrow{p_{V'}}$ are the visible energy and three-momentum in the final states, and

$$\alpha = \frac{m_{\chi_2}^2 - m_{\chi_1}^2}{4E^2}$$

For each event, we can receive a relation between the mass of DM and mass splitting.

If the excited DM is long-lived, can we determine its mass at colliders ?

The crossing point from these events and kinematic endpoint measurement $m_{f\bar{f}}^{max}$ can help us to determine the mass of DM and mass splitting. This method is based on "Kinematic focus point" from arXiv:1906.0282 (Kim,Matchev,Shyamsundar).

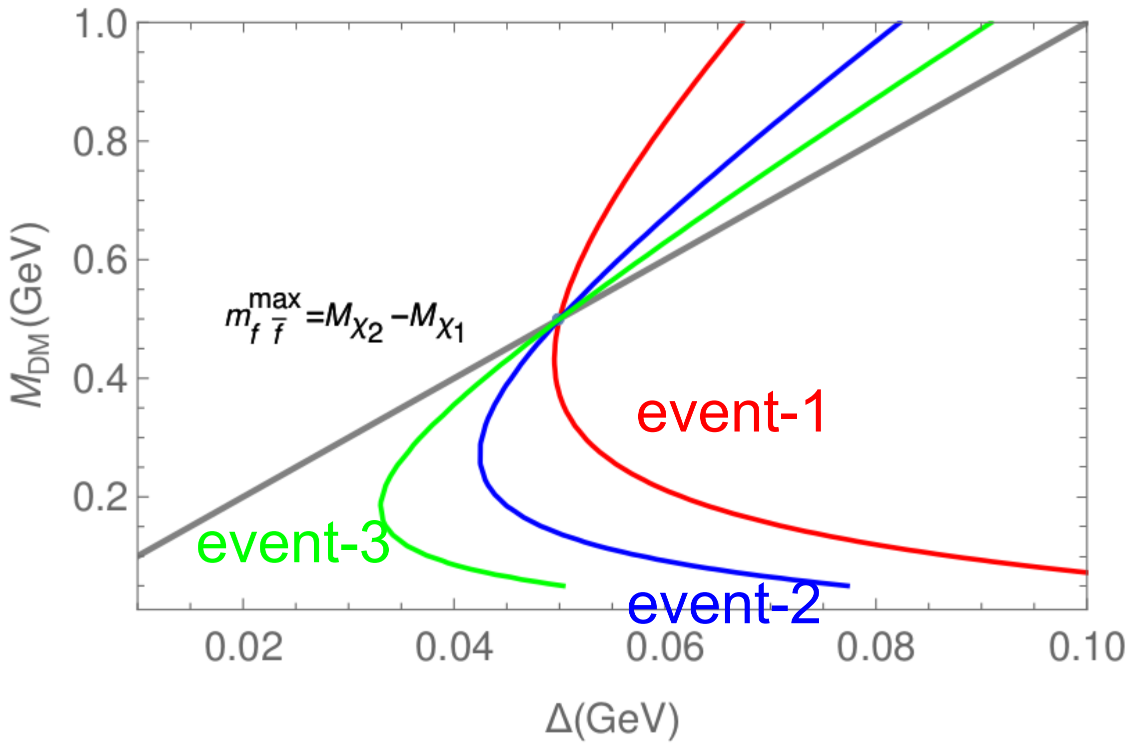

$(\Delta, M_D) = (0.05, 0.5)$ GeV

If the excited DM is long-lived, can we determine its mass at colliders ?

Assume we can have 100 signal events at the Belle II, then we will get 4950 solutions from each two events !

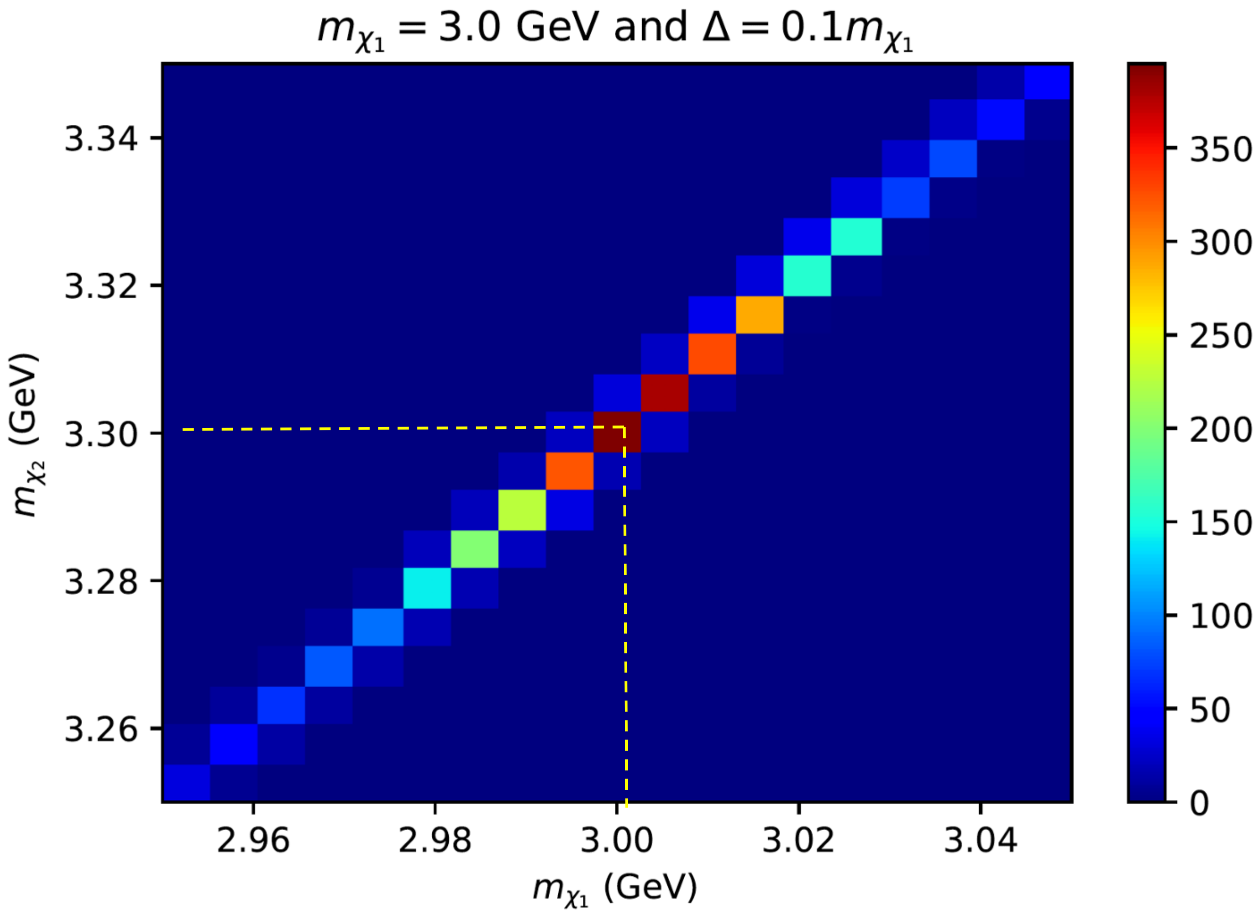

If the excited DM is long-lived, can we determine its mass at colliders ?